6-2017

A Lipid Binding Structure and Functional Analysis of Human ARV1

Jessie Lee Cunningham
Rowan University

A LIPID BINDING STRUCTURE AND FUNCTIONAL ANALYSIS OF
HUMAN ARV1

Jessie Lee Cunningham, B.S.

A Dissertation submitted to the Graduate School of Biomedical Sciences,
Rowan University in partial fulfillment of the requirements for the M.S. Degree.

Stratford, New Jersey 08084

June 2017

Table of Contents

Acknowledgments

One might suspect that of all the sections that are included in the construction of a Master's dissertation, the "acknowledgements" section would be the easiest to complete; however, I have found it to be the most difficult. The remaining sections have been written, figures have been formatted, all is complete to the best of my current abilities and I am left with a physical representation of two years of fortitude and efforts; sourced both from myself and from others. The products of this dissertation and the developments that I underwent as a scientist are the results of many people and organizations who invested in me their time, financial support, and guidance for which I will be forever grateful for.

To the program director, Dr. Diane Worrad, faculty, and the many coordinators of the Master of Science in Molecular Pathology and Immunology (MSMPI) program at Rowan University Graduate School of Biomedical Sciences (GSBS), thank you for giving students the opportunities to develop their minds and skillsets in the pursuits of careers in research of the sciences. To Dr. Eli Mordechai, the founder of Genesis Biotechnology Group, and all of its members, thank you for opening your laboratories and making resources available for the next generation of scientists to hone their skills and for providing them the confidence that comes with experience to further their careers.

I would like to personally thank the members of my thesis advisory committee which include, Dr. Sal J. Caradonna, MSMPI Program Chair, Dr. Grant Gallagher, Senior Team Leader at the Institute for Biomarker Research and Coordinator of the GBG-Rowan MSMPI program, Dr. Scott Gygax, Vice President & Managing

6

Director of Product Development, and Dr. Joseph T. Nickels, Director of the Institute of Metabolic Disorders. From the very beginning, these individuals facilitated each step of this journey as an unwavering support system and it is from their efforts that I have been able to complete this program.

I have to extend a special thanks to Dr. Joseph T. Nickels and every single member at the Institute of Metabolic Disorders (IMD). This group is full of amazing people who are passionate about their work. Even when I troubled them during off hours or on weekends with questions or concerns, they were always so happy and willing to help me whenever the assistance was needed. Dr. Nickels was more than just faculty for me during the course of this program. He was a true mentor that inspired me to have passion for my work and demanded of me nothing less than my best; standards I will strive to uphold for the remainder of my career.

I would lastly like to thank my friends and family for all of the love and encouragement when all other hope seemed lost. Leonid Kalik, a man who had to endure me at my most stressed, and still found every reason to make me smile. To Jacqueline Cunningham, dearest sister of mine, who convinced me to apply to this program and *be an oyster*. To Charles and Zoraida Cunningham, I am most thankful for all that you have done. It is so much more than the late-night coffee deliveries, phone calls to resolve fears, or the countless acts of love you have provided me. You have always believed in me, even when this world convinced me I could not. I dedicate this degree to you as you have contributed more to its completion than I did. "There is no success that comes for free. I've paid for every good in my life with pain, and blood, and sorrows. And for the good that I could not afford, I was blessed

with the sacrifices of others." I hope that someday I can find a way to repay all of the

sacrifices you have made for me.

Abstract

Metabolic Syndrome (MetS) is a combination of risk factors that can over time increase the probability of developing diseases, including cardiovascular disease, type 2 diabetes, non-alcoholic fatty liver disease (NAFLD), and non-alcoholic steatohepatitis (NASH). Acyl-coenzyme-A: cholesterol O-acyl transferase related enzyme required for viability-1, abbreviated as Arv1, is an evolutionarily conserved putative lipid binding protein. Several studies have implicated hArv1 as a critical regulator of lipid transport and trafficking.

Recent work using an Arv1 knock out (KO) mouse model have established a clear link between Arv1 function and the progression of MetS and NAFLD/NASH [*unpublished data*] [1]. Overall, studies show that KO animals exhibit a reduction in body weight, have less blood circulating cholesterol, are more glucose tolerant and insulin sensitive, and show severely reduced signs of NASH.

Little is known about whether Arv1 binds lipids directly and if it is involved in their transport in any way. Here, we explored whether Arv1 could bind lipid, and if so what was its lipid specificity for binding. Moreover, we undertook a structure/function approach to define the critical residues within the hArv1 homology domain (AHD) required for function. Homogeneous time resolved fluorescence (HTRF) assays were used to assess the interactions between Arv1 and specific phospholipids. We found that hArv1 directly binds to phosphatidylglycerol (PG), phosphatidic acid (PA), cardiolipin (CL) and phosphatidylserine (PS) with decreasing affinity. Using site directed mutagenesis, we identified specific residues that are required for AHD lipid binding. Overall, we have verified that the AHD of Arv1

does have lipid binding activity. Moreover, we have defined critical residues within the AHD that are required for this binding. Understanding the molecular basis for Arv1 lipid binding will further our understanding of how hArv1 may be contributing to the initiation and/or progression of MetS related diseases.

1. Introduction

1.1. Metabolic Disorders

Advances in the fields of science and medicine have contributed to an increase in the average American lifespan, yet even with this increase, the quality of overall health remains less than ideal. Obesity has been linked to the appearance of detrimental risk factors, many of which have been tied to the metabolic syndrome (MetS) [2]. MetS is characterized by the accumulation of risk factors, that when present concurrently, increases the probability of developing potentially fatal diseases that include type II diabetes, atherosclerosis, cardiovascular disease (CVD), and NAFLD/NASH [3]. Because the rate of incidence of MetS has been steadily on the rise, there has been a surge in urgency for the discovery of new and effective treatments for these diseases [4].

The degree of MetS is largely patient specific, without a clearly defined progression of symptoms; however, it is known that both genetic and environmental factors contribute to its development. Some risk factors include, increased abdominal fat accumulation, obesity, high blood pressure, high blood sugar levels, insulin resistance, increased expression of inflammatory or coagulation factors, high triglyceride levels and low levels of HDL (Figure 1). According to the US National Heart, Lung and Blood Institute and the American Heart Association Consensus Statement, accumulation of three or more of these risk factors is thought to be sufficient for initiation of MetS [2]. Obesity and insulin resistance are thought to have the most impact on disease severity as they both contribute to the further

accumulation of additional risk factors. It should be pointed out that obesity itself is not a prerequisite, as it is possible to develop MetS with a healthy BMI [3,5].

The US National Health and Nutrition Examination Survey have indicated that approximately one third of adults have some form of metabolic syndrome, with 40% of adults over the age of 40 affected [2]. Although some MetS disorders (risk factors) have been well defined and targeted drug therapies are available, the efficacy of these pharmaceuticals ranges. Often, patients cannot tolerate them as the undesired side effects that present can outweigh the benefit of the drug [6]. There are also instances where few to no effective therapies are available; a situation that can be further compounded by a lack of indicators for early detection or progression, as is the case with NAFL/NASH [7]. In order to develop new strategies for earlier detection and treatment, more work is needed to further dissect the intricately intertwined pathways that are involved in metabolic syndrome.
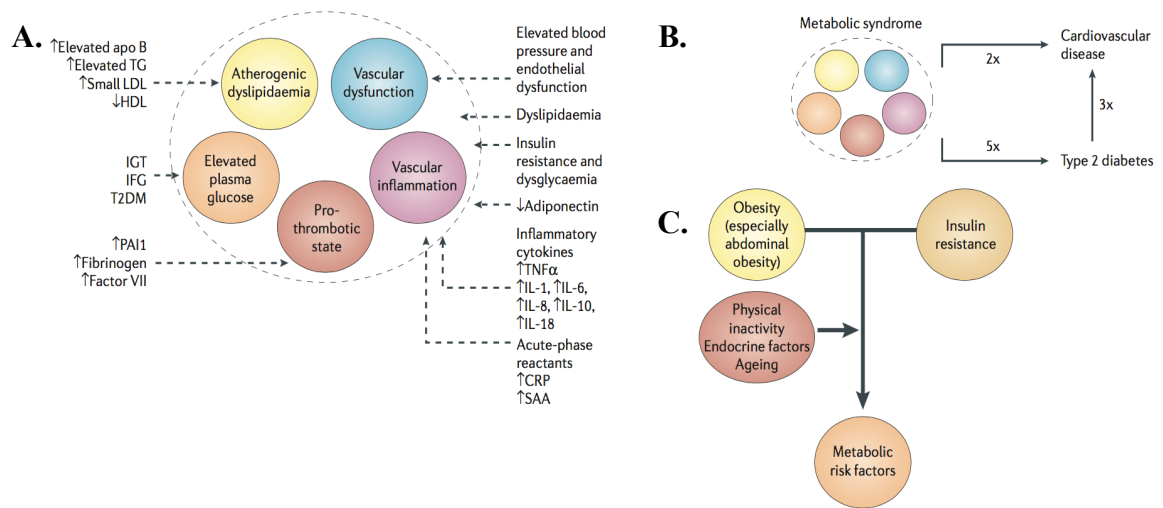
Figure 1. Contributing risk factors of Metabolic Syndrome. [A.] Some primary contributing risk factors of metabolic syndrome (MetS) include dyslipidemia, elevated blood pressure, elevated blood sugar, a pro-thrombotic state and a pro-inflammatory state. Each factor involves several components, some of which can be interrelated. [B.] The chances of developing life threatening diseases increase with the accumulation of more risk factors. Atherosclerotic cardiovascular disease (ASCVD) is twice as likely in those with metabolic syndrome and the risk of type II diabetes is increased five-fold. Presence of a MetS related disease increases relative risk of promoting an additional disease. If a patient has type II diabetes already, they are then three times more likely of *also* developing CVD. [C.] Central obesity and insulin resistance are described as being key initiators of metabolic syndrome. This can be further compounded by secondary factors such as level of activity, hormones, and age.

triglycerides (TGs), apolipoprotein B (apo B), small low-density lipoprotein (LDL) particles, high-density lipoproteins (HDLs), plasminogen- activator inhibitor 1 (PAI1), CRP, C-reactive protein; IFG, impaired fasting glucose; IGT, impaired glucose tolerance; IL, interleukin; SAA, serum amyloid A protein, T2DM, type 2 diabetes mellitus, TNFα, tumor-necrosis factor-α. [5].

1.2. Lipid Classifications

The term lipid encompasses a diverse collection of organic compounds whose chemical and structural attributes allow for their solubilization in most organic solvents while remaining insoluble in water [8]. Lipids can be subdivided into classifications contingent on specific localization within the cell, distinctive capabilities, chemical composition, or the involvement to defined metabolic or signaling pathways. While some functions may be unique to a particular classification, in general, lipids serve the main functions of storing energy, creating membrane structures, and allowing the induction or conduction of signaling pathways [8].

1.2.1. _Fatty acids_

Fatty acids are an integral structural component for the synthesis of complex lipids including triglycerides and phospholipids, while also serving as efficient energy storage molecules. They are comprised of a carboxylic acid and an aliphatic chain that can be either saturated or unsaturated [9, 10]. Fatty acid synthesis is performed largely in adipose tissues and in the liver. In the cytosol of the cell, fatty acids can be synthesized through end products of the enzyme mediated glycolytic pathway or broken down via beta oxidation within the mitochondria. The conversion of fatty acids to or from acetyl-CoA is mutually exclusive for each pathway [9, 10].

1.2.2. *Glycerolipids*

Glycerolipids are obtained through diet, recycled through storage mechanisms, or can be synthesized de novo in the liver. They are composed of a glycerol backbone produced from the metabolism of carbohydrates, the hydroxyl groups of which can be esterified with multiple fatty acids. Mono-, di-, and tri-prefixes indicate the number of fatty acid additions, the most common form being triacylglycerol (TAG), also referred to as triglyceride [11]. TAG is the predominant form of energy storage in animals and it also serves as a storage molecule for otherwise toxic fatty acids [12]. The fatty acids stored in triglycerides accumulate in adipose tissues. There, they are reduced and anhydrous, however when lipolysis occurs there is a hydrolysis of ester bonds which liberates fatty acids from the glycerol backbone and provides a rapid source of energy for the organism [11, 12].

1.2.3. *Sterol lipids*

Sterol lipids, which include cholesterol, are obtained through dietary intake or produced from acetyl-CoA through the mevalonate HMG-CoA reductase pathway. The canonical structure of the sterol molecule contains four linked hydrocarbon rings with a hydrocarbon tail at one end, and a hydroxyl group at the other [13]. These amphipathic lipids play crucial roles in maintaining the membrane structure and fluidity, representing 30% of membrane composition [13]. When embedded in the membrane, cholesterol is orientated in such a way that its polar hydroxyl group has access to interact with the head groups of phospholipids and the remainder of its structure is parallel to the fatty acid chains [9, 10]. In addition to its roles in the

structural aspects of cellular membranes, cholesterol is required for intracellular

transport, cell signaling and is also the precursor component for bile acid, steroid, and

vitamin synthesis [14].

1.2.4. *Sphingolipids*

In addition to their structural function in cell membranes, sphingolipids are

used largely in cell recognition and signal transduction [13]. Their structure is not

glycerol based, but rather, is built up with long chain sphingoid bases as a backbone,

amino alcohols including sphingosine, and a fatty acid chain. Sphingolipids are also

the precursor for the production of phosphsphingolipids, glycosphingolipids, and

ceramides [13].

1.2.5. *Glycerophospholipids*

Glycerophospholipids, commonly referred to as phospholipids, are the most

abundant class of lipids in cellular membranes and vesicles. Their structures are

composed of a backbone that is often glycerol, where C1 and C2 of the backbone is

esterified to the carboxyl group of a fatty acid chain that is saturated or unsaturated, a

phosphate group, and an alcohol group [15]. The fatty acid portion promotes

hydrophobicity, while the remaining head group remains hydrophilic and able to

interact with the environments on either side of a lipid bilayer. The specific

characteristics of each phospholipid are dependent on the status of their hydrocarbon

tails and the features conferred to it by the addition of the head group [16]. Major

groups of phospholipids include phosphatidylcholine (PC), phosphatidylethanolamine

(PE), phosphatidylserine (PS). Minor groups include phosphatidic acid (PA),

phosphatidylglycerol (PG), diphosphatidylglycerol also known as cardiolipin (CL), phosphatidylinositol (PI), and the phosphoinositides (PIPs) [15]. Each type of phospholipid not only confers structure to lipid membranes; they also function in cell-cell signaling and as signaling promoters through their interactions with intra and intercellular lipid binding proteins [15, 16].

1.3. Lipid Metabolism and Synthesis Pathways

One can obtain lipids through their diet or by endogenous *de novo* biosynthesis within cells. Below is a review of the enzymes and pathways involved in lipid biosynthesis, uptake, and metabolism (Figure 2).

1.3.1. Dietary Lipid Metabolism

The predominant lipid taken in through diet is triglyceride. Other lipids taken up in less quantities include esterified cholesterol, fatty acids, and phospholipids. During digestion from the stomach to the intestine, cholesterol becomes de-esterified, while triglycerides are broken down into monoacylglycerols and fatty acids by lipase enzymes and emulsifiers [12]. Once these triglyceride intermediates are absorbed into the intestine, monoacylglycerol acyltransferase (MGAT) produces diacylglycerol from monoacylglycerol and fatty acid. Diacylglycerolacyltransferase (DGAT) then catalyzes the re-synthesis of triglycerides [17].

Triglycerides and cholesterol are packaged by enterocytes of the intestine into chylomicrons that can be circulated throughout the periphery [18]. In addition to containing triglycerides and cholesterol, chylomicrons are also made up of apolipoproteins apo B-48, apo A-I, II, IV, apo-C, apo-E and apo-CII that aid in proper

lipid nucleation of the various apolipoproteins [19]. Cells that require these lipids

utilize lipases that hydrolyze the triglycerides, whereby they obtain fatty acids and

exchange them for excess cholesterol. During these lipid exchanges, apolipoproteins

of varying densities are formed and broken down in order to maintain normal lipid

homeostasis [18].

1.3.2. _G3P Mediated Synthesis and Endogenous Lipid Metabolism_

De novo biosynthesis triglyceride biosynthesis occurs in adipose and liver

tissues through the sn-glycerol-3-phosphate (G3P) pathway [12]. Glycerol-3-

phosphate, an end product of carbohydrate metabolism via the glycolytic cycle, is the

first acyl acceptor for glycerol-3-phosphate acyltransferase (GPAT) [12]. This yields

lysophosphatidic acid (LPA) whose acylation by acylglycerol-3-phosphate

acyltransferase (AGPAT) produces the phospholipid, phosphatidic acid (PA), which

acts as a precursor for other phospholipids and neutral lipids [12, 20].

The neutral lipid DAG is produced from the dephosphorylation of PA by PA

phosphatase, which can then be converted to triglycerides using the same DGAT

enzyme as described in the MGAT mediated synthesis of TAG [12].

Once in the liver, triglycerides synthesized either _de novo_ or recycled from

dietary sources, are used in the in the formation of very low density lipoproteins

(VLDL). This apolipoprotein is used by various tissues as a lipid source that includes

cholesterol, fatty acids, and triglycerides. Acquisition of additional apo-CI, II, III and

E apolipoproteins matures the VLDL. VLDL lipid breakdown converts the VLDL to

intermediate density lipoproteins (IDL). From this point, IDL can either be absorbed

and degraded by the liver or further catabolized into low density lipoproteins (LDL), which differ from VLDL in that they have lost apo-E, have a high cholesterol content instead of the previous high triglyceride content, and express apo B-100, which is required for ligand mediated endocytosis. LDL enters cells by binding to the LDL receptor, a glycoprotein that can be selectively expressed on target cells or by the liver. Endosomal uptake followed by merging with lysosomes allows for the recycling of the receptors and the degradation of cargo lipids into principal constituents [19].

High density lipoproteins (HDL) are responsible for transporting surplus lipids from cells to the liver, a process termed "reverse cholesterol transport" [12, 20]. It does this by scavenging cholesterol from cells through the transfer of cholesterol esters, competing for ligand binding sites to prevent internalization of cholesterol from LDL, through direct lipid trafficking to endocrine glands for steroid or hormone synthesis, and by transporting lipid to the liver for elimination and/or continued recycling [19].

Exogenous Pathway

Endogenous Pathway

Dietary fat

(1)

(5)

Bile acids and cholesterol

Nonhepatic cells

(10)

LDL (Apo B-100)

Liver

Intestine

(4)

(6)

(8)

(9) LPL HL

Chylomicron remnants (Apo B-48, E)

VLDL (Apo B-100, C, E)

IDL (Apo B-100, E)

Chylomicrons (Apo B-48, A,C, E)

(3)

(7)

(2) Apo C, E

Lipoprotein lipase

Apo C, E (CETP)

Lipoprotein lipase

HDL

FFA

HDL

FFA

Muscle Adipose tissue

Muscle Adipose tissue
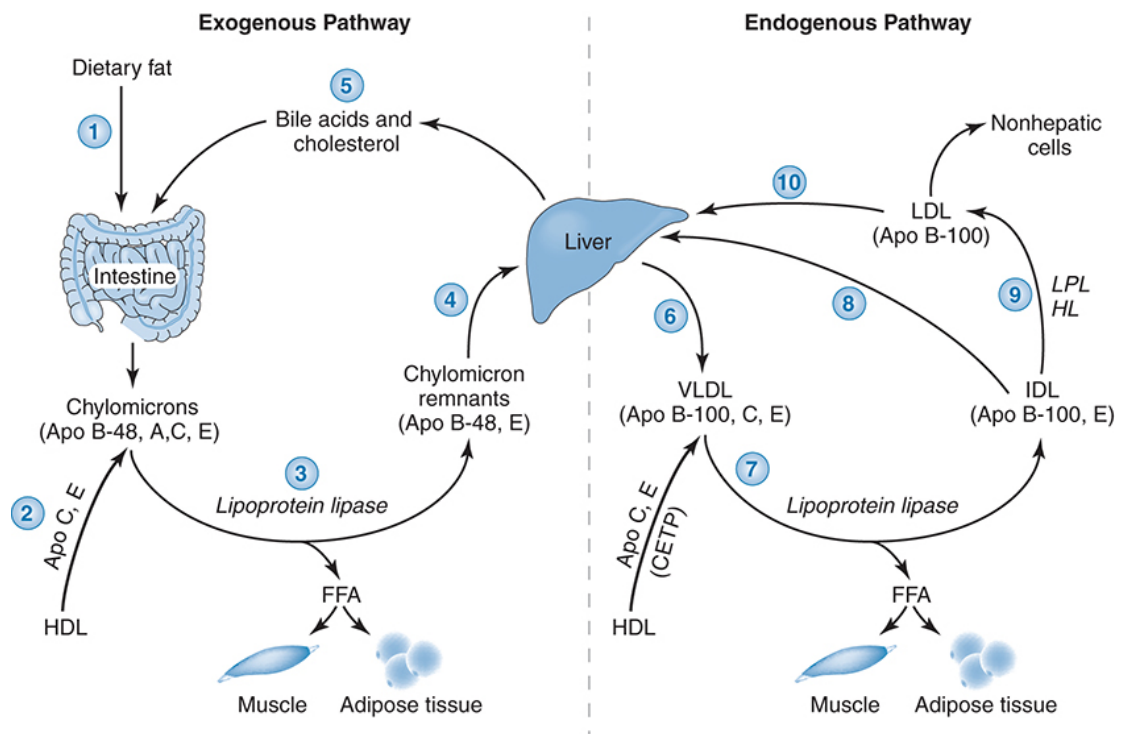
Figure 2. Exogenous and endogenous pathways. (Left) Exogenous (Intestines) pathway (1.) involves the intake of dietary fats that are absorbed and repackaged as apoB containing chylomicrons, rich in triglycerides. (2.) Chylomicrons circulate in the lymph and are further modified with additional apoE and C from HDL. (3.) ApoC promotes chylomicron-lipoprotein lipase (LPL) interactions at target cell allowing the hydrolysis of triglycerides to free fatty acids to be stored in adipose or used by muscles. (4.) ApoE mediates the removal of remnant chylomicrons. (5.) resulting cholesterol at the liver has several fates, one of which is hydroxylation into bile acid. (Right) Endogenous (Liver) pathway (6.) ApoB-100 containing VLDL particles are formed by packaging high levels of triglycerides and some cholesterol. (7.) VLDL are modified with addition of cholesteryl esters, apoC and E from HDL. VLDL catabolized by LPL for lipid transport at target cells. (8.) Approximately half VLDL remnants (IDL) are taken up by the liver and (9.) remaining IDL generate LDL by removal of triglycerides, apoE, and C. (10.) ApoB-100 and E permit LDL receptor mediated endocytosis at the peripheral cell or liver to remove LDL from circulation. [19].

1.3.3. *Mechanisms of Regulation*

To prevent toxicity as a result of over accumulation of lipids, several mechanisms are in place to detect levels present and moderate the biosynthetic pathways that lead to its production. Expression of numerous transcription factors including the sterol regulatory element binding protein (SREBP), carbohydrate response element binding protein (ChREBP), liver X receptor α, and peroxisome proliferator-activated receptor-γ regulate lipid gene transcription and lipid metabolism [21,22, 23]. Increases in the intake of dietary lipids such as cholesterol will activate or inhibit these pathways in order to maintain normal lipid homeostasis.

There are three isoforms of the transcription factors SREBPs (SREBP1-a, SREBP1-c, SREBP2) that are kept as inactive precursors. SREBP is normally found in the ER bound to two proteins, SREBP cleavage-activating protein (SCAP) and Insulin induced gene 1 (INSIG-1) [24]. Loss of cellular cholesterol causes INSIG1 to disassociate, freeing the remaining SREBP-SCAP complex to travel to the Golgi where SREBP is further cleaved by SCAP activated site 1 and 2 proteases (S1P, S2P). The final cleavage product of SREBP is a soluble active transcription factor that enters the nucleus to bind to the sterol regulatory element (SRE) where it activates the transcription of different genes including *LDLR* and *HMGCR* (HMG-CoA reductase) [21]. (Figure 3). This ultimately leads to increases in the production of cholesterol. Interestingly, in response to high levels of cholesterol, HMG-CoA becomes inhibited through phosphorylation or increased proteasome degradation. [21, 24].
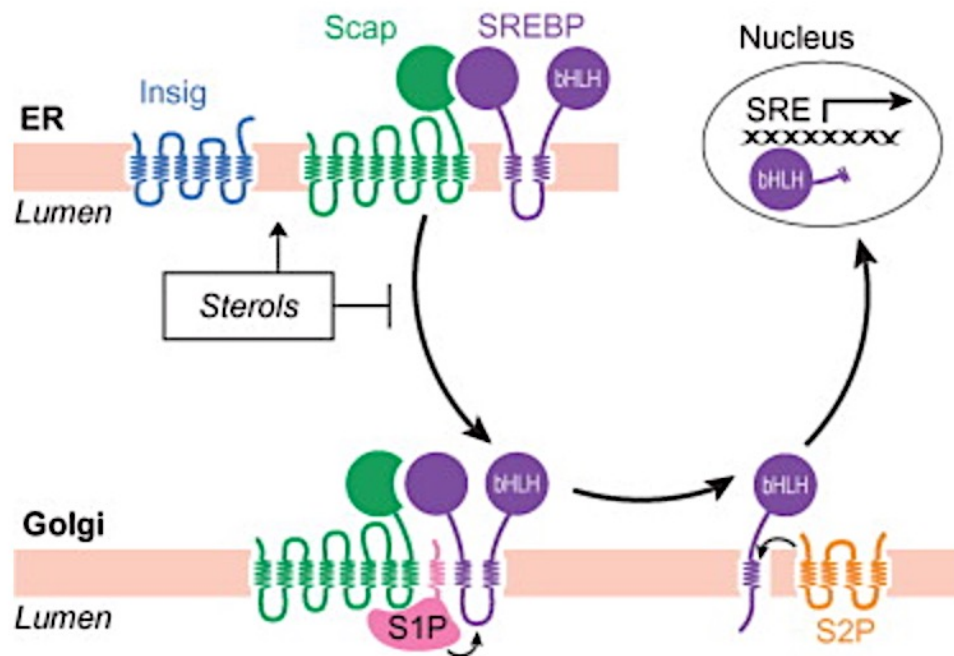
Figure 3. Regulation by SREBP. In the absence of sterols such as cholesterol,

INSIG dissociates from the complex, allowing SCAP to escort from the ER to the

Golgi where proteases S1P and S2P sequentially cleave SREBP thereby releasing the

NH2-terminal transcription factor domain. This travels to the nucleus where

transcriptional activation of genes lead to increased cholesterol synthesis and uptake.

In the abundance of cellular sterols, this mechanism is inhibited by tight binding to

SCAP(SREBP) to INSIG1, the ER retention protein. [25].

1.4. Phospholipid Membrane Composition and Asymmetry

To consider the phospholipid bilayer as simply a rigid structure that acts as a barrier, significantly diminishes its importance in the number of processes affected by its disruption. The lipid bilayer is composed of two layers of lipid molecules whose amphiphilic nature directs the hydrophilic head groups of phospholipids outwards while positioning the hydrophobic tails inwards. The result is the creation of three independent areas that are selectively isolated from each other, the extracellular side, the transmembrane region, and the intracellular side [26]. This is not only a means of separating the outside of a cell from the inside, but also a means of creating isolated subcellular compartments, with each having specific environmental conditions. Depending on the abundance of membrane bound proteins and cholesterol, the lipid membrane itself is approximately 40 Å and capable of selectively inhibiting the transfer of units that are as small as ions [27]. The concentration of ligands, embedded proteins, and phospholipids regulate the activity of specific regions of the membrane [20]. Portions of specific phospholipids, such as the head groups, can serve as signaling molecules by either altering the regions charge, interacting directly with other molecules, forming vesicles, or by functioning as docking sites for the recruitment of multicomponent complexes. The membrane must be able to adapt to the needs of the cell by altering size, restricting passage, modifying electro-chemical gradients or by fluctuating its phase state [27].

As previously described, the particular attributes of a phospholipid are largely dictated by the nature of its head group. These attributes are responsible for the specificity of each lipid for various interactions [9, 10]. Phospholipids can be divided into major and minor species. The major groups of phospholipids include PC, PE, and PS, while the minor groups cover CL, PG, PI and the PIPs. Although PA plays a major role in fat and phospholipid synthesis, as it is a precursor in the production of the majority of other phospholipids and metabolites, it is considered a minor lipid species, as its abundance is maintained at a lower concentration due to its rapid turnover [16].

The *de novo* synthesis of PA can be accomplished using the previously described glycerol 3-phosphate pathway or by using the dihydroxyacetone phosphate pathway. The resulting product is then acted on by additional enzymes in order to produce other phospholipids (Figure 4). Once a phospholipid is assembled its conformation is not final; based on the needs of the cell and the catalytic environment, lipid remodeling can occur to either alter the phospholipid or break it down into its primary components to be used in a metabolic pathway [26]. PA can be hydrolyzed into diacylglycerol by phosphatidate phosphatase. Diacylglycerol can either be utilized in the production of TAG or can be carried through the Kennedy pathway to produce PC or PE [28]. Action of cytidine triphosphate on PA can produce cytidine diphosphate diacylglycerol (CDP-DAG) which is required for the productions of PG, PI, and PS depending on locations within the ER or mitochondria

[28]. Production of PG directly results in production of CL and phosphorylation modification of PI produces the PIPs. Several parallel pathways exist for phospholipid formation with heavy overlap existing from the shared use of common intermediates.
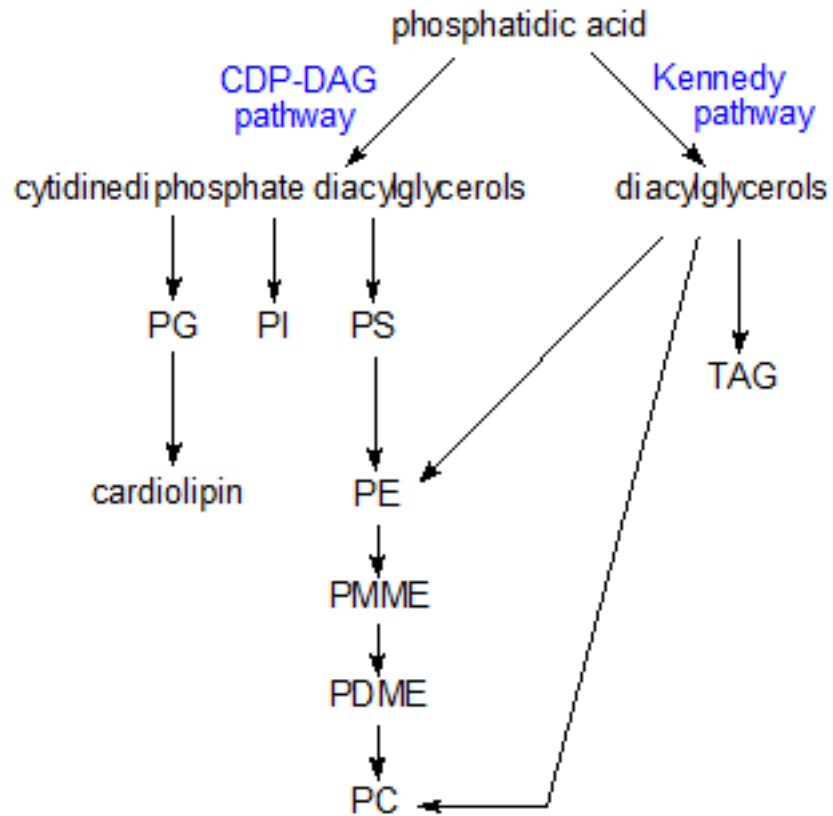
Figure 4. Phosphatidic acid derived phospholipid synthesis. Produced by the glycerol 3-phosphate pathway or the dihydroxyacetone phosphate pathway, once phosphatidic acid is formed, other phospholipids can be generated by the cytidine diphosphate diacylglycerol pathway yielding PG, CL, PI, PS, PE, phosphatidyl-N-monomethylethanolamine (PMME), phosphatidyl-N,N-dimethylethanolamine (PDME) and PC or the Kennedy pathway which produces triglycerides (TAG), PE, or PC [16].

1.4.2. *Lipid Membrane Asymmetry*

The amphipathic nature of phospholipids enables for spontaneous assembly of structures in aqueous environments. In regard to the lipid bilayer, the immediate assemblage is for the hydrophobic acyl chains to avoid interaction to water while the polar heads remain exposed [29, 30, 31]. The conformation and resident localization, however is not strictly dictated by physicochemical properties alone. The varied localization in phospholipid distribution is not caused by asymmetry in the production or hydrolysis of phospholipids, but rather is an intended manifestation [31]. There is a proportion of metabolic energy expenditure associated with maintaining the localization and concentration of specific lipids. This is an indication that there are complex mechanisms in place to properly organize the components of membranes.

1.4.3. *Location and Distribution of Phospholipids*

In most eukaryotic cells, phosphatidylcholine is the most abundant phospholipid and is readily found along with sphingomyelin in the outer leaflet of plasma membranes [26]. It forms the "bulk" of lipid membranes and is suited to do so with its neutral charge and kinked, unsaturated acyl tails that impart fluidity to the structure without inducing curvature [16]. Phospholipids with terminal primary amino groups, such as PE and PS, are located in the cytoplasm facing inner leaflet. PE is the second most abundant phospholipid, accounting for 20% of liver phospholipids. PE on its own is unable to form bilayers, but rather forms hexagonal phases [16, 26]. It is able to contribute to lipid bilayers only in the presence of other phospholipids and in doing so, is able to stabilize the conformations of these

phospholipids by applying a lateral compression force that helps to control the curvature of the membrane [16]. PS, an anionic phospholipid with three ionizable locations, contributes to signaling in both intracellular and intercellular mechanisms. It can interact with lipid binding proteins or enzymes directly or promote membrane interactions by causing an accumulation of a negative surface charge; this acts as a nucleation site for polycationic proteins to bind [16]. Altering its location enzymatically to the outer leaflet of plasma membranes promotes macrophage intervention in pro-apoptotic mechanisms; a cell death mechanism which can be detected through the PS specific binding by Annexin V [33]. Contributing to this charge status is phosphatidylinositol, located within the inner leaflet, which is acted upon by kinases responsible for the PI phosphorylation, giving rise to the seven members of the phosphoinositide (PIPs) family [26]. While these phospholipids may provide structurally to membrane integrity, they are also responsible for significant portions of several signaling pathways that contribute to cell growth, differentiation, protein trafficking, membrane docking, and vesicle formation. The location of each of the PIPs is thought to function as a location specific signature [16, 34].

Not only is there asymmetry between the two monolayers of a lipid membrane, there is also discrimination in the phospholipid make up of different organelles (Figure 5). The mitochondrial outer membrane, inner membrane, and cristae structures functions are dependent on their phospholipid composition. Some phospholipids such as PG and CL are predominately located in this organelle and can be directly synthesized there, while other phospholipids and/or their derivatives are synthesized at the endoplasmic reticulum and are transported to the mitochondria.

28

The outer mitochondrial membrane (OMM) is predominately PC (54%) PE (29%), and PI (14%) with trace amounts of PS, PG, CL, and PA, however the inner mitochondrial membrane (IMM) has CL as 20% of its lipid composition [35]. The relatively low concentration of PG is conserved due to its conversion to CL by cardiolipin synthase within the IMM. Structurally, CL is unique in that is resembles a dimer of two PG molecules. The structure and charge of PG allow for it to interact and activate mitochondrial proteins, including enzymes involved in oxidative phosphorylation as well as function as a cofactor for OMM to IMM cholesterol translocation [35].

Collectively, the asymmetric distribution of phospholipids is required for maintaining the proper structure and function of lipid bilayers as well as for the functioning of the cellular membrane-bound proteins [34]. It is required for the conversion of signals from extracellular sources in order to propagate intracellular signaling. To sustain this asymmetry, several types of proteins including phospholipid scramblases, phospholipid translocases, and ATP-binding cassette (ABC) transporters, work to regulate the assembling and movement of lipids across membranes [36].
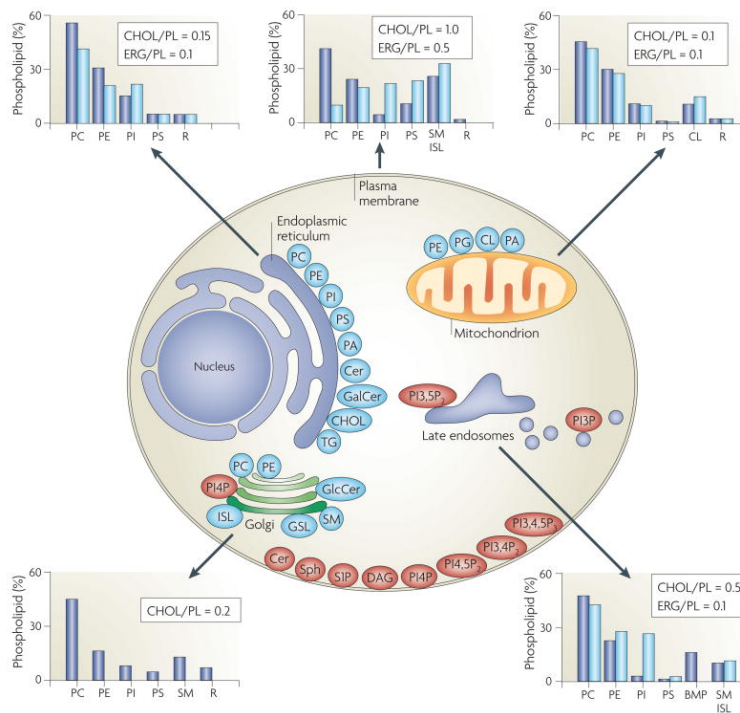
Figure 5. Organelle specific synthesis and residency of phospholipids. Bar graphs on the perimeter express the phospholipid composition as a percentage of total phospholipid at each cell location in in mammals (blue) and yeast (light blue). The molar ratio of cholesterol (CHOL in mammals) and ergosterol (ERG in yeast) to phospholipid is also included as a measure of sterol content. The center portion of the figure depicting a cell represents the primary synthesis locations for each phospholipid (blue circles) and signal recognition phospholipid (red circles). The endoplasmic reticulum (ER) is the site of production for phosphatidylcholine (PC), phosphatidylethanolamine (PE), phosphatidylinositol (PI), phosphatidylserine (PS) and phosphatidic acid (PA), Cer, galactosylceramide (GalCer), cholesterol/ergosterol. Almost half of the total amount of phospholipids of the mitochondria are synthesized there. The predominate ones are PE, PA, PG, CL. Sphingomyelin (SM), PC, complex glycosphingolipids (GSLs) and yeast inositol sphingolipid (ISL) are synthesized at the Golgi.

PI(3,5)P$_2$, phosphatidylinositol-(3,5)-bisphosphate; PI(4,5)P$_2$, phosphatidylinositol-(4,5)-bisphosphate; PI(3,4,5)P3, phosphatidylinositol-(3,4,5)-trisphosphate; PI4P, phosphatidylinositol- 4-phosphate; R, remaining lipids; S1P, sphingosine-1-phosphate. [26].

1.4.4. *The Methods of Lipid Transport and Movement*

There are multiple directions of movement and transfer for lipids within the
cell. However, the ability to transfer lipids from one organelle to another is
dependent on the physiochemical properties of the lipid, the proteins involved in the
transfer, and the organization of the accepting membrane (Figure 6). At the most
basic, some phospholipids such as PC with its small head group and no charge, can
flip from one side of a membrane to the other and diffuse laterally on either side. This
can be both energy independent through movement of generated gradients or
dependent through ATP driven enzymes [37]. Increases in the charge status of a head
group results in more difficulty in lipid movement flipping, whereas alterations to the
tails that increase its hydrophobic nature, produce a lipid that can translocate easier
[37]. Lipids can also be carried by isolated portions of lipid bilayers including
endosomes or vesicles. Vesicle formation is a common mode of transport between the
ER, Golgi, and plasma membrane, which requires portions of membranes to bubble
out into curved structures that pinch off, maintaining the bilayer and loaded contents
[37]. This process may require receptor and docking proteins such as soluble NSF
attachment protein receptor (SNARE), and the process itself can be calcium
dependent. Contact site formation is thought to be another method by which
organelles can contribute to the movement of lipids. The plasma membrane
associated membranes (PAM) and mitochondrial associated membranes (MAM) are
two examples of this [38]. The first of which is contact (<30nm distance) between the
ER and the PM, while the second is ER contact with the mitochondria [39, 40].

These structures not only allow for transfer of lipids that may otherwise be restricted to their sites of synthesis, but also bring binding proteins and enzymes within proximity to possible substrates.
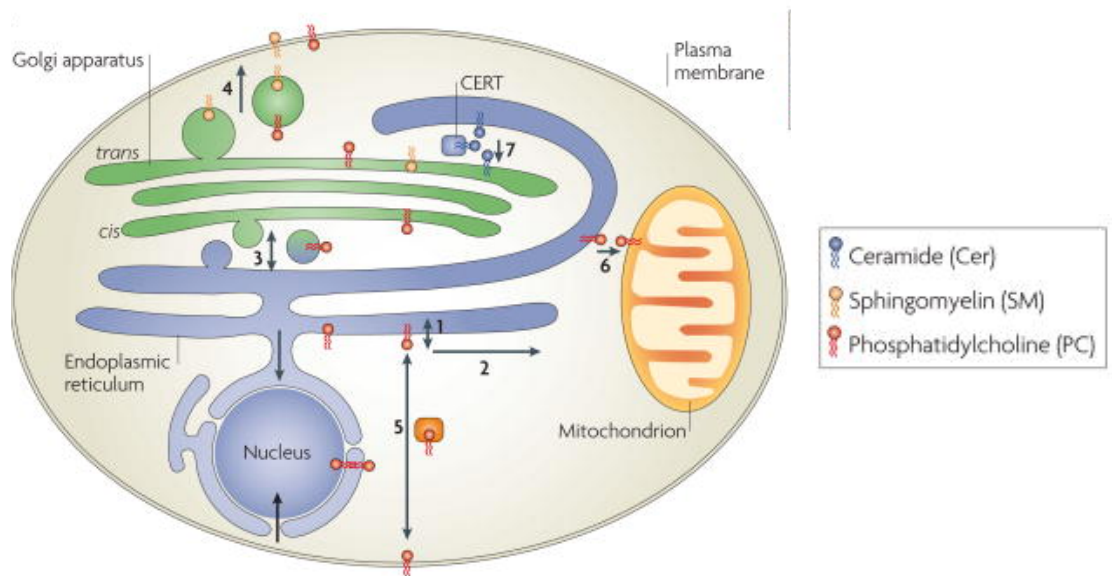
Figure 6. Mechanisms of lipid transport. (1) PC created in the cytosolic ER surface can freely flip across the ER membrane. (2) It can also laterally diffuse in any membrane. (3) Lipids can travel through the formation of vesicles traveling to the Golgi or the (4) plasma membrane. Transporter proteins have several modes of trafficking. (5) They can bind to lipids and freely travel through the cytosol from one surface to another. They can also transport across contact sites that are already stabilized or they themselves can bind to each membrane and "tether" them together while also shuttling their lipid cargo across. Contact sites can form (6) between the mitochondria/ER (MAM) or between the (7) trans- Golgi/ER. [26].

Non-vesicular lipid transport is possible through lipid transporter proteins such as Osh4, a yeast homolog of the oxysterol binding proteins [41, 42]. This mechanism relies on a transporter protein that can move in between initial membrane components and destination components. When a protein binds to lipid at the initial membrane, conformational changes allow for the cargo lipid-protein complex to travel. This complex diffuses to the site of docking where the destination membrane contains ligands that compete for binding with the protein, which effectively releases the lipid the protein was transporting, allowing it to bind to a new substrate. Interestingly, the affinity that the transporter has for binding to the initial cargo is decreased, allowing it to return to its initial location to repeat this process [26].

In the case of Osh4, it was previously known to bind sterols; however, later studies revealed that it was able to also transport them against gradients to produce lipid gradients [41, 42]. Osh4 uses a counter exchange mechanism to bind sterols in the ER, transport them against a concentration gradient to their destination at the trans Golgi network or the plasma membrane, where interaction of PI(4)P with Osh4 causes the protein to release the sterol and return to the ER [43]. Here, PI(4)P-phosphatases can hydrolyze PI(4)P to PI, preventing accumulation and further driving the cycle. Similarly, oxysterol-binding proteins (OSBP) and other transporters like CERT can promote tethering of two membranes between the Golgi and ER that are brought into closer proximity and whose components also engage in counter exchange [42].

1.5. ACAT (Acyl-coenzyme-A: cholesterol O-acyl transferase) Related Enzyme Required for Viability-1 (Arv1)

In eukaryotic cells, sterols, specifically cholesterol, are instrumental in a plethora of biological processes, each fulfilling independent functions. Not only are sterols required for the structures of cell membranes, which are almost one third comprised of cholesterol, they are also essential to modify the fluid dynamics of membranes by changing the packing of lipids through interactions with phospholipids [9, 10]. Cholesterol is required for endocytic mechanisms involved in intracellular transport, as well as cell signaling by inducing or amplifying communications through lipid raft formation. Biochemically, cholesterol also serves as a precursor from which other metabolic derivatives can be produced.

Even with the many roles for cholesterol within the cell, over accumulation of this lipid in its un-esterified form produces undesirable stress that must be reduced if the cell is to avoid apoptosis [44]. To prevent apoptosis, free sterol is esterified by the actions of acyl-coenzyme A: cholesterol O-acyltransferase (ACAT) enzymes, whose expression level are dependent on substrate concentration [45]. In response to elevated sterol, transcriptional activation of sterol regulatory element-binding proteins (SREBPs) result in the decrease of LDL uptake through the LDL receptor, and an inhibition of biosynthesis pathways for production of sterols and fatty acids.

In 2000, the Sturley laboratory conducted a screen looking for genes required for viability in the absence of ACAT related enzymes, ARE1 and ARE2, which are proteins required for sterol esterification. The results of which led to the first

identification of the gene *ARV1* (ARE2 required for viability) in *Saccharomyces cervisiae* and in humans [46]. Mutations that disrupted *ARV1* expression resulted in an increased sensitivity to the sterol targeting antibiotic nystatin, decreased uptake of sterols, 50% increase in the accumulation of free sterols, and a 75% increase in steryl esters. The mutants also demonstrated alterations in the distributions of these lipids, in that the ER and vacuolar membranes had large increases in their concentrations at the plasma membranes. Based on these results, it was hypothesized that Arv1 functions to traffic or transport sterols to the plasma membrane, thereby mediating their distribution in order to prevent toxicity [46].

Human Arv1 is a 271 residue (yeast Arv1is 321residues) transmembrane protein that has a putative zinc binding motif and a conserved region designated as the Arv1 homology domain (AHD). The zinc binding motif was proposed to facilitate transport across membranes, recruit signal molecules, and bind to charged lipid species [47, 48]. It has been shown that zinc-binding proteins can bind sterols and play a role in sterol maintenance, in that this motif increases luminal zinc resulting in increased cholesterol uptake of endosomes composed of phospholipids that are largely of a negative charge [49].

Having previously established a correlation in the regulation of sterol biosynthesis to sphingolipid biosynthesis, work completed by our laboratory addressed the influence of altered yeast Arv1 on the rate of synthesis and steady state levels of complex sphingolipids, ceramides, and phospholipids [50, 51]. The results indicated that not only did loss of Arv1 produce defects in sterol trafficking, but also created accumulation of ceramides and defects in both the synthesis and metabolism

35

of sphingolipids. Whether the defects of one lipid pathway were causative of the other was not established. We were also the first to demonstrate defects in the production and clearance of certain phospholipids. Altering the expression of Arv1 in cells demonstrated significant decreases in the production and steady state of phosphatidylethanolamine and phosphatidylserine while generating increases in the synthesis of phosphatidylglycerol, with overall increased accumulation of phosphatidylcholine and phosphatidylglycerol levels [51]. These changes were thought to be caused by defects in phosphatidylserine synthase (PSS) activity by long chain sphingoid bases. The inhibition of PSS could lead to decreased production of phosphatidylethanolamine and with the decreases in PS and sphingolipid synthesis that would also occur, phosphatidylglycerol production and accumulation could be favored by the increased production of cytidine 5'-diphospho-1,2-diacyl-sn-glycerol: myo-inositol, 3-phosphatidyltransferase (CDP-DG), a phosphatidylglycerol precursor [51].

In humans, liver specific cholesterol localized to the ER can either be transported to the plasma membrane of cells, utilized in the production of VLDL particles, esterified, or hydroxylated to produce bile acids [14]. The Sturley and Rader laboratories were the first to target Arv1 in mice [55]. In these studies, hArv1 was targeted by repeated injections of antisense oligonucleotide (ASO) for tissue specific knockdown of Arv1 in liver, adipose. They saw increases in plasma LDL cholesterol from decreased LDLR expression, and increased synthesis of bile acids with an altered hydrophobic index. Increased availability of cholesterol provided high enough substrate to increase bile acid production. The increase in bile acid caused the

activation of the bile acid-sensing nuclear Farnesoid X receptor (FXR) [55]. Liver

knockdown of Arv1produced an over accumulation of intracellular cholesterol caused

by deficiency in ER cholesterol removal, as well as SREBP-2 suppression. Based on

the data, it was hypothesized that the function of Arv1 was to facilitate the transfer of

cholesterol from the ER to the plasma membrane through either vesicle formation or

non-vesicle methods. When the protein's expression is decreased, this cholesterol

shuttling becomes inefficient, creating the aforementioned consequences. [14, 52, 55].

As previously stated, the regulation of sterols, specifically cholesterol, is

strictly maintained through several mechanisms that influence its synthesis,

esterification, and transport into or out of cells [46]. A critical threshold of 5% molar

basis of sterol content is tolerated in the ER. When levels surpass this threshold,

activation of these pathways is mandatory to prevent cytotoxicity induced cell death

[53]. In 2011, the Sturley laboratory described activation of an ER stress response

pathway thought to be triggered by Arv1 deletion. Within the lumen of the ER,

buildup of misfolded or unfolded proteins activates a signal cascade initiated by a

membrane stress transducer, a path known as the unfolded protein response (UPR)

[54]. Induction of the UPR activates the inositol-requiring enzyme-1 (IRE1), the

activating transcription factor-6 (ATF6), and the protein kinase RNA (PKR)-like ER

kinase (PERK). In some circumstances, the C/EBP homologous protein (CHOP)

transcription factor becomes activated and induces cell death. It has been shown that

deleting Arv1 in primary macrophages causes an increase in transcript levels of ATF4

and CHOP, indicating activation of the pro-apoptotic, ATF6 dependent arm of the

UPR. In a second yeast screen looking for mutants hypersensitive to fatty acid

accumulation, Arv1 activation was found to be required. It was suggested that Arv1 is required for fatty acid detoxification [55].

Yeast topology studies uncovered the orientation of full length Arv1 within the ER membrane (Figure 7). The protein is anchored to the membrane by 3 transmembrane regions. The N-terminal region faces out into the cytoplasm with residues 3-63 comprising the AHD in yeast and 34-94 in humans. The C-terminus is luminal facing and there exists a ER luminal loop, thought to function in protein-protein interactions, and it has been shown to be necessary to suppress defects associated with Arv1Δ phenotypes [56].
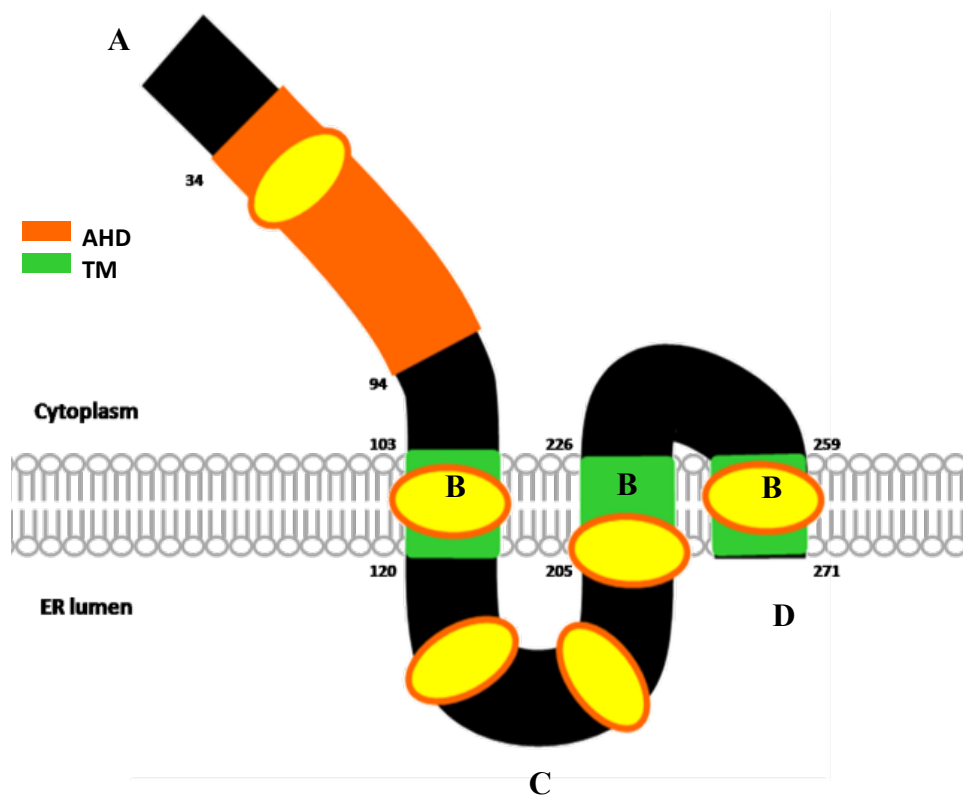
Figure 7. Topology and domains of human Arv1. Acyl-Coenzyme-A: cholesterol O-Acyl Transferase related enzyme required for viability-1 (ARV1) is putative a lipid transporter protein. In humans, it is 271 amino acids long, composed of a [A] 103 amino acid N-terminus facing into the cytoplasm, [B1-3] three transmembrane regions anchoring it into the ER membrane, [C] a lumen loop, and [D] C-terminus directed in the lumen of the ER. Of the initial 103 N-terminal, there exists a highly-conserved sequence known as the Arv1 homology domain (AHD in orange), which contains a zinc binding domain and is suspected to be responsible for the majority of the protein's actions. In yellow are six cholesterol recognition/interaction amino acid consensus sequences (CRAC).

(Model from Villasmil et al 2011, adapted by Dr. Hsing-yin Liu, 2015.)

The Menon laboratory has published work that has suggested that Arv1 does not transport lipids but is required for lipid organelle homeostasis [57]. They first showed that while Arv1Δ cells did have increased sterol, steryl ester, and phospholipid content, their ratio of sterol to phospholipid was comparable to wild type. Fractionation profiles of Arv1Δ and wild type cells following surcrose gradient centrifugation indicated the majority (70%) of ergosterol was located in the PM of both cell types and that an increased fraction of 22,33-dihydroergosterol (DHE) was identified in intracellular fractions [57]. Transport between PM and ER appeared normal in both cell types. DHE was shown to be esterified at the same rate, but took longer to appear in lipid droplets in mutant cells compared to wild type. The morphology of these lipid droplets was also drastically different. Lack of Arv1 resulted in defects in cortical and cytoplasmic ER, and in changes in the sterol availability and organization of the trans-bilayer of the plasma membrane. Certain transmembrane domains of proteins were altered by defects indicating that Arv1 might contribute to the regulation of membrane insertion for tail-anchored proteins necessary in maintaining homeostasis of the membrane [57].

These conflicting results convey a need for further work focusing on establishing the true role of Arv1 in lipid transport and trafficking. The work done by Georgiev et al. was restricted to yeast. New data generated from mouse studies performed in our laboratory has shed some light the physiological role of Arv1 and its role in the progression of several metabolic disorders.

In 2015, we generated a whole body Arv1 knockout mouse and used this model to see what were the consequences of deleting Arv1 on lipid metabolism. The

Rader laboratories were pursuing the same studies and were able to publish their work prior to us submitting a manuscript. Overall, the studies came to the same conclusion. Several metabolic parameters were analyzed including blood lipid and lipoprotein levels, changes in body weight, body composition, glucose tolerance, insulin sensitivity, and energy expenditure [1]. In the Lagor et al. study, Arv1 KO mice fed normal chow had less white adipose tissue (WAT) compared to their wild type counterparts. The KO had significant decreases in lean and fat masses. The cellular composition of various depots revealed differences in adipose morphology including smaller adipocytes. These animals consumed more food, but also demonstrated increased activity and energy expenditure. It was suspected that knock out of Arv1 decreased the storage of triglycerides in adipose leading to increased fatty acid clearance [1]. Arv1 knockout mice produced less HDL cholesterol, were leaner with decreased WAT, and demonstrated normal organ morphology with normal TG content in mice on a normal chow diet. Female knockout mice were found to be infertile and both sexes were prone to spontaneous death as well as death induced by overnight fasting. Interestingly, these mouse results conflicted with their ASO mediated tissue specific knockdown of Arv1 studies, alluding to possible off target effects of ASO treatment [1].

As stated earlier, during the time of the Rader KO study, we conducted a study to look at how loss of Arv1 affected various metabolic parameters during a challenge with a western style, high fat, high carbohydrate diet. The ultimate purpose of which was to characterize the influence of Arv1 on the progression and severity of

diet induced symptoms observed in nonalcoholic fatty liver disease and metabolic syndrome.

A Cre-Lox system was used to generate the knockout mouse, targeting exons 5 and 6 (Rader targeted exons 2 and 3). Mice were fed normal chow until 12 weeks of age to establish a baseline and then fed the high fat diet or were left on normal chow. Over the course of 15 weeks, wild type mice on HFD doubled in size while KO maintained a normal lean phenotype. Consistent with Rader's findings, KO mice consumed more food, both on normal and high fat chow (4 times more) but did not increase in size significantly. An increase in metabolic rate was observed in KO animals, which became more apparent when switched to the HFD. Lower blood cholesterol and reduced HDL levels were shown regardless of diet, while decreased triglyceride levels were seen in response to the HFD. WT mice had increases in all three parameters in response to HFD. Insulin and oral glucose tolerance tests performed showed WT mice had elevated blood glucose levels that remained high in response to HFD, indicating glucose intolerance, where KO mice were more sensitive to glucose and demonstrated increased sensitivity to insulin. When the livers of both animals were assessed, WT mice on the HFD had enlarged livers with microsteatosis and macrosteatosis, hepatocyte ballooning, and Malory bodies present with increased inflammation, while KO animal livers were healthy with no abnormalities. There were increases in cholesterol, triglycerides, LDL, and HDL in the livers of HFD fed WT mice along with the altered morphologies that mimicked those seen for NAFLD/NASH. Arv1 KO mice had reduced levels of these lipids compared to WT on the same diet and excreted higher levels of fecal cholesterol, and they activated

lipid and insulin-signaling pathways including increases in FXR and PPARγ expression. Collectively the results of the Nickels HFD study with Arv1 KO mice produced strong evidence for the role and influence that the Arv1 protein has in relation to the initiation and progression of lipid related diseases (Figure 8).   In conclusion, the mouse model studies indicate that loss of Arv1 confers protection against obesity induced disorders.

A. **Lower body weight**
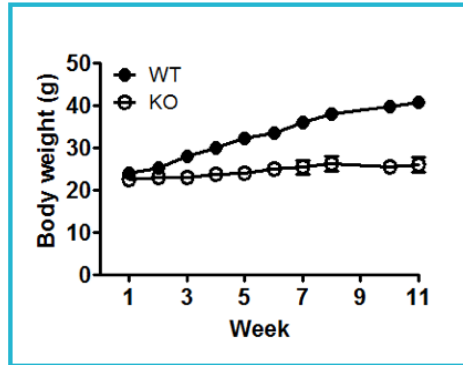
B. **Reduced blood lipid**
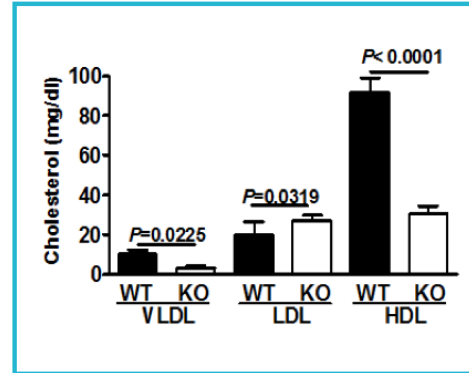
C. **Lower tissue fat**
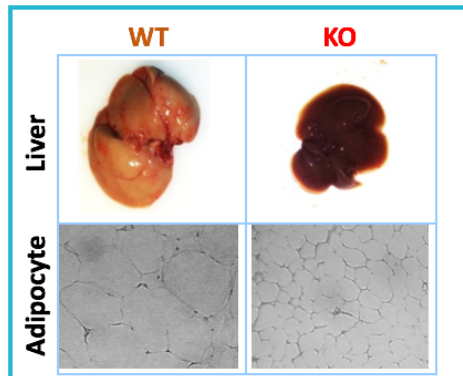
D. **Better glucose metabolism**
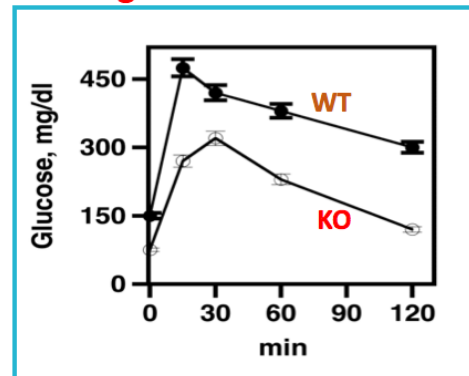
Figure 8. Arv1 KO mouse HFD study. The above represents data selected from the work done using the Nickels lab Arv1 whole body KO mouse generated with a Cre-Lox system for the excision of exons 5 and 6 or Arv1 coding. Wild type (WT) and knock out (KO) animals were kept of a high fat diet. Arv1 KO animal demonstrated [A.] a lower body weight that also had fewer deposits of fat, [B.] decreased circulation of cholesterol VLDL, LDL, and HDL than WT animals on the same diet. WT animals produced [C.] larger fatty livers with abnormalities while KO animal livers remained healthy. The KO animal also displayed [D.] better glucose metabolism and sensitivity to insulin (not shown).

(Gallo-Ebert et al., manuscript submitted)

2. Rationale

A clear association has been established linking obesity and the development of metabolic syndrome pathologies. Although there exists some controversy as to whether or not nonalcoholic fatty liver disease (NAFLD) belongs in the groupings of metabolic syndrome as a consequence of the disease or as a contributor of its progression, the manifestation of both is directly affected by the presence and degree of obesity [58]. Importantly, it has been shown that NAFLD can contribute and amplify the severity of metabolic disorders such as MetS by promoting liver dyslipidemia and inflammation, which lead to development of nonalcoholic steatohepatitis (NASH), hepatocellular carcinoma, and cardiovascular disease [58, 59].

NAFLD is the most prominent form of chronic liver disease and is defined as the over accumulation of hepatocellular fats, predominately triglycerides, that is not the result of alcohol consumption. It is a disease that has several stages that it can progress through, however early stage intervention allows for reversal. It first begins at simple steatosis which can develop into steatohepatitis, cirrhosis, and possibly hepatocellular carcinoma. Approximately 70% of obese individuals develop fatty livers, but this can also present in non-obese (10-15%) individuals [60]. The earliest stage of simple steatosis is characterized as a fatty liver in the absence of further abnormalities such as inflammation or fibrosis. If detected as this stage, intervention therapy can reverse the fatty liver back to a healthy state; conversely, if left to progress, fibrosis and inflammatory factors, such as interleukin 6 (IL-6), tumor

necrosis factor-alpha (TNF-α), and C-reactive protein production move it to the steatohepatitis stage, the damage of which is irreversible [7, 60]. Of the 20% of NAFL that progresses to NASH, a subset can also develop into hepatocellular carcinoma. The stage transition is thought to be the product of multiple "hits" to the liver. The first "hit" is an insult to the liver induced or encouraged by additional MetS risk factors like insulin resistance that causes the steatosis that primes the liver for the subsequent hit, oxidative stress. This second hit results in inflammation, fibrosis, and necrosis symptoms of NASH and cirrhosis with further complications from possible involvement of adipokines and mitochondrial dysfunction [59, 60, 61].

NAFLD is difficult to detect in the earlier stages, where intervention has most success. The first indicators of liver related insult are elevated liver enzymes levels, but in order to be diagnosed as NAFLD, every other liver related condition must first be ruled out and an ultrasound performed. This does not give physicians indications of the exact degree of damage that is present. The gold standard for the detection of fibrosis are liver biopsies, but this is far from an ideal means of identification as results are not always a reliable assessment of how much damage is present in the whole organ. Effective therapies are not available at this point and the primary treatment is organ transplant when liver functions drop below threshold, leaving patients even more at risk for cancers associated with the lifelong use of immune system suppressors to avoid rejection [60]. The United States alone spends $103 billion dollars each year on NAFLD detection and treatment. Projected costs could rise to $1.005 trillion if the annual rate of increase of NAFLD parallels the prevalence of obesity in the United States [62].

It is clear that more treatment options must be developed and made available to curtail the increased growth of NAFLD populations in the United States and beyond. Developing a more sensitive and less invasive method for NAFLD detection would be ideal in that intervention at this point prevents permanent damage that occurs once NASH progression takes place. This would increase positive outcomes for patients and avoid the higher cost of care that results from the necessity of transplants and/or cancer therapies. Only with greater understanding of the mechanisms by which the body regulates the production, metabolism, and distribution of lipids can new therapies be established. The purpose of the research conducted in this study is to contribute to the growth of this knowledge in the areas of lipid trafficking and regulation, in order to contribute to the development of earlier detection and drug treatment options for those who suffer from NAFLD or MetS related diseases. Arv1 is suggested to be a lipid transporter protein whose deletion in mice was shown to be protective against NAFLD like symptomology when fed a high fat "western" diet. By resolving whether Arv1 is a lipid binding protein or transporter will not only help to understand the molecular mechanisms Arv1 uses to function, but will contribute to our understanding of the factors involved in the initiation and/or progression of MetS related diseases. This will open up the opportunity for the development of novel pharmacological therapeutics for the treatment of lipid-mediated disease states.

3. Materials and Methods

3.1. Inducible Recombinant Protein Expression and Synthesis

3.1.1. Plasmids and Bacterial Strains

Due to the low expression levels of endogenous Arv1, an inducible recombinant system for protein expression was utilized. The pET28b+ plasmid flanked with NdeI and EcoRI restriction sites was designed to code for the 98-amino acid long N-terminal portion of human Arv1 with the addition of a polyhistidine tag (Figure 9). Rather than using the full-length protein sequence containing multiple transmembrane regions, the N-terminal region containing the AHD believed to retain the majority of the protein's activity was selected for. Previous truncation studies conducted by Nickels lab on the N- terminal region indicated that inclusion of residues 1 through 98 would generate a more stable protein product than merely ending the sequence at the endpoint location of the AHD (N94). The N98 plasmid was obtained from current lab members (Dr. Christina Gallo-Ebert and Kinnari Modi) and functioned as a means of generating the N98 form of the protein, as well as served as a template from which protein variants could be produced using site directed mutagenesis.

3.1.2. Site Directed Mutagenesis and Plasmid Expression

Scanning through the hArv1 AHD protein sequence, (Figure 10) conserved residues were selected in regions associated with punitive binding sites for lipid interaction, glycosylation or based on charge of residue.
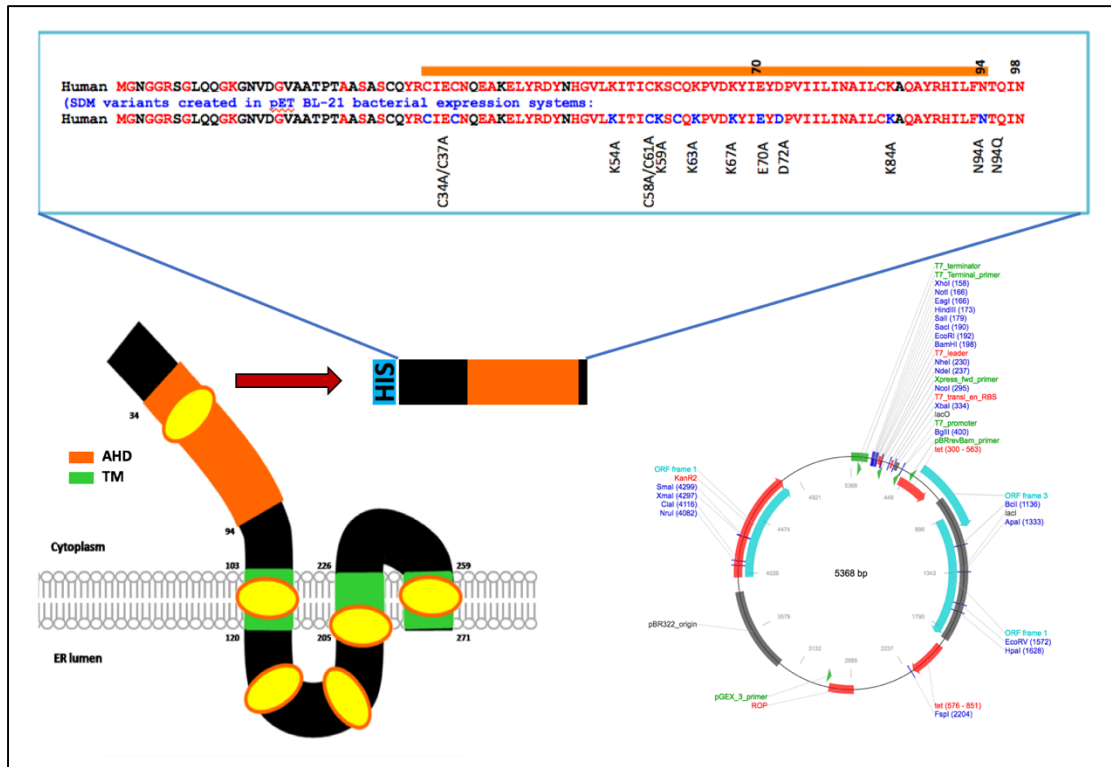
Figure 9. Designing plasmids for the inducible recombinant protein synthesis of hArv1 N98 WT and variants. (Bottom, Left) The topology of the full length Arv1 and the Arv1 homology domain (AHD) was identified as the location responsible for the majority of the protein's functions as it has zinc binding ribbon and cholesterol binding domains. (Top) The N98 protein product was designed to code for a stable form that included the entire AHD (in orange) with addition of a his-tag. The highly-conserved sequence is shown above with desired mutations that were made in blue. (Bottom, Right) Both the N98 WT and site directed mutagenesis variants were created off the pET28b+ plasmid flanked with NdeI and EcoRI restriction sites.
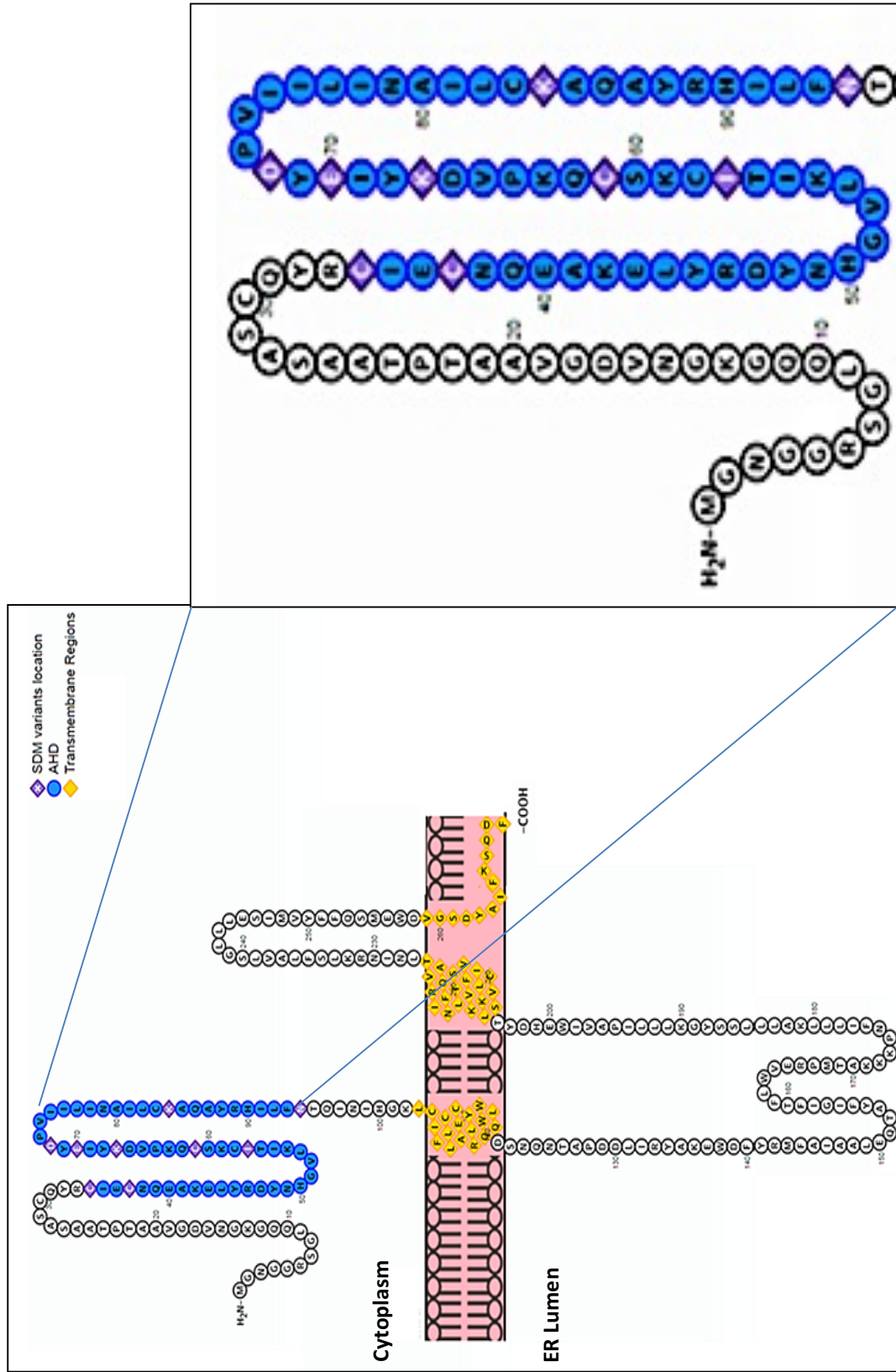
Figure 10. Amino acid sequence of hArv1 and selected residues for mutation. (Left) Schematic representation of hArv1 orientation in the ER membrane. Provided is the specific amino acid sequences for each region. The region of blue covers the AHD , with residues that were mutated, highlighted in purple. Trans membrane region residues are yellow. (Right) enlarged region of the AHD and altered residues. [63].

Forward and reverse primers for the desired mutations were designed and ordered through Integrated DNA Technologies or complete plasmids were obtained from the strain collections of Dr. Joseph Nickels. Primers were diluted to working stocks of 100pmol to be used with QuikChange™ Site-Directed Mutagenesis kit (catalog # #200518).

Table 1. Site directed mutagenesis primer sequences.

Variant Name	Primer Sequence	JNB Strain Number
K67A	F 5' CGAGAAACCTGTAGACGCATATATCGACTATGATC 3'	JNB2121
	R 5' GATCATAGTCGATATATGCGTCTACAGGTTTCTCG 3'	
E70A	F 5' TGTAGACAAATATATCGCG TATGATCCTGTTATCA 3'	JNB2120
	R 5' TGATAACAGGATCATACGCGATATATTTGTCTACA 3'	
D72A	F 5' CAAATATATCGAGTATGCTCCTGTTATCATCTTGA 3'	JNB 2119
	R 5' TCAAGATGATAACAGGAGCATACTCGATATATTTG 3'	
K84A	F 5' TAATGCTATATTGTGCGCAGCTCAGGCCTACAGAC 3'	JNB 2118
	R 5' GTCTGTAGGCCTGAGCTGCGCACAATATAGCATTA 3'	
N94A	F 5' CAGACATATTCTTTTCGCTACTCAAATAAATTAGG 3'	JNB2208
	R 5' CCTAATTTATTTGAGTAGCGAAAAGAATATGTCTG 3'	
N94Q	F 5' CAGACATATTCTTTTCCAGACTCAAATAAATTAGG 3'	JNB2209
	R 5' CCTAATTTATTTGAGTCTGGAAAAGAATATGTCTG 3'	
C34/37A	Obtained from JNB strain collection.	JNB2133
C57/61A	Obtained from JNB strain collection.	JNB1923

Polymerase chain reaction mixes were composed of 50ng of template DNA, 125ng of forward and reverse SDM designed primer, 5μl of 10X PCR buffer, 1 μl DNTPs, with molecular grade water used to bring the mix to a final volume of 50 μl. To this, 1 μl of the PfuTurbo Taq polymerase enzyme was added. The reactions were cycled on a table top MJ Research PTC-150 Minicycler as described in Table 2.

Table 2. PCR cycling conditions.

Cycle Step	Temperature	Time
Initial denature	95°C	00:30
Denature	95°C	00:30
Anneal	55°C	01:00
Extend	68°C	10:00
Repeats	25-40 times	

To digest the parental supercoiled dsDNA, 1 μl of DpnI restriction enzyme added directly to the PCR product and the total reaction was transferred to Eppendorf to be gently mixed. Reactions were spun in a microcentrifuge for 1 minute at low speed and incubated at 37°C for 1 hour.

3.1.3. Top10 Competent Cell Transformation

ThermoFisher one shot TOP10 chemically competent *E. coli* (catalog # C404006) were transformed using 1 μl of the DpnI digested PCR product. Cells were immediately put on ice for 30 minutes before heat shocking at 42°C for exactly 45 seconds. Following this, cells were kept on ice for 2 minutes, 500mL of SOC media was added, and shaken at 37°C for 1 hour. Cells were plated on 10cm Corning

Falcon polystyrene bacteriological plates (catalog# 351029) containing 10mL of solidified Luria broth (LB) agar made previously with a Kanamycin (KAN) concentrations of 50μg/mL. Plated cultures were grown overnight at 37°C. Single colonies were taken from each plate to inoculate 5mL liquid cultures in Kanamycin selection LB media of the same concentration. Cultures were shaken between 200-250rpm at 37°C for 12-24 hours.

3.1.4. Bacterial Plasmid DNA Isolation

Plasmid DNA was isolated using Qiagen Qiaprep Spin Miniprep Kit, (catalog # 27104) according to the manufactures' instructions. Alkaline conditions lyse the bacterial cells, the reaction is neutralized, and salt concentrations increased to promote binding of product to the silica membrane after the lysate and debris have been removed via multiple centrifugation step and washes. Plasmid DNA concentration was measured on a Nanodrop spectrophotometer (Thermo Fisher). The pedestal was first thoroughly cleaned with deionized water, before 2μl of sample was loaded and the arm closed, allowing the optical density to be measured at A260. Purified plasmids that failed produced A260/280 ratios around 1.8 were rejected for further assessments.

3.1.5. Plasmid DNA Sanger Sequencing

The DNA sequences of each plasmid were verified using Genewiz Sanger sequencing services. Each plasmid sample was diluted with nuclease free water to a concentration of 80ng/μl in 10μl and to this, the N98 forward primer was diluted to yield 5pmol in 5μl for a total primer amount of 25pmol. DNA sequences were aligned

using SeqBuilder and MegAlign programs to confirm the desired substitution
mutations were present in the plasmids.

3.1.6. BL21 Chemically Competent E. coli Transformation

ThermoFisher BL21 chemically competent E. coli cells (catalog# C6000-03)
were used for their capacity to highly express a desired protein product. With the
ability to selectively induce protein expression and a higher threshold for RNA/DNA
over accumulation, this strain reduced the toxicity of some recombinant proteins
while generating high output. BL21 cells were transformed in 1.5mL Eppendorfs
with 3µl of plasmid isolations that had confirmed sequences. Cells were placed on ice
for approximately 15 minutes before being relocated to a 42-42°C water bath for 2
minutes, followed by returning to ice for 2 minutes. To expand the cultures, 250µl of
recovery media was added and cells were incubated for 1 hour in a 37°C shaker set at
200-250rpm. Of this, 100µl was plated onto LB/KAN agar plates and grown
overnight at 37°C.

3.1.7. Bacterial Strain Collection, Freezing, and Culturing

Grown liquid cultures of transformed BL21 cells with confirmed sequences
were stored at -80°C as glycerol stocks in the bacterial strain collection of Dr. Joseph
Nickels. Volumes of 500-1000µl of grown cell cultures in LB/KAN media were
retained and mixed with 500µl of 30% glycerol (USB/Affymatrix) stocks that had
previously been aliquoted into cryotubes and autoclaved for 20 minutes before being
brought to room temperature for addition of cultures. Stocks were recorded with an

identifying serial number that was then logged into the strain collection database

which recorded all pertinent information to recover and utilize strains.

To recover stocks, LB/KAN plates were streaked using a sterile inoculation loop that

was scrapped along the inside of the still frozen cryotube. Plates were incubated

overnight at 37°C to allow colony growth. Plates were stored wrapped in parafilm

(catalog # # P7793-1EA) at 4°C for easier access to cultures.

3.1.8. *Recombinant Protein Induction*

BL21 cultures were grown in 50mL of LB/KAN overnight at 37°C, shaking at

200-250rpm. From each culture, 100μl was taken and diluted in LB to have the

optical density of the culture measured at 600nm. The 50mL cultures were diluted to

a volume of 1000mL of LB such that their OD was between 0.1-0.2. Cultures were

allowed to grow with routine OD checks until their OD600 measured around 1,

requiring approximately 1-2 hours. The 1L cultures were cooled on ice for 2 minutes

and a 500μl pre-induction sample was retained and stored at 4°C. Isopropyl β-D-1-

thiogalactopyranoside (IPTG), (catalog (# I6758-1G) was added to a final

concentration of 0.5mM, dissolved in 500μl of LB, and added to each 1L culture.

Cultures were relocated to a 25°C incubation shaker set at 250rpm for 2.5 hours.

Following induction, a 500μl post-induction sample was retained and stored at 4°C.

The 1L induced cultures were evenly distributed by weight into 4, 250 mL

bottles that were then spun at 5000-7000 rpm for 20 min. The supernatant of the

pelleted cultures was removed completely. The pellets were re-suspended in 5mL of

1X Phosphate Buffered Saline (PBS) (catalog#21040CM) that was kept on ice and

transferred to a 50mL falcon conical. The conical tubes were spun at 4000rpm for 10-15 minutes to re-pellet the induction product and they were stored for future purification at -80°C.

3.1.9. _Sodium Dodecyl Sulphate-Polyacrylamide Gel (SDS-PAGE) Electrophoresis and Coomassie Triphenylmethane Staining_

Precast Polyacrylamide NuPAGE Bis-Tris Gels from Invitrogen ThermoFisher (catalog # NP0322BOX) or GenScript PAGE gel (catalog # M42015) were used to determine whether or not the induction of protein expression was successful before proceeding to the extensive protein purification procedures. Both precast gels were 4-20%, contained 10-15 wells, and had a well loading capacity of 40μl. From each pre- and post-induction sample, 200μl was mixed with 40μl of 6X SDS dye. Samples were boiled in a 90°C heat block for 5 minutes then centrifuged for 1 minute at low speed. Approximately 20μl of each sample was loaded into the gel with 5uL of PageRuler Plus Prestain ladder (Thermo) and run at 140V for 45-60 minutes in an Invitrogen MiniGel Tank.

Gels were stained for 15 minutes with InstantBlue from Expedeon (catalog #ISB1L) to visualize the results of induction. Failure to demonstrate a significant increase in overall expression indicated that no purification should be conducted on the protein pellets obtained from un-induced cultures. Gels could also be used in western blot analysis of proteins described in section 3.2.3.

3.2. Protein Purification

3.2.1. *Chemical Lysis and Immobilized Metal Ion Affinity Chromatography*

Previous methods utilized several short cycles of sonication followed by Immobilized Metal Ion Affinity Chromatography (IMAC), however the purified protein product had an unstable activity and a high degree of impurities within some samples, thought to be caused by degradation from the sonication process. For this reason, chemical lysis methods were employed with several collection aliquots between washes to follow the point at which the most preserved protein was eluted. Induced protein pellets were re-suspended to a final volume of 20mL for purification of two pellets with lysis buffer containing 50mM sodium phosphate, (pH 7.2), 300mM NaCl, 30mM Imidazole (first dissolved and sterile filtered) brought to a final volume of 500mL with deionized water and the addition of 1 EDTA-free protease inhibitor (PI) cocktail tablet per 10mL of lysis buffer. The sodium phosphate stock solution was produced through the addition of 1M sodium phosphate monobasic, $NaH2PO4$, and 1M sodium phosphate dibasic, $NaHPO4$. When the complete lysis buffer was mixed, it was brought to desired pH with HCL. To the re-suspended pellets, 100μl of 200mg/ml of lysozyme (Sigma # L6876-100G) was added while kept on ice to disrupt the cellular membranes. This solution was gently mixed until the lysate became viscous. Next, 6μl of benzonase (Sigma # 9025-65-4) was added to the lysate to degrade all DNA/RNA and was rocked at room temperature until the viscosity of the lysate was removed. To extract protein from inclusion bodies resulting from eukaryotic protein expression in E. *coli,* 1.6 mL of 25% sarkosyl

(Sigma # 137-16-6) was added to the lysate in 0.8mL increments with gentle mixing following each addition. The lysate was rocked at room temperature for 20 minutes or until the lysate changed to a brown color. The entire lysate was then poured into a 250mL Erlenmeyer flask and 140mL of lysis buffer containing 2 dissolve PI tablets was added in 20mL increments and swirled. The lysate lost all viscosity and changed from a darker brown color to a lighter beige color.

Polypropylene columns (Thermo Scientific #29924) were acclimated prior to addition of the lysate. This was done by inserting a filter disk into each 10mL column and packing them with 1.8mL of TALON superflow metal affinity resin (Clontech #635506). The resin contains tetradentate chelators charged with cobalt which allowed for purification of his-tagged proteins. To acclimate the columns, lysis buffer without PI tablets was used to fill the column twice and flow through from gravity. The total volume of complete lysate was passed through the column in 10mL increments two times and the darkening of the resin indicated the protein had successfully bound. First the columns were washed with 30ml of 50mM sodium phosphate, pH7.2/300mM NaCl/30mM imidazole, 30ml of 20mM sodium phosphate, pH7.2/500mM NaCl/30mM imidazole, 30ml of 20mM sodium phosphate, pH7.2/150mM NaCl/30mM imidazole, 30ml of 20mM sodium phosphate, pH7.2/150mM NaCl/100mM imidazole, 30ml of 20mM Na-phosphate, pH7.2/150mM NaCl/100mM imidazole/0.5% Tween20, and last washed with 50ml of 20mM sodium phosphate, pH7.2/150mM NaCl/300mM imidazole. To elute the protein, 20mM sodium phosphate, pH7.2/150mM NaCl/1M imidazole/5% glycerol was used in step wise elution where each run through was collected an aliquoted. The

first elution (E1) was .5mL of the elution buffer and was allow to pass through. Protein was very rarely ever detected in this fraction. The following elution steps were carried out by capping the bottom end of the column and adding .75mL of the elution buffer, allowing it to rest for 10 minutes before removing the bottom cap and replacing the lid to expel the volume from the column. This process was repeated for at least 9 more elutions or until the resin went from a dark red (protein still present) to a light pink (little to no protein remaining). All elutions were aliquoted into smaller storage volumes and kept on ice or stored at -80°C. Freeze-thaw cycles per protein aliquot were limited to a maximum of 2.

3.2.2. _Protein Confirmation and Concentration Quantification_

The protein concentration for each elution step aliquot was determined using Pierce detergent compatible Bradford reagent (Thermo catalog #1863028). Into a 96 well plate (catalog # 41111327), bovine serum albumin (BSA) at a concentration of 1mg/mL was added for standard curve consisting of 0mg/mL, 1.25 mg/mL, 2.5 mg/mL, 5 mg/mL, 10 mg/mL, and 15 mg/mL. For each sample 5-10uL was added in triplicate, followed by 300uL of undiluted detergent compatible Bradford reagent and allowed to incubate at room temperature for 4 minutes. Absorbance of the plate was read on the FLUOstar Omega microplate reader at A620.

For each purification, 2 SDS-PAGE gels as previously described, were run with 10-20uL of each elution sample. One gel was stained with InstantBlue Coomassie stain to identify elution's with possible increased levels of contamination such as degraded proteins.

3.2.3. *Western Blotting*

To ensure that complete protein with tag was purified, the second SDS-PAGE gel had its separated products transferred to a 0.2μm nitrocellulose membrane with transfer buffer containing 25 mM Tris, 192 mM glycine, and 20% methanol to aid in the stripping of SDS and increase adherence to the membrane. Transfers were done in BioRad Trans-Blot transfer tanks containing 450mL of 1X transfer buffer and the preparation of the gel and membrane sandwich was done in accordance to manufacture's specifications. Transfers were run at 100V for 60 minutes. Following transfer, membranes were blocked with 2% nonfat milk in 1X TBS-Tween20 (TBST) for 60 minutes at room temperature prior to the addition of primary antibodies overnight at 4°C. Three washes with were performed on the blots for 30 minutes each prior to addition of necessary secondary antibody for 60 minutes at room temperature. Three washes of the membrane were done at room temperature each lasting 30 minutes. All washes consisted of 2% nonfat milk in 1X TBST excluding the wash preceding imaging which was done only in 1X TBST. All antibodies were stored in 2% nonfat milk in 1X TBST and those without HRP conjugation also had 1X sodium azide, NaN3 (Sigma catalog # 26628-22-8), added. Membranes were visualized using a 1:1 solution of 8mL of Immobilon Western Chemiluminescent horseradish peroxidase (HRP) Substrate (Millipore catalog #WBKLS0500) for 10-15 seconds before detection by GE ImageQuant LAS 3000 imager and its associated program.

The following antibodies were used at the specified dilution ratios: 1:250-1:500 rabbit anti-hArv1 (abgent #64801), 1:1000 HRP conjugated 6x-His tag antibody

(Invitrogen #MA-1-21315-HRP), 1:500 ECL HRP conjugated donkey anti-rabbit IgG (GE healthcare life sciences #NA934), 1:1000 mouse anti-Beta Actin (thermofisher #MA1-91399), 1:500 ECL HRP conjugated sheep anti-mouse IgG (GE healthcare life sciences #NA931V)

3.3. Characterization of Lipid Binding

3.3.1. Protein Lipid Overlay "Far Westerns"

Protein lipid overlays (PLO) also referred to as "far westerns" are a means of qualitatively assessing the ability of a protein to bind to the head group of an immobilized lipid. Lipid overlay strips (Echelon #P-6002) are 2x6cm membranes that have been spotted with 100pmol of 15 different lipids that are commonly found in the composition of lipid membranes that include triglyceride, phosphatidylinositol (PI), phosphatidylinositol (4)-phosphate (PI(4)P), phosphatidylinositol (4,5)-bisphosphate, (PI(4,5)P$_2$), phosphatidylinositol (3,4,5)-trisphosphate (PI (3,4,5)P$_3$), phosphatidylserine (PS), phosphatidylethanolamine (PE), phosphatidic acid (PA), diacylglycerol (DAG), cholesterol, phosphatidylcholine (PC), sphingomyelin, phosphatidylglycerol (PG), 3-sulfogalactosylceramide (Sulfatide), and cardiolipin (CL).

Membranes were blocked for 1 hour at room temperature with 10mL of TBS with 3% fatty acid free, bovine serum albumin. To single membranes, different his-tagged proteins of interest were added in 5mL of TBS/BSA at 5μg/mL for 1 hour at room temperature. The protein solution was discarded and three washes were done with TBS/BSA for 30 minutes each. Anti-His tag antibody (1:1000) in TBS/BSA was

added to the membranes and rocked overnight at 4°C. The following day, the antibody was removed and the membranes were washed three times for 30 minutes each with PBS containing no BSA. Membranes were visualized using a 1:1 mix of 8mL of Immobilon Western Chemiluminescent horseradish peroxidase (HRP) Substrate (Millipore catalog #WBKLS0500) for 10-15 seconds before detection by GE ImageQuant LAS 3000 imager and its associated program. If a protein was able to bind to a bound lipid, the his-tag was detected as a dark spot on the membrane, the location of which indicated the lipid that said protein had bound to [64].

3.3.2. *Homogenous Time resolved Fluorescence (HTRF)*

3.3.2.1. *Assay Mechanism*

HTRF (Homogeneous Time Resolved Fluorescence) is a common high-throughput screening technology that allows one to measure analytes through its combination of fluorescence resonance energy transfer technology (FRET) and time-resolved measurement (TR) [65]. In this assay, the interactions between two molecules can be quantified by binding each molecule involved with a fluorescent label, and then analyzing the transfer of energy between the initial donor fluorophore and the secondary acceptor fluorophore [65, 66]. Following excitation of the first fluorophore, transfer of energy can only occur if the molecules bound with the fluorescent tags are within proximity to each other.

For this research, TR-FRET is measured between Europium kryptate linked to an anti-histidine antibody targeted for the histidine tagged hArv1 protein, as the donor, and Streptavidin-d2 conjugate that binds to biotinylated phospholipids that

was suspected to interact with hArv1, as an acceptor if it is in proximity to the donor [65]. (Figure 11). The emissions are measured with two differing wavelengths (acceptor and donor at 665nm and background at 615nm) allowing the reduction of variations that may occur well to well [66]. Through the use of these two detection reagents, it is possible to analyze and quantify the interactions between individual lipids in the presence of hArv1 as well as the ability of one type of lipid to displace a different lipid that was previously bound, through competition assays.
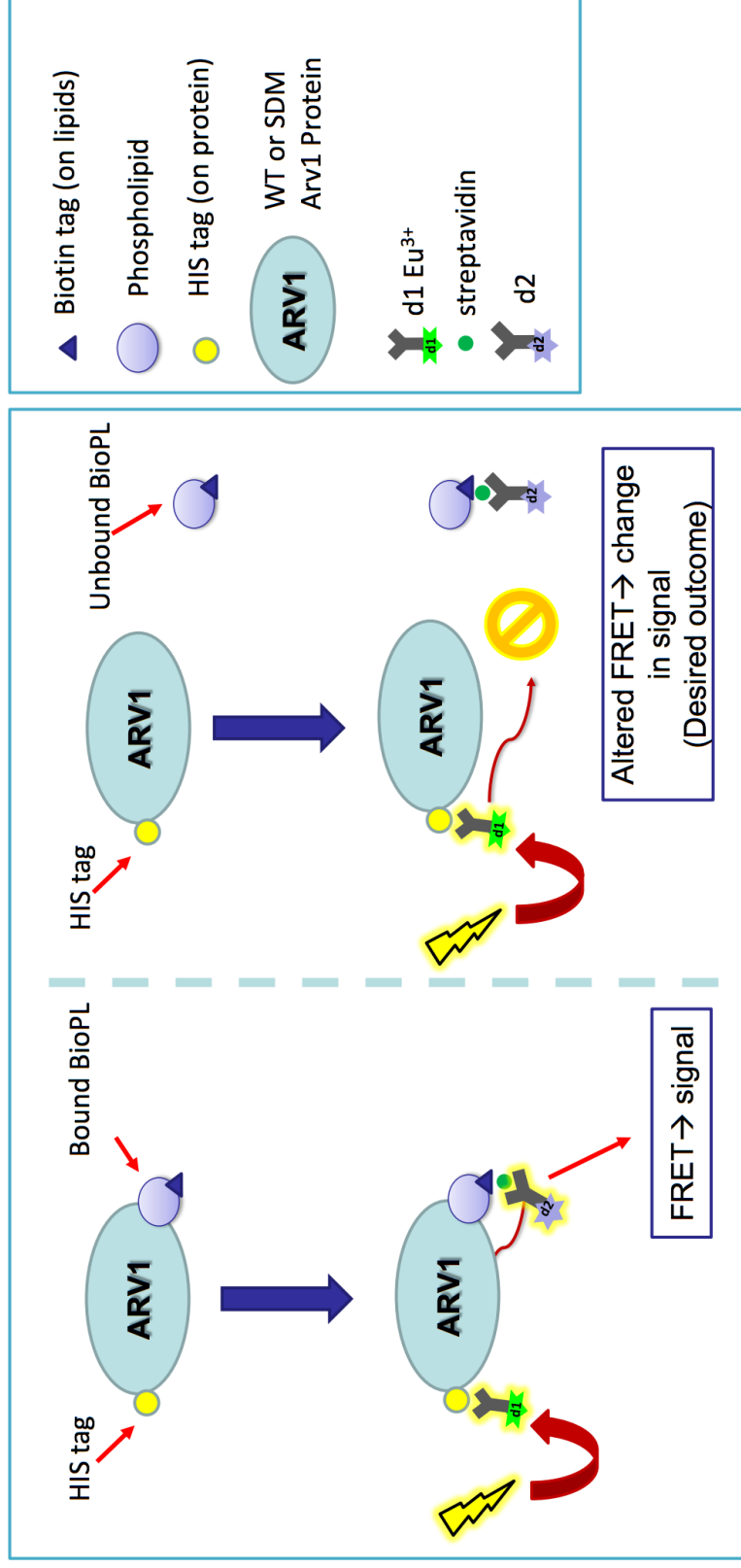
Figure 11. Homogenous Time Resolved Fluorescence (HTRF) assay mechanism. Protein-lipid binding was assessed by measuring the interaction of Europium kryptate linked to an anti-histidine antibody targeted for the histidine tagged hArv1 protein, as the donor, and Streptavidin-d2 conjugate that bound to the biotinylated phospholipids. If a protein was able to bind the phospholipid, the antibodies were brought within proximity such that excitation of one allowed for florescence resonance energy transfer (FRET). Emissions were measured at two wavelengths for the acceptor and donor at 665nm and background at 615nm.

(modified from Fleury et al, 2015).

3.3.2.2. *Protein Activity Validation*

It was determined that not only does the concentration of available purified protein vary from elution to elution between purifications of different mutated variations of the hArv1 protein, but also the activity of the protein itself. It is for this reason, the elution activity was quantified and selectively pooled based on this activity. Earlier work had established the ability of Arv1 to bind well to phosphatidylglycerol. For each protein variant, an HTRF was performed (see section 3.3.2.3 Phospholipid Binding Quantification) and the highest demonstrated binding elution aliquots for the phospholipid were used for characterization in additional binding assays.

3.3.2.3. *hArv1/Biotinylated Phospholipid HTRF Assay for Phospholipid Binding Quantification*

Assays were plated on 384 well flat bottom microplates (Greiner Bio catalog #784075-25). First, all reagents used in the assay were taken out cold storage and brought to room temperature. Proteins were diluted using binding buffer to a stock concentration of 0.75μM and biotinylated phospholipids phosphatidic acid (bioPA), phosphatidylserine (bioPS), phosphatidylglycerol (bioPG), phosphatidylcholine (bioPC), cardiolipin (bioCL), and phosphatidylethanolamine (bioPE), see Table 3, were dispensed under ventilation hood, dried under nitrogen gas to remove the storage chloroform, and re-suspended with binding buffer to a stock concentration of 50uM.

Table 3. Biotinylated phospholipids used in HTRF assays.

	Phospholipid	Structure	MW
860581C	Biotinylated Phosphatidylglycerol		956
840475C	Phosphatidylglycerol		797
860561C	Biotinylated Phosphatidic Acid		877
840875C	Phosphatidic Acid		723
860560C	Biotinylated Phosphatidylserine		964
840035C	Phosphatidylserine		810
L-C16B	Biotinylated Cardiolipin		1652
710335C	Cardiolipin		1501
860563C	Biotinylated Phosphatidylcholine		945
850375C	Phosphatidylcholine		786
850725C	Phosphatidylethanolamine		744

Binding buffer consisted of 1M HEPES (4-(2-hydroxyethyl)-1-piperazineethanesulfonic acid) at pH 7.2, 1% BSA, 25% Tween20. The lipid was then further diluted by 1:2 for a series of 12 serial dilutions. First 6μl of binding buffer was loaded into the plate in triplicate for each dilution of phospholipid. To this, 2μl of 0.75μM his-tagged protein was added, followed by 2μl of biotinylated phospholipid. Immediately following each addition loaded into the plate, the plate was centrifuged for 1 minute at 1000rpm to bring the contents added to bottom of the well. Next, detection antibodies were mixed with detection buffer that consisted on 1M HEPES, pH 8.5, 1%BSA,1M KF. The two antibodies were monoclonal MAb anti-6HIS Europium kryptate conjugated D1 fluorescent antibody (Cisbio 61HISKLA) and Streptavidin conjugated d2 fluorescent antibody (Cisbio 610SADLA). For each 1000μl of detection buffer, 5μl of each antibody was added just prior to loading 10μl into each well. The plate was again centrifuged for 1 minute at 1000rpm and stored in a sealed container to incubate overnight, away from direct light. Total reaction volume per well was 20μl and all additions of protein and lipid would result in a 1:10 dilution of concentration when plated. Plates were read on a PerkinElmer EnVision Xcite Multilabel plate reader located at Venenum Biodesign the following day. For each assay, the fluorescence values are recorded at each of the 12 dilutions of lipid to generate a binding curve specific for that protein-lipid combination.

3.3.2.4. *Phospholipid Binding Competition assays*

The competition assays followed a similar protocol as described for the standard HTRF described in section 3.3.2.3. In the standard assay, protein is loaded

in a constant concentration and the concentration of biotinylated phospholipid increases, however; in a competition assay, both protein and biotinylated lipid were plated constant and the non-biotinylated lipid that was to compete for binding areas of the protein was loaded in an increasing concentration. Reagents used in the assay were taken out cold storage and brought to room temperature. Proteins and biotinylated phospholipids were diluted with binding buffer and plated to a constant concentration. Protein concentration was again 0.75uM while the concentration of the biotinylated phospholipid was determined by the concentration required to reach 80-100% binding capacity in the previously determined Binding HTRF described in section 3.3.2.3. Untagged lipid was diluted to a stock concentration of 50X the loading concentration of the tagged lipid and diluted further for twelve 1:2 serial dilutions.

The assay was plated first with 4μl of binding buffer, followed by 2μl of each protein, and 2μl of the biotin tagged lipid. After centrifuging the plate in between additions for 1 minute at 1000rpm each, the 12 dilutions of competing cold lipid was added and the plate was centrifuged again. The detection buffer containing the MAb anti-6HIS Europium kryptate conjugated D1 fluorescent antibody and Streptavidin conjugated d2 fluorescent antibody was added to each well, followed by a final spin before overnight incubation. Plates were read PerkinElmer EnVision Xcite Multilabel plate reader to measure the variance in fluorescence output for the 12 dilutions of competing lipid to generate an inhibition curve for that lipids ability to outcompete the binding of the biotinylated lipid.

3.3.2.5.   *Generating Graphs and Statistical Analysis*

Data generated from homogenous time resolved florescence assays was processed and graphed using GraphPad Prism 6 software [67]. Curves were generated with three points per concentration point, per replicate and graphed as an XY scatter demonstrating the mean and standard error of the mean. Points that produced a "hooking" effect were excluded on the basis of phospholipid as to not skew analysis of curve fitting, a common practice for results generated by high throughput screening assays [68]. The "hook" effect results at a point when the titration of biotinylated lipids saturates the available protein, and the drop in signal is caused by consumed detection reagents.

Curves were logarithmically transformed and normalized to a common scale before being fit with a nonlinear regression of the agonist against the normalized response. This generated half maximal effective concentration, EC50, values that could then be compared between different lipids or variant proteins as well as between assays plated at different times [67]. In the context of this study, any interpretation or reference of an EC50 for the purpose of "apparent affinity" was defined as a measure of the protein's or variant's, sensitivity to binding to a particular lipid within a dose response curve. Changes in the EC50 of the same lipid between altered versions of the same protein implied a change in this apparent affinity.

The EC50 values for replicate experiments per lipid/protein combination were recorded and graphed to compare their distributions between replicates to determine reproducibility and also between lipid/protein combinations to determine differences

in apparent affinity of binding. A one-way analysis of variance (ANOVA) was performed to first identify if there were differences in the distributions of EC50s. When significant differences were calculated, a student's 2-sample T-test was used to establish if independent curves were statistically different from one another.

4. Experimental Results

4.1. Protein Induction, Expression, and Confirmation

The 271-amino acid sequence of the human Arv1 protein is anchored into the membrane of the endoplasmic reticulum by three transmembrane regions which impedes the studies of the functional implications of its structure. Complications arise when attempting to purify membrane bound proteins due to flexibility of the protein, a lack of stability without the membrane giving structural consistency, and issues with hydrophobicity [69]. These obstacles taken collectively with Arv1's relatively low endogenous expression within the cell, have prevented researchers from successfully crystalizing the native structure thus far. The sequence and the topology of the protein have been elucidated, but further work is required to not only confirm the true structure of the full-length protein, but to characterize the importance of the tertiary structures in the context of lipid transport.

To overcome the lack of expression of Arv1, an inducible recombinant system for protein purification was utilized in *E. coli*. The N terminal 98 residues encompassing the Arv1 Homology Domain was chosen to be expressed in order to avoid the limitations of managing membrane bound proteins, which was supported by work performed by Jamie Francisco in our laboratory that showed that the majority of the protein's function resides in this region. Figure 10 includes a schematic of the protein's topology and orientation in the membrane as well as the AHD portion designated in blue amino acids with mutation locations in purple.

Both the N98 wild type and mutant variant constructs of N98 were generated and expressed in BL21 cells, which are specifically used for high level protein expression. Protein overexpression was induced with IPTG and confirmed through Coomasie staining and western blotting, Figure 12 includes a representative western blot (A) showing increased protein expression for N98, K67A, and E70A around the expected 13 kDa region in only the post induction samples.

The induced samples were purified under chemical lysis conditions in order to preserve the integrity of the protein, as sonication methods caused higher levels of impurities attributed to protein degradation. Immobilized metal ion affinity chromatography was used to purify the His-tagged protein. The representative Coomasie stained gel in Figure 12 shows the protein product of each elution (E) around the 13kDa range. The final purified proteins were quantified with Bradford assays and used in the western blot.
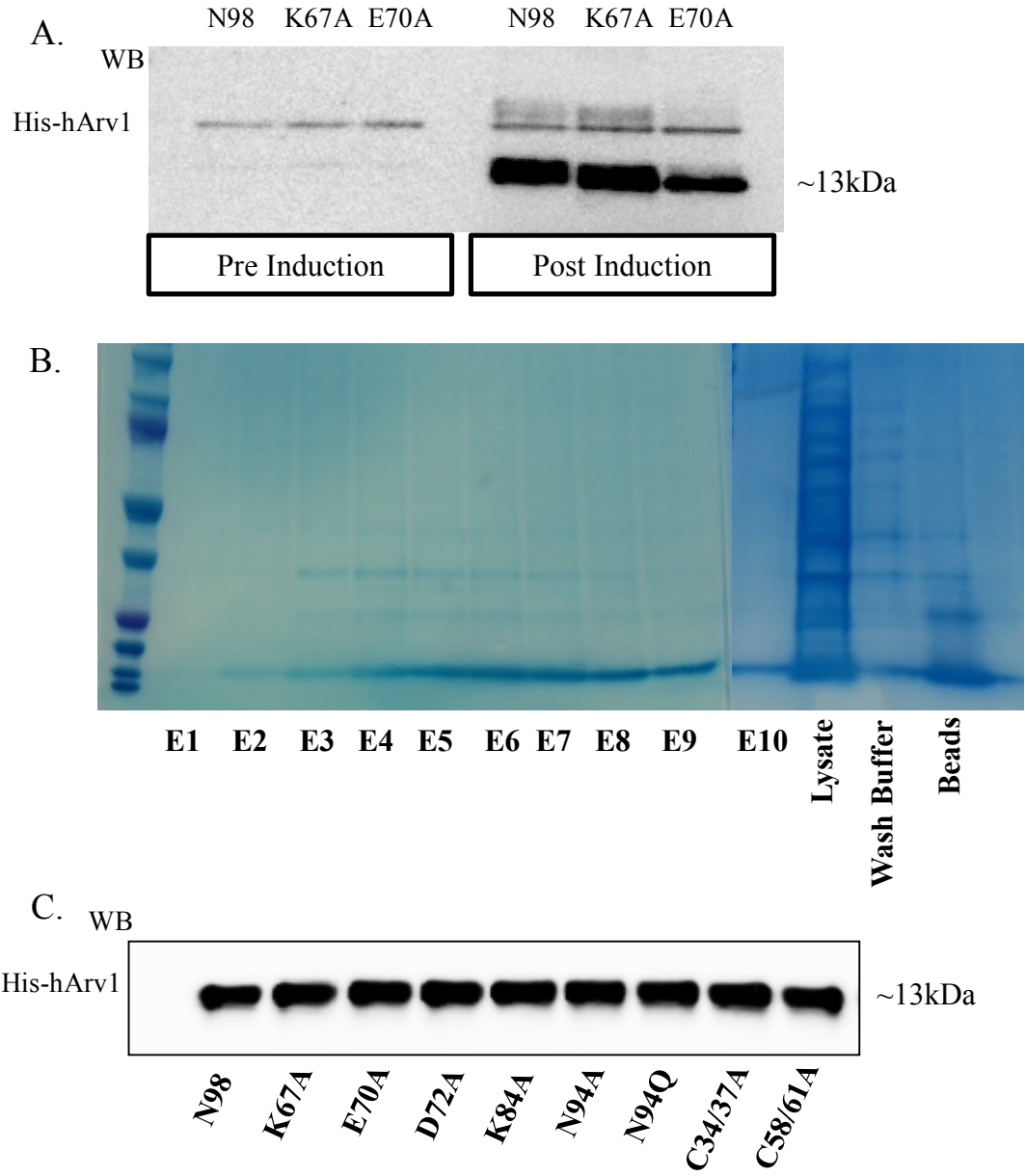
Figure 12. N98 and SDM hArv1 induction, expression and validation. [A.]
Western blot of 20 μl of lysates pre-and post-addition of IPTG to confirm successful
induction of protein overexpression. [B.] Coomassie stained SDS PAGE gel with 15
μl from each purification stage to assess purity of product. [C.] Western blot of 15ug
total protein per well of each protein to confirm identity of the proper his-tagged
protein.

4.2. Far Western Protein-Lipid Overlays

To begin to address the lipid binding specificity of N98 and the mutants, far

westerns were performed using 5μg/mL of protein and Echelon lipid immobilized

strips. The Echelon membranes contain 15 spots of different lipids, with each spot

containing 100pmol of a particular lipid. After the membranes were incubated with

protein and multiple wash steps of washing, the protein bound to the lipids were

visualized by probing with anti-His antibody (Invitrogen MA-1-21315-HRP). Figure

13 contains representative lipid overlays from experiments repeated in triplicate.
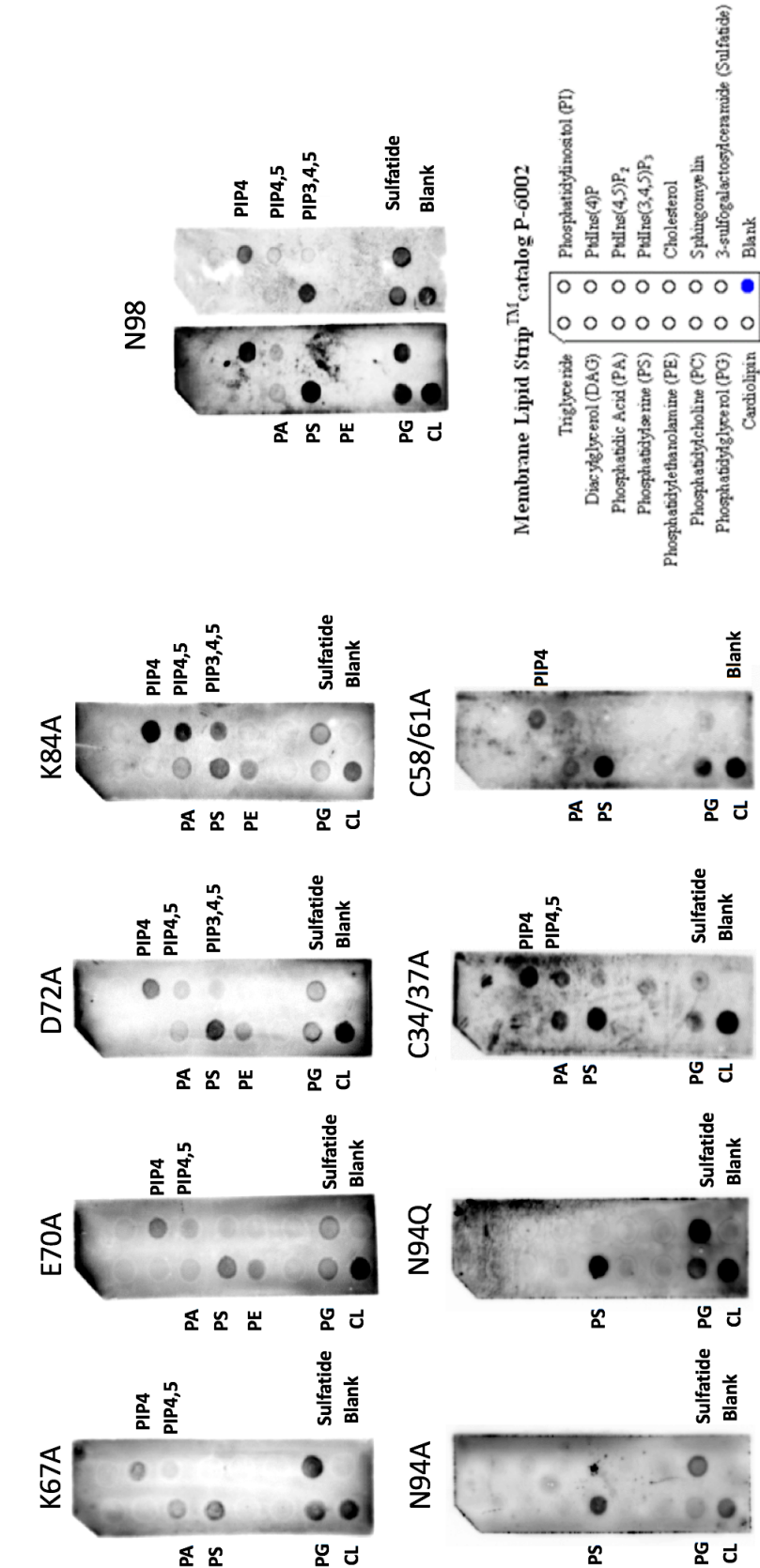
Figure 13. Far Western Lipid-Protein Overlays. Membranes that contained 15 spots of 100pmol of different lipids found in phospholipid membrane compositions were incubated with 5μg/mL of protein in 1XTBS with 3%BSA overnight Proteins that bound to the lipids were visualized by probing with anti-His antibody. The location determined the identity of the lipid that the protein was bound to. (Bottom, Right) Schematic of lipid location. (Top, Right) Representative results obtained with N98 protein. (Left) results obtained with SDM variant proteins.

The N98 bound to phosphatidylglycerol with strong intensity. Strong phosphatidylserine binding was shown, however only moderate phosphatidic acid binding was seen. A high intensity signal was seen for cardiolipin and sulfatide. Interestingly, the N98 overlays indicated it had the ability to bind to phosphatidylinositol (4)-phosphate (PI(4)P) and to far less degree, phosphatidylinositol (4,5)-bisphosphate. These phospholipids play central roles in several signal cascade pathways as either target substrates or as localization scaffold proteins that aid in the enlistment other proteins and/or enzymes to a specific region [16]. No binding was seen for all other embedded lipids including PI, PC, or PE, and cholesterol, (Figure 13, Right).

Analysis of the lipid binding of various mutants indicated showed changes in lipid binding affinity. Proteins E70A, D72A, K84A, N94A, and both cysteine cluster protein variants showed a loss of binding to sulfatide, while N94Q showed increased binding to this lipid. Increases binding to PIP4, PIP4,5 and PIP3,4,5 was seen for K84A and C34/37A mutants. As far as phosphatidylglycerol binding, K67A, E70A, D72A, K84A, N94A, C34.37A and C58/61A had decreased intensity affinity. Loss of phosphatidylserine binding was observed for the K67A, E70A, K84A, and N94A variants. Finally, there was an increase in phosphatidic acid binding by K67A, K84A, C34/37A and C58/61A as well as increases in phosphatidylethanolamine binding by E70A, D72A, and K84A (Figure 13 Left).

Far westerns of this type are highly qualitative and the immobilization of the lipids to the planar surface of the membrane may have reduced the physiological relevance of the results. Depending on the orientation of the lipids, access to portions

of the lipids by the proteins may have been more readily available or restricted to binding interactions just by means of anchorage to the overlay membrane. This would be different compared to how the spatial arrangement would be if floating in a dynamic medium. For this reason, applications of this method were predominately limited to identifying proteins that lacked reproducible binding activity before applying them to more physiologically relevant experiments for the characterization of binding interactions. The lipid overlays did allow for fast identification of proteins that were in the process of losing activity either by extended storage times or multiple freeze-thaw cycles.

4.3. *Homogenous Time Resolved Fluorescence Assays*

4.3.1. *Elution Activity Selection*

When first optimizing conditions for the HTRF assay, it was discovered that differences in binding of protein to the same lipid varied within some batches of purified proteins. Before attempting to characterize the binding affinities of the variant proteins for each lipid, it was decided to identify the elution fraction(s) that demonstrated the best lipid binding affinity. Preliminary work in our laboratory identified a high affinity binding between hArv1 and phosphatidylglycerol. The biotinylated form of this lipid was used in our HTRF to select the elution producing peak activity denoted by left shifts of the EC50 value (Figure 14). Elution selection varied to only a minor degree between mutated proteins and was reasonably consistent when purifying a new collection of the same protein.

E70A Elution Test for Biotinylated Phosphatidylglycerol Binding
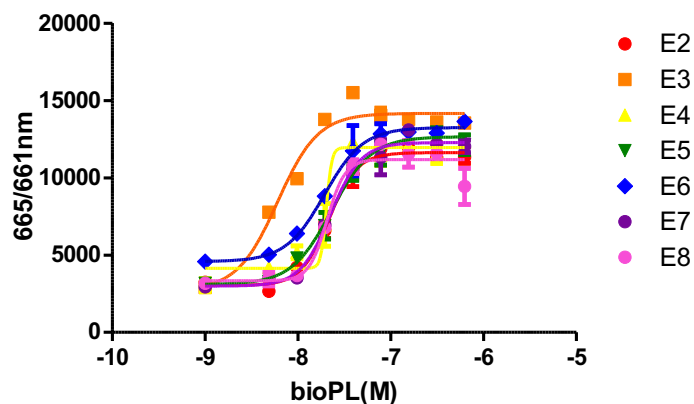
	E2	E3	E4	E5	E6	E7	E8
Best-fit values							
Bottom	3033	2730	4140	3106	4576	2994	3339
Top	11627	14165	11951	12654	13248	12276	11182
LogEC50	-7.665	-8.218	~ -7.693	-7.638	-7.713	-7.648	-7.686
HillSlope	2.867	1.998	~ 15.12	2.025	2.074	2.651	4.484
EC50	2.160e-008	6.051e-009	~ 2.029e-008	2.300e-008	1.934e-008	2.250e-008	2.061e-008

Figure 14. Protein purification elution selection by HTRF assay. Following

protein purification, several elutions were aliquoted for each protein that was purified.

It was determined that the activity of the protein varied between these elutions

sometimes. To remove the chance of masking a mutated protein's ability to bind,

each elution was tested with a binding HTRF. Above is an example of an elution

activity HTRF performed on protein E70A. Protein was loaded at a constant

concentration of 0.75 μM and BioPG at 50 μM.

4.3.2. _Characterizing Phospholipid Binding of N98 hArv1 Protein_

4.3.2.1. _HTRF-PG, PS, PA, CL, PC, PE_

A constant concentration of 0.75μM N98 hArv1 protein was plated with a 1:2 serial dilution of biotinylated phospholipids phosphatidic acid (PA), phosphatidylserine (PS), phosphatidylglycerol (PG), phosphatidylcholine (PC), cardiolipin (CL), and phosphatidylethanolamine (PE) that ranged from 0 to 50μM. The curves generated required points that produced a "hook" to be removed based on the rate the particular lipid saturated the protein. PG had the 3 highest concentrations excluded, PA and PE had the 2 highest removed, CL had 1 point removed and PS and PC did not produce a "hook" so no points were removed. These data points are most likely skewed due to the lipids transitioning from monomeric form to micellular form or the consumption of detection reagents.

The N98 protein demonstrated the highest apparent affinity for binding to PG with a half maximal effective concentration of 4.270e-008. The lowest affinity binding was produced in PC assays which demonstrated an EC50 of 1.282e-006, a 29-fold difference from PG. Similar to the binding patterns exemplified by PG, PA yielded an EC50 around 8.673e-008, only a 1-fold difference from PG. CL (3.756e-007), PS(4.547e-007), and PE (6.008e-007) all produced curves with EC50s similar in range and 7, 10, and 13-fold difference from PG respectively (Figure 15 A). Overall, there was a preferential order of binding by N98 from high to low order for PG, PA, CL, PS, PE, PC.

A. **Biotinylated Phospholipid Binding Charactization of hArv1 N98 Protein**

	BioPG	BioPS	Bio
Best-fit values			
LogEC50	-7.370	-6.342	-7.062
HillSlope	2.072	1.570	2.564
EC50	4.270e-008	4.547e-007	8.673

- ● Bio-Phosphatidylglycerol
- ■ Bio-Phosphatidylserine
- ▲ Bio-Phosphatidic Acid
- ▼ Bio-Phosphatidylethanolamine
- ◆ Bio-Phosphatidylcholine
- ○ Bio-Cardiolipin

	BioPG	BioPS	BioPA	BioPE	BioPC	BioCL
Best-fit values						
LogEC50	-7.370	-6.342	-7.062	-6.221	-5.892	-6.425
HillSlope	2.072	1.570	2.564	2.327	1.398	1.542
EC50	4.270e-008	4.547e-007	8.673e-008	6.008e-007	1.282e-006	3.756e-007

B. **Half Maximal Effective Concentration Distribution of ARV1/BioPL BindingCurves**

One-way analysis of variance	
P value	< 0.0001
P value summary	***
Are means signif. different? (P < 0.05)	Yes

Results of Student T-test:	* = P<0.05 ** = P<0.005 *** = P<0.0005

Figure 15. hArv1 N98 HTRF Binding Curves and EC50 Distributions. [A.] Established binding patterns generated by HTRFs using biotinylated PG, PS, PA, PE, PC, and CL. Apparent affinity is indicated by a left shift decrease in the half maximal effective concentration (EC50). [B.] Statistical analysis was applied to determined significances between the distributions of EC50 of differing phospholipids. N98 was found to have the ability to specifically bind anionic PL with an apparent affinity of PG>PA>CL>PS>PE>PC.

Statistical analysis of these EC50 distributions determined that there were in fact, significant differences produced from the binding curves of the lipids by the N98 hArv1 protein (ANOVA P value <0.0001). Having determined that differences were significant, the next query was how different each phospholipid assay's EC50 differed from phosphatidylglycerol, an already established strong binding ligand of hArv1. A t-test determined that each curve was in fact statistically different from the PG binding with P values of 0.05 or less. The last comparisons made were to assess if each phospholipid binding curve was statistically independent from the other lipids used. Results indicated that there was a lack of significant differences when comparing PS to CL binding and PC to PE binding, however all other comparisons produced a P value of 0.05 or less (Figure 15, B).

4.3.2.2. *Preliminary Data: Competition HTRF*

With the binding affinities of hArv1N98 being successfully characterized, preliminary work was done that determined if these phospholipids were binding to the same site on the protein. Competition assays were performed with constant concentrations of N98 protein (0.75µM) and constant concentrations of biotinylated phospholipids. The concentrations for bioPG, bioPA, and bioPS, were selected to be the concentration at which the protein indicated saturation in the HTRF assays described in section 4.3.2.1 (Figure 16). To this end, a 1:2 serial dilution of non-biotinylated lipids were added beginning at 50X the concentration of bioPL, followed by detections reagents as previously described. In this reaction, if a non-biotinylated lipid displaced the biotinylated lipid, it would result in a decrease in signal. The more

rapid the decrease, the stronger the inhibition of the bioPL binding, denoted by the

half maximal inhibitory concentration.

	BioPG	BioPS	BioPA	BioPE	BioPC	BioCL
Best-fit values						
LogEC50	-7.370	-6.342	-7.062	-6.221	-5.805	-6.329
HillSlope	2.072	1.570	2.564	2.327	1.415	1.639
EC50	4.270e-008	4.547e-007	8.673e-008	6.008e-007	1.567e-006	4.691e-007
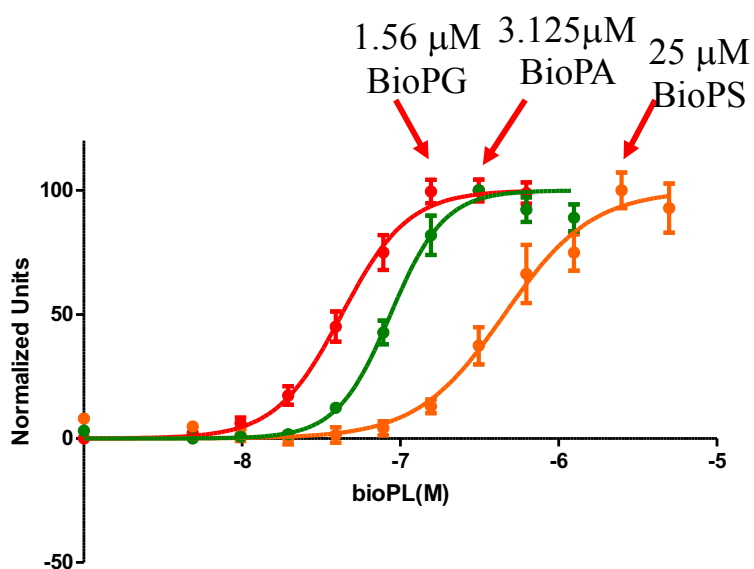
Figure 16. Selection of competition HTRF assay concentrations for phospholipids. Competition assay allowed for the preliminary assessment to

determine if binding of phospholipids was occurring at different locations or if the

same region was being competed over. For each phospholipid, the concentration at

the point of saturation was selected for. This would determine the plating constant

concentration of biotinylated phospholipid. 50X the concentration of bioPL at

saturation determined the highest concentration of non-biotinylated PL which was

then diluted 1:2 12 times.

4.3.2.2.1. *Competition of Biotinylated Phosphatidylglycerol*

0.75μM of protein and 1.56μM bioPG were used. Non-biotinylated PG, PC, PS, PA, and Cl were plated beginning at 78μM with a 1:2 dilution afterwards. Results indicate that PA and CL successfully inhibited bioPG binding with the lowest IC50 of 4.945e-009 and 6.655e-009 respectively. PS appeared to have similar turnover as PG in competing for bioPG binding. PE and PC did not bind or inhibit PG binding (Figure 17, Bottom, Left).

4.3.2.2.2. *Competition of Biotinylated Phosphatidylserine*

Protein was plated at constant 0.75μM and bioPS plated at constant 25μM. Non-biotinylated PG, PC, PS, PA, and Cl were plated beginning at 1250μM with a 1:2 dilution afterwards. PA most likely has the ability to compete (IC50 1.731e-008) but more replicates will be required to reduce the influence of error. PC did not bind or inhibit Arv1 binding to PS. PG, PS, and CL produced IC50s of 1.063e-007, 3.383e-008, and 4.031e-008. Substantial overlap in error bars limits the possibility of any of these being significant (Figure 17, Top, Right).

4.3.2.2.3. *Competition of Biotinylated Phosphatidic Acid*

Protein was plated at constant 0.75μM and bioPA plated at constant 3.125μM. Non-biotinylated PG, PC, PS, PA, and Cl were plated beginning at 156.25μM with a 1:2 dilution. PA demonstrated strong competition with an IC50 of 7.616e-009. PS and CL were also able to compete with IC50s of 4.587e-008 and 3.239e-008 respectively.

Competition with PG produced an IC50 of 1.355e-007. Once again, PC neither bound

or inhibited PA binding. (Figure 17, Top, Left).

Competition of Biotinylated Phosphatidylserine Binding

	PG	PC	PS	PA	CL
Best-fit values					
LogIC50	-6.973		-7.471	-7.762	-7.395
HillSlope	-0.9564		-0.8572	-1.107	-0.9210
IC50	1.063e-007		3.383e-008	1.731e-008	4.031e-008

Competition of Biotinylated Phosphatidic Acid Binding
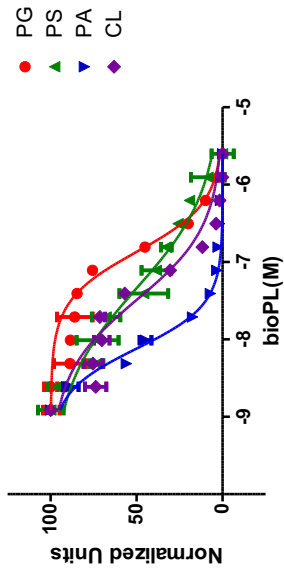
	PG	PC	PS	PA	CL
Best-fit values					
LogIC50	-6.868		-7.338	-8.118	-7.490
HillSlope	-1.390		-0.6839	-1.558	-0.9166
IC50	1.355e-007		4.587e-008	7.616e-009	3.239e-008

Competition of Biotinylated Phosphatidylglycerol Binding
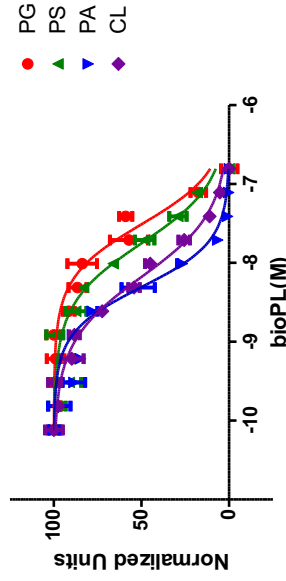
	PG	PC	PS	PA	CL
Best-fit values					
LogIC50	-7.509		-7.750	-8.306	-8.177
HillSlope	-1.301		-1.145	-1.522	-1.061
IC50	3.095e-008		1.778e-008	4.945e-009	6.655e-009

Figure 17. Preliminary results for PA, PS, and PG competition assays.

(Top, Left) Competition assay of 3.125 µM of phosphatidic acid with

dilutions starting at 156.5 µM PL. (Top, Right) Competition assay of 25 µM

of phosphatidylserine with dilutions starting at 1250 µM PL. (Bottom, Left)

Competition assay of 1.56 µM of phosphatidylglycerol with dilutions

starting at 78 µM PL. N=2

4.3.3. _Characterizing Phospholipid Binding of SDM Variant hArv1 Protein_

4.3.3.1. _Phosphatidyglycerol_

Our HTRF assays characterizing the binding affinities of individual mutant variants using phosphatidylglycerol as a substrate produced half maximal efficiency concentration distributions that were determined to be significantly different through application of an ANOVA (Figure 18, A, P value <0.0027). Comparisons made with a Student's T-test determined that there were significant increases in the average EC50 values with proteins that had the asparagine at position 94 altered to an alanine or a glutamine. This increase in EC50 value indicated a decrease in the affinity of those proteins to bind to phosphatidylglycerol (Figure 18, A).

4.3.3.2. _Phosphatidic Acid_

Results generated using phosphatidic acid also produced half maximal efficiency concentrations that significantly differed from the N98 values (Figure 18, B, P value < 0.0001). Mutant variant C58A/61A resulted in an increase in the EC50 values, which indicated a loss of binding affinity. Interestingly, there was a cluster region that produced a decrease in the EC50 values. Mutating positions 67, 70, or 72 to alanine resulted in similar significant decreases from 8.673e-008 to around 5.0e-008. A drop in EC50 values indicates that these mutant proteins have an increased propensity to bind to phosphatidic acid.
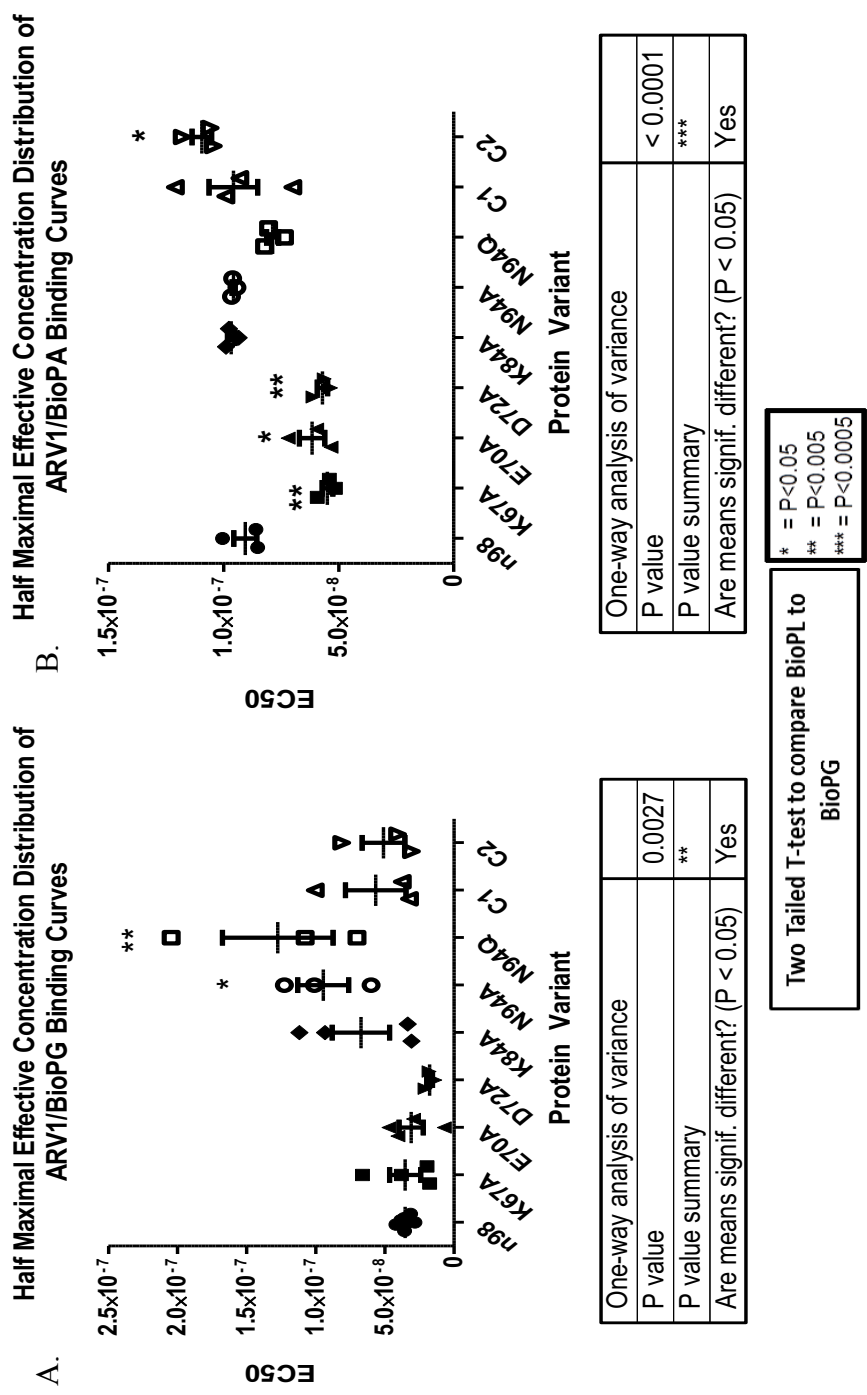
Figure 18. SDM hArv1 protein characterization of PG and PA binding. Three or more assays were performed for each protein variant which was plated in triplicate. HTRF binding curves were generated and the statistical significance of the distribution of their resulting EC50 values were determined for [A.] phosphatidylglycerol and [B.] phosphatidic acid.

4.3.3.3. _Phosphatidylserine_

Although binding interactions to phosphatidylserine were successfully assessed with the N98 hArv1 protein, the use of a new lot of biotinylated phosphatidylserine resulted in unwanted variations in HTRF assay values. Both literature and manufacture specifications indicated that there are issues concerning this lipid and the propensity of it to fall out of solution. We did store PS in chloroform at -20°C, however once the vial was unsealed, the lipid became increasingly more difficult to work with. When the lipid was out of solution, manufacture's specifications dictated the use of a 40°C water bath for 60 second increments until the majority of the lipid was back in solution. This may over time have further damaged the lipid. The average storage life of the biotinylated lipids is five months following breaking of the seal, however each time the lipid is used, exposure to the air resulted in alteration of lipid concentration due to chloroform evaporation. Storage volatility resulted in disparities between assays using this lipid immediately after its acquisition and those conducted two months after opening the vessel.

These problems were associated with a large overlap in the distributions of the half maximal effective concentrations for additional replicates of the N98 protein and studies conducted on the mutated variants (Figure 19). Future work will require working with the manufacture to provide this lipid from selective lots or narrowing the window of expiration dates when working with phosphatidylserine.

Half Maximal Effective Concentration Distribution of ARV1/BioPS Binding Curves

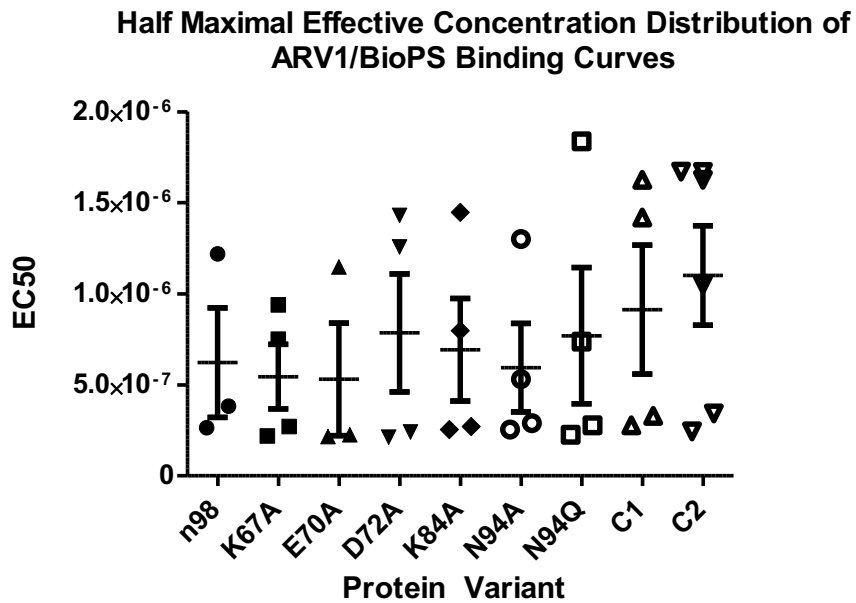| One-way analysis of variance	
P value	0.8776
P value summary	ns
Are means signif. different? (P < 0.05)	No

Figure 19. SDM hArv1 protein characterization of PS binding. Three or more assays were performed for each protein variant which was plated in triplicate. HTRF binding curves were generated and the statistical significance of the distribution of their resulting EC50 values were determined for phosphatidylserine. Due to issues with the stability of biotinylated phosphatidylserine, large amounts of variation were present between replicate experiments. Further work will be required to characterize the impact of binding for this phospholipid.

4.3.3.4. *Phosphatidylethanolamine*

Characterization of the N98 protein determined that hArv1 does not bind very well to phosphatidylethanolamine. Binding curves generated with the mutated variants did contain increases in the error bars for each concentration plated in three wells per concentration in experiments repeated three times. While these curves were not as "clean" as those generated with other phospholipids, they did produce reproducible EC50s whose distributions were determined to be significantly different (Figure 20, A, P value <0.0007). K84A, N94A, and N94Q yielded decreases in their EC50 values compared to those produced by the N98 assays. The alteration of residues at those locations produced a protein that had an increased ability to bind to a phospholipid that the unaltered version of the protein does not bind to very well.

4.3.3.5. *Phosphatidylcholine*

No statistically significant differences in the distribution of the half maximal effective concentrations for biding curves generated by HTRF assays using phosphatidylcholine were observed (Figure 20, B, P value 0.3818). On average, biding curves were flat, with only very small increases in signal seen at the highest concentrations of lipid.

A. Half Maximal Effective Concentration Distribution of ARV1/BioPE Binding Curves
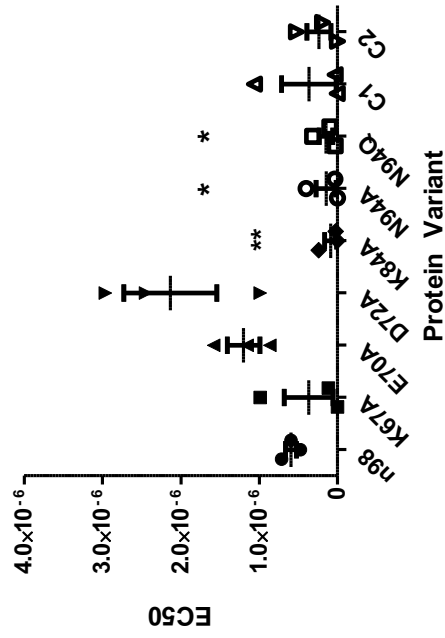
One-way analysis of variance	
P value	0.0007
P value summary	***
Are means signif. different? (P < 0.05)	Yes

B. Half Maximal Effective Concentration Distribution of ARV1/BioPC Binding Curves
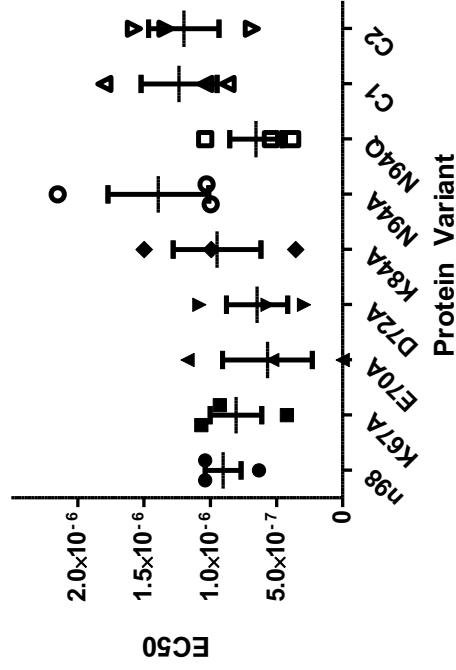
One-way analysis of variance	
P value	0.3818
P value summary	ns

*	= P<0.05
**	= P<0.005
***	= P<0.0005

Two Tailed T-test to compare BioPL to BioPG

Figure 20. SDM hArv1 protein characterization of PE and PC binding. Three or more assays were performed for each protein variant which was plated in triplicate. HTRF binding curves were generated and the statistical significance of the distribution of their resulting EC50 values were determined for [A.] phosphatidylethanolamine and [B.] phosphatidylcholine.

91

5. Discussion

Arv1: A critical factor in the progression of Metabolic Syndrome

The importance of Arv1 was first recognized in S. *cerevisiae* when it was determined to be essential when cells accumulate toxic un-esterified sterol intermediates [46]. Human ARV1 is highly conserved with its yeast counterpart, as its expression in yeast can functionally compensate for the changes in lipid distribution and synthesis induced by the loss of yeast Arv1. The importance of Arv1's conserved domains have been established in several fungal species. While each domain has the potential to contribute to function, the AHD found within the N-terminus has been shown to possess the majority of the documented activities associated with full length Arv1. Here, our results indicate that the AHD of human Arv1 can bind several phospholipids with varying affinities. In addition, it was discovered that several amino acids within the AHD were found to be critical for conferring lipid specificity. This work brings up the possibility that hArv1 acts as a lipid-binding protein that somehow regulates pathways involved in the initiation and progression of diseases caused by altered lipid homeostasis.

Studies using both yeast and human cell cultures have provided evidence that Arv1 is responsible in some way for maintaining the balance of lipids, including fatty acids, glycerolipids, sphingolipids, and sterols. Recent work by multiple laboratories have made a strong connection between Arv1 function and the onset of lipid disorders associated with MetS and/or NAFLD/NASH *(manuscript submitted)* [1]. Arv1 knock out mice did not gain weight, did not have an excess circulation of cholesterol, had

livers with reduced cholesterol, triglycerides, and fatty acids, and showed no signs of NAFLD/NASH. These animals also showed better sensitivity to insulin and were more glucose tolerant even when fed a high fat, high carbohydrate diet. The overall hypothesis is that loss of Arv1 prevents the absorption of surplus dietary fats as higher cholesterol, bile acid, and fatty acids are found in the feces of these animals *(manuscript submitted)*.

Maintaining Proper Lipid Distribution and Concentrations

In order to function at optimal conditions, each organelle has a specific repertoire of lipids it must maintain in specific quantities. Some lipids may be synthesized in a location/organelle specific manor, however the principal location for the production of lipids, their intermediates, and derivatives is the endoplasmic reticulum (ER) [70, 71]. To retain the ideal compartmentalized distributions, intracellular transport must be orchestrated in such a way that lipids are not over accumulated or depleted in any one location. The types of movement of lipids include lateral diffusion along bilayers, crossing between closely associated bilayers, flipping leaflets, and vesicular/tubular carriers [37]. Some methods may require use of specific lipid binding/transfer proteins [70].

A critical feature of some lipid transfer proteins is their ability to provide inter-organelle transport of lipids that would otherwise have limited contact [41]. Relating differing membranes allows for not only transfer of lipids, but also provides increased accessibility to enzymes or substrates to promote synthesis, signal transduction, or transport of cellular cargo [70]. Examples of this include the production or

movement of phospholipids such as phosphatidylserine for apoptotic signaling, or the transfer of cholesterol away from the ER in response to increases in dietary sources. The characteristic symptoms of many metabolic diseases including Niemann–Pick disease, Tangier disease, obesity, type II diabetes, nonalcoholic fatty liver disease, and atherosclerosis are direct consequences of the failure to regulate the steady state levels of specific lipids [72, 73]. This may be from a lack of ability to synthesize particular lipids, inability to properly metabolize lipids, or the failure to properly allocate them to required locations within cells in order to maintain the asymmetry seen between different membranes as well as different organelles [71, 74]. In order to further the understanding of theses pathologies and ideally develop mechanism specific drug therapies, it is imperative that more research be conducted on the cellular regulators of lipid homeostasis.

N-terminal AHD Region Retains Binding Abilities of Full Length Arv1

Based on knock out mouse studies, Arv1 has the potential to be a novel drug target to treat multiple lipid-mediated diseases. However, the molecular structure and function of this protein is still unknown. In order to contribute to resolving these issues, here our work focused on developing a computable means of assessing and measuring the protein-lipid interactions of hArv1, determining the lipid specificity of the protein, and identifying amino acids required for lipid binding.

We first wanted to confirm that the AHD would retain lipid binding in the absence of the transmembrane regions and the ER lumen loop. The human AHD spans residues 34-94 of the first 103 amino acids facing the cytoplasmic side of the

ER. Previous work attempting to use residues 1-94 produced a protein that yielded some inconsistences in purification, for that reason, the segment was extended to terminate at the 98th amino acid. This N-terminal 98 Arv1 protein was used in protein-lipid overlay assays. Results indicated that N98 was able to directly bind to phosphatidylglycerol (PG), cardiolipin (CL), phosphatidylserine (PS), the signaling lipid phosphatidylinositol 4-phosphate (PI(4)P), and cerebroside 3-sulfate (sulfatide). Moderate to low binding was achieved with phosphatidic acid (PA) and phosphatidylinositol (4,5)- bisphosphate (PI(4,5)P). The ability to bind to PG and CL was an interesting result in that these phospholipids are almost exclusively located in the membrane of the mitochondria. Several publications have shown that Arv1 localizes to the ER membrane, although Sundvold et al. demonstrated it could translocate and localize at centrosomes, the cleavage furor, and the intercellular bridge during cell division [75]. If Arv1 does interact with PG and CL in the cell it could either do so where the ER and mitochondria are brought within proximity to each other or during telophase. Structurally, CL resembles two fused units of PG. Whether or not this would result in differences of binding affinity could not be determined by the overlay.

Sulfatide can be found in pancreatic cells and along with other functions common to glycosphingolipids, it is involved in glucose-induced insulin secretion and has been known to stabilize insulin crystals [76]. In type II diabetes, low levels of sulfatide can occur along with increases in the pro-inflammatory cytokine TNF-α and insulin resistance (IR). If Arv1 recapitulates the binding pattern demonstrated for sulfatide in the lipid overlay, it could indicate its role in promoting progression of

type II diabetes by transporting available sulfatide to be degraded by arylsulfatase A [77].

It was surprising that the N98 Arv1 did not appear to bind cholesterol, considering the protein is known to bind cholesterol and has six cholesterol recognition/interaction amino acid consensus sequence (CRAC) sites, one of which is within the AHD. A CRAC site is denoted by a branched apolar leucine or valine that is next to 5 or less residues, followed by an aromatic group that is most often a tryptophan, then another 5 random residues, terminated with a basic group of lysine or arginine [78]. It is possible that there is a limitation in the orientation and availability of cholesterol when immobilized on an overlay, as, it was confirmed that the AHD alone can bind cholesterol using liposome binding assays, which allows for a more 3-dimensional access of the lipid to the protein (*J. Francisco and J.T. Nickels, unpublished data*). Further characterization of Arv1/cholesterol binding is warranted.

hArv1 AHD (N98) Binds Lipids with Specificity

Protein-lipid overlay results support that Arv1 is able to directly bind to anionic lipids with some degree of specificity. This is noted in the differences in intensity between lipids that appeared to bind very well like PS and lipids with only moderate binding, such as PA and PI(4,5)P. While the degree of difference could not be calculated, they were visibly observable. Not only did Arv1 bind to anionic lipids, it also did so selectively. No binding for phosphatidylinositol (PI) was visible, which has a negative charge, indicating that this is not simply a nonspecific charge related interaction occurring. Arv1 did not bind to the non-charged lipids PC or PE, which

seems reasonable since these lipids are in high quantities and make up the bulk of membranes. If Arv1 is to play a selective contributing role in the discriminatory transfer of sterols or phospholipids, it would not be beneficial to have significant binding for a substrate that is found in abundance and is not limited in specific regions as is the case with PC and PE.

hArv1 AHD (N98) Binds Lipids with Quantifiable "Apparent Affinity"

The application of the overlay allowed for the preliminary identification of lipid binding partners of Arv1, however the inability to quantitate the degree of binding prevented comparisons from being made between lipids required to rank the apparent affinity of binding to a particular lipid. A 2015 publication by Fleury et al., demonstrated a novel use in application of homogeneous time-resolved fluorescence technology. The HTRF assay had previously been used commonly as a means of studying the interactions between associated proteins by supplying specific ratio concentrations of protein substrate and enzyme. In this publication, HTRF was used to analyze protein-lipid interactions involved in sphingolipid metabolism, specifically, the transfer of ceramide to the Golgi by ceramide transfer (CERT) proteins [64]. By doing so, they were able to determine the ability of pharmaceutical compounds to inhibit this interaction by quantifying the change in the half maximal effective concentration (EC50). This value is defined as the concentration of agonist (in this case, lipid concentration) that is required to produce a response (protein binds the lipid) that is half of the maximal response. The EC50 determines the position of the dose-response curve and is used as a means to measure the effectiveness of an

agonist binding and is often referred to as the "apparent affinity". In the context of this study, any interpretation or reference of an "affinity" was defined as a measure of the protein's or variant's, sensitivity to binding to a particular lipid within a dose response curve. Changes in the EC50 of the same lipid between altered versions of the same protein implied a change in this apparent affinity.

Of the six biotinylated phospholipids available, the N98 hArv1 demonstrated the ability to bind to PG, CL, PS, and PA. Binding of PG, CL, PS, and PA agreed with the findings seen with our protein lipid overlays, although the degree to how well each lipid bound highlighted some divergences between these methods. The "intensity" of binding in the overlays led to the prediction that PG, CL, and PS would have robust binding in comparison to PA or the neutral lipids. Interestingly, it was determined that the EC50 distribution for certain lipid binding curves were statistically independent from others. It was decided to compare the lipid that showed the highest degree of apparent affinity (lowest EC50) as a benchmark to which the other lipids could be compared. Validation of significance was done through application of a student's T-test. The N98 hArv1 had the highest sensitivity for binding to PG with an EC50 0f 4.278e-008. Unexpectedly, this sensitivity is not shared with cardiolipin binding which indicated strong binding in the protein-lipid overlay, but when analyzed with HTRF, yielded a significantly different EC50 of 3.756e-007. It was earlier questioned if the structurally similarity of CL to PG would influence its binding. Here it has been determined that although CL shares the structural components of two PG moieties, these two lipids are bound by Arv1 with differing efficiencies. Possible rationalization for this include the size differential or

that PG as a (-1) charge, and CL (-2). The results produced by CL binding were comparable to the binding patterns generated with PS, whose EC50 was 4.547e-007. Limited binding of PE and PC was seen, generating EC50s that were not statistically different from each other, but were independent of the other phospholipids, 6.008e-007 and 1.282e-007 respectively. Second to PG, PA binding was very robust and generated 8.673e-008 as an EC50. Addressing these five lipids alone, the order of preferential lipid binding by N98 hArv1 was determined to be PG > PA >> CL – PS > PE - PC. Because the protein did not bind to all anionic lipids in the protein lipid overlays and because the charge of the phospholipid did not strictly predict the binding order in the HTRF, strong evidence indicates Arv1 does bind lipids with a quantifiable sensitivity and a degree of specificity that does not appear to be limited to the charge status of the phospholipid. With the binding patterns documented, future studies can address the efficacy of tool compounds that inhibit binding or ascertain if the binding action is calcium dependent, as is the case with other lipid binding proteins, such as Annexin V [33].

Amino Acid Mutations Alter Binding Specificity and Apparent Affinity for Some Phospholipids

Having established the order of binding, it was possible to determine the identity of amino acids contributing to lipid binding and specificity. As was the case with the N98 protein, none of the site directed mutant variants demonstrated any clear binding with PC either by overlay or HTRF assay, and no significant differences were apparent when comparing the distributions of the EC50 values. This phospholipid is

readily found in high abundance in the composition of the outer leaflets most lipid bilayers. Specific trafficking would most likely not occur in a PC dependent manor, as it is not drastically restricted to any singular location.

When evaluating the binding of variant proteins with overlays, some notable disparities were seen in the binding of sulfatide and the PIPs compared to N98 binding. Of the eight mutations used, all but one, lysine 67, affected the ability of sulfatide to be bound when each residue was changed to an alanine. With sulfatide having a suspected role of contributing to the initiation and/or progression of metabolic syndrome, including type II diabetes, it is not inconceivable that in response to the long term over accumulation of dietary fats, Arv1 could help in the depletion of sulfatide by transporting it to be degraded. Within pancreatic cells, insulin is produced and its circulation is regulated in response to blood glucose levels. Sulfatide is known to chaperone the inactive folding and preserve the structure of insulin crystals that are stored prior to exocytosis [76]. This lipid is co-localized to the insulin crystals and within the Golgi apparatus. The results obtained suggest that sulfatide binding occurs with the AHD region of the protein. Zinc molecules are found within the Golgi and could contribute to the binding of the cytoplasmic portions of the ER bound Arv1, specifically within the AHD, which has a punitive zinc-binding motif [76]. Sulfatide bound by Arv1 could promote its shuttling from the ER to the Golgi, facilitated by zinc interaction which would promote proper insulin preservation. Based on the results of the Arv1 KO mouse study, where glucose and insulin tolerance was improved by deletion of Arv1, it is likely the Arv1 binds to sulfatide and promotes its transport to be degraded. The enzyme arylsulfatase-A is

responsible for hydrolyzing sulfatide within lysosomes, however the enzyme needs assistance from proteins such as saposin B (SapB) which remove the sulfatide from membranes [77]. Arv1 may also perform a function of depleting sulfatide levels. Knockout of Arv1 in mice resulted in decreases in the amount of insulin produced on either HFD or normal chow adds support to this explanation.

Found in low concentrations in the cell, phosphoinositides are often distributed in a location specific manor. PIPs are produced by kinase interactions with phosphatidylinositol predominantly at the Golgi, $PI(4,5)P_2$, $PI(3,5)P_2$ at early endosomes, $PI(3)P$ at late endosomes and $PI(3,4,5)P_3$ at the plasma membrane [16]. In this study, mutation of lysine 84 conferred a notable increase in the protein's ability to bind to $PI(4)P$, $PI(4,5)P_2$, and $PI(3,5)P_2$, whereas the N98 protein showed less binding to $PI(4)P$, and little binding to other PIPs [16]. The change in charged residue at Lys67 allowed for the mutant protein to bind several differently phosphorylated species of phosphoinositide. What is interesting about this is that PIP binding is often determined by the electrostatic interactions of the phospholipid's negative charge with basic amino acids. The native lysine residue has a positive charge, which means the WT protein should have had potentially better binding then when this basic residue is removed. It is possible that this switch in charge may have allowed for improved access to the arginine at position 89, also a basic residue. Mutating Lys 84 also allowed for an increase in the binding of PE, as did mutating asparagine 94. Studies designed to express the full length K84A mutant in HepG2 cells may reveal whether this amino acid is involved in the transport of cholesterol

from the ER, in that the mutation improved binding to both signal docking PIPs as well as PE, both of which are found in the plasma membrane.

The increase in apparent affinity for PE through mutating Asp 94 also caused a decrease in its propensity to bind to PG, a lipid that the N98 Arv1 had the highest apparent affinity for. Any mutation made beyond amino acid 84 seemed to produce an increase in the error associated with PE binding using our HTRF assay. Whether or not this occurrence is artifact requires determination. Asp 94 was altered to address questions regarding the influence of possible glycosylation (asparagine to glutamine) or removal of a polar residue that participates in hydrogen bonding of protein structure (asparagine to alanine). Both mutations produced similar results, in that there was an increase in binding a phospholipid (PE) that the N98 protein did not bind well to, and decreasing the ability to bind to a phospholipid the WT Arv1 has the highest apparent affinity for (PG). Taken collectively, it appears that Asp94 is required to confer lipid binding specificity.

A possible cluster/motif was identified with respect to PA binding that included positions 67, 70, and 72. Single changes from lysine, glutamate, or aspartate to alanine at these locations, respectively, significantly reduced the EC50 values for PA. One would expect that the positive charge on either a lysine or arginine residue would allow for hydrogen binding of the phosphate group on PA, allowing for specific binding by distinguishing this phospholipid from others. It may be that this region is important in restricting undesired binding of PA, a lipid known to induce negative curvature in the membrane, act as a precursor for several lipid species, and functions in signaling cascades when converted to lysophosphatidic acid (LPA).

Results suggested that PA binding was specific and not only a consequence of charge. Here, lysine (positive charge), glutamate (negative charge), and aspartate (negative charge) alterations produced very similar binding curves with EC50 distributions that overlap each other. Further analysis of this area would involve double and triple amino acid mutations, as well as expanding in both directions to identify the complete region of this motif, and also determine if this increase in apparent affinity for PA can be further amplified by altering more than one residue at a time. Cysteines changed at positions 57 and 61 reduced the proteins ability to bind PA, indicating the need for those residues to maintain the affinity. Further altering residues between these two locations may further impair this binding.

Arv1 Does Not Appear To Have Multiple Binding Sites

Competition assays were performed to ascertain whether Arv1 contained more than one lipid-binding site. BioPG, which was used as the representative Arv1 binder, as it had the highest degree of binding affinity, was able to be displaced with increasing concentrations of PA or CL. The displacement by CL is interesting in that the N98 did not demonstrate a high propensity for binding this lipid in standard HTRF, and yet it was able to displace the bound bioPG better than PG itself. BioPA binding was inhibited with increased amounts of CL and PS. Both CL and PS overlapping inhibitory trends however did not do so well enough to surpass the turnover rate of PA to bioPA binding.

While the results produced from competition assays are preliminary, having only been replicated 1-2 times, if these trends are verified through statistical analysis,

it would appear that there is competition over the same site of binding with regards to PG, PS, PA, and CL, or that the conformational changes associated with binding can be altered with binding of a different phospholipid. The rate of each bioPL binding by N98 at set concentration of bioPL was able to be reduced in the presence of increasing amounts of non-biotinylated phospholipid.

Theoretical Mechanisms of Action of hArv1

The role of Arv1 in lipid metabolism has been studied in yeast, mouse, and human cell culture. Major advancements have been made since its discovery, however the direct mechanism through which Arv1 functions remains unknown. Several hypothetical mechanisms dealing with lipid binding are conceivable. The results of this study have been used to formulate a working model of how Arv1 functions to regulate lipid transport and metabolism.

Arv1 resides in the ER, anchored by three transmembrane regions [51, 56]. Various knock down studies in different species hint at the possibility that Arv1 may regulate cholesterol [46], sphingolipids, phospholipids [51], and bile acids [14]. Our laboratories HFD KO mouse study showed strong relationship between Arv1 function and dietary fat toxicity. KO mice had healthier livers with less cholesterol, triglycerides, and fatty acids, were leaner, and had better tolerance and sensitivity to glucose and insulin; a mouse that is resistant to diet-induced obesity (*manuscript submitted*). Assuming that Arv1 is a lipid transporter protein that is regulating lipid homeostasis, the paradox in this is, why when its knocked down in cell culture, there

appears to be cellular lipid dysregulation and yet when it was removed in mice it appears to be "beneficial" in the context of metabolic diseases?

It is suspected that the over consumption of dietary fats being sent to the liver result in the over accumulation of cholesterol within the ER. Normal distribution of cholesterol in cells should be low in the ER and higher in the plasma membranes. To maintain this balance, cholesterol needs to be secreted by lipoproteins, hydroxylated into bile acids, or esterified [14]. Knockdown of Arv1 has been shown to lead to an inverse distribution causing ER cholesterol buildup [14]. The buildup of cholesterol in the absence of Arv1 leads to activation of ER stress pathways such as the unfolded protein response, which aim to resolve the burden or undergo apoptosis [79]. In the KO mouse studies, the loss of Arv1 prevented the animals from absorbing more fats from the diet and the result was increased amounts of fatty acids, cholesterol, and bile acid in the feces. Our KO mice survived in the absence of Arv1 while on a HFD, however the Rader's study produced mice that were prone to spontaneous death on normal chow, and did not tolerate extended overnight fasting. Some mechanism was operating to tolerate the ER lipid burden, but only when the composition of the diets could contribute a larger cholesterol gradient to push the lipids in. An oversimplified view could be that the high ER cholesterol presents signals that the cell is "full" and does not need to continue to take in more fat. The HFD might have generated something similar to a gradient that promoted intake of some fat regardless of the "full" signal while excreting the rest, allowing the animal to survive. When on a normal chow diet, the "full" signal prevents uptake, and eventual depletion of fat storage leaves the animal more prone to death from fasting. Our KO mice responded

metabolically differently depending on the diet they were put on; some differences were minor compared to wild type that became more apparent when switched to a HFD.

When Arv1 is readily available, it is conceivable that just as the lipid environment generated by the content of the diet could influence the outcome of the animal, it could also alter the activities of Arv1 in response to ER lipid burden. The trafficking functions of Arv1 may differ in the framework of the degree of ER burden and lipid environment. In healthy cells, Arv1 may transport lipids to one of the above-mentioned fates of cholesterol. Conversely, long term over accumulation of lipids in the ER could lead to Arv1 promoting a different route of traffic, perhaps an unbeneficial one with undesirable consequences as seen with WT mice that are fed a HFD.

The molecular basis underlying the protein-lipid interaction between Arv1 and various lipids has not been elucidated. From this study, it was determined that Arv1 can specifically bind to PI(4)P and sulfatide in the overlays, and to PG , PA , CL, and PS with defined apparent affinity using HTRF. Since these phospholipids are found in varying concentrations at different locations, it is plausible to assume that since Arv1 binds very well to some of these lipids, the protein may have some form of contact with the residential organelle of those lipids. This suggests that communication in some form may be possible between Arv1 in the ER, and the plasma membrane, Golgi, and/or the mitochondria.

Arv1 deficient cells present a significantly different organization of lipids than wild type cells, which are altered in the asymmetry of the phospholipid bilayer [57].

Arv1 could aid in arranging the phospholipids within membranes to promote binding

of secondary proteins or enzymes to clusters of a specific phospholipid. By doing so,

it may improve accessibility to a particular phospholipid or further stabilize the

binding to one. The presence of multiple lipid species in the membrane may also

contribute to its structural qualities and phospholipid geometry. Where PC and PS are

considered "cylindrical" in shape and produce flat bilayers, PE and PA are "conical"

and PIPs "cone" shaped which promote curvatures [80]. Curvatures can lead to

increased formation of vesicles at the Golgi. Changes in the "shape" of membranes

can promote binding of other proteins to these regions. This is a required event in the

formation of contact sites between organelles [80]. Arv1 may contribute to contact

site formation through its binding and rearranging of PA and PS in specific

membranes.

As a transmembrane protein, Arv1 has the potential to act as a lipid

transporter by directing lipid cargo across membrane at contact sites and/or

contributing to the tethering of structures at contact sites [26]. As described earlier,

members of the oxysterol-binding protein (OSBP) family have been shown to bind

sterols in the ER, move them against a sterol gradient, and transfer them to a specific

destination [43]. This is done through counter exchange of lipid binding. After

binding the sterol and bringing it across the contact sites, the OSBP's affinity for its

cargo would be compromised through interaction and binding of a PIP member,

allowing the sterol to be released for the cycle to be repeated [26]. Additional proteins

are often required to further stabilize this complex. Although not validated, when

Arv1 was first identified, the sequence gave strong indications that the protein might

operate as a dimer, an interesting concept that has yielded some support in the form of co-immunoprecipitation and yeast 2 hybrid (Y2H) studies (*H-Y Liu, unpublished data*).

If, Arv1 has this ability to dimerize, and dimerization is required for function, maintaining the dimer would be crucial for the transport of lipids such as cholesterol to the mitochondria at MAM contact sites. Arv1 is able to bind to both PG and CL which are both predominately restricted to the mitochondria. Competition assays with CL and PA have indicated a strong ability to outcompete other bound lipids. This could mean that the transport of Arv1's lipid cargo terminates at its destinations by inhibitory influences of competing lipids. CL is found in higher concentrations at the IMM, however it is still present in a lesser extent on the OMM [81]. Mitochondria maintain low levels of sterols and sphingolipids which need to be synthesized at the ER and transferred to the mitochondria which strictly regulates the localization and concentration of lipids such as cholesterol [81]. Failure to do so may result in oxidative stress and apoptosis. The accumulation of cholesterol at the mitochondria has also been characterized in several metabolic disorders, including NAFLD [82]. The progression of NAFLD to NASH is designated at the point when hepatic steatosis progresses to steatosis with inflammation, known as steatohepatitis. While NAFLD is a reversible condition with proper intervention therapies, once a patient transitions to steatohepatitis, there is no prospect for reversal. A key point in the transition of this commitment step is the overloading of cholesterol in the mitochondria, which leads to increased production of TNF-α [82]. This pro-inflammatory cytokine promotes chronic inflammation in the liver, increasing the risk

of hepatocellularcarcinoma, promotes further cholesterol dysregulation by increasing its synthesis, and also contributes to promoting type II diabetes by facilitating the resistance to insulin [82].

Based on all the data, we hypothesize that in response to long term over accumulation of lipids through diet, Arv1 that might otherwise traffic lipids to the Golgi or plasma membrane in a beneficial manner, instead directs lipids to the mitochondria, which can lead to key features of several metabolic diseases (Figure 21, A). Arv1 in the ER, either as a monomer or dimer, promotes the formation of contact sites to the mitochondria. Cholesterol from the ER is bound at one of the protein's CRAC sites, where it is shielded from the cellular contents as is transferred across membranes to the mitochondria. Interaction and binding of PI(4)P or possible inhibition by CL at the mitochondria facilitates the release of cholesterol, allowing the contact site interaction to end (Figure 21, B).
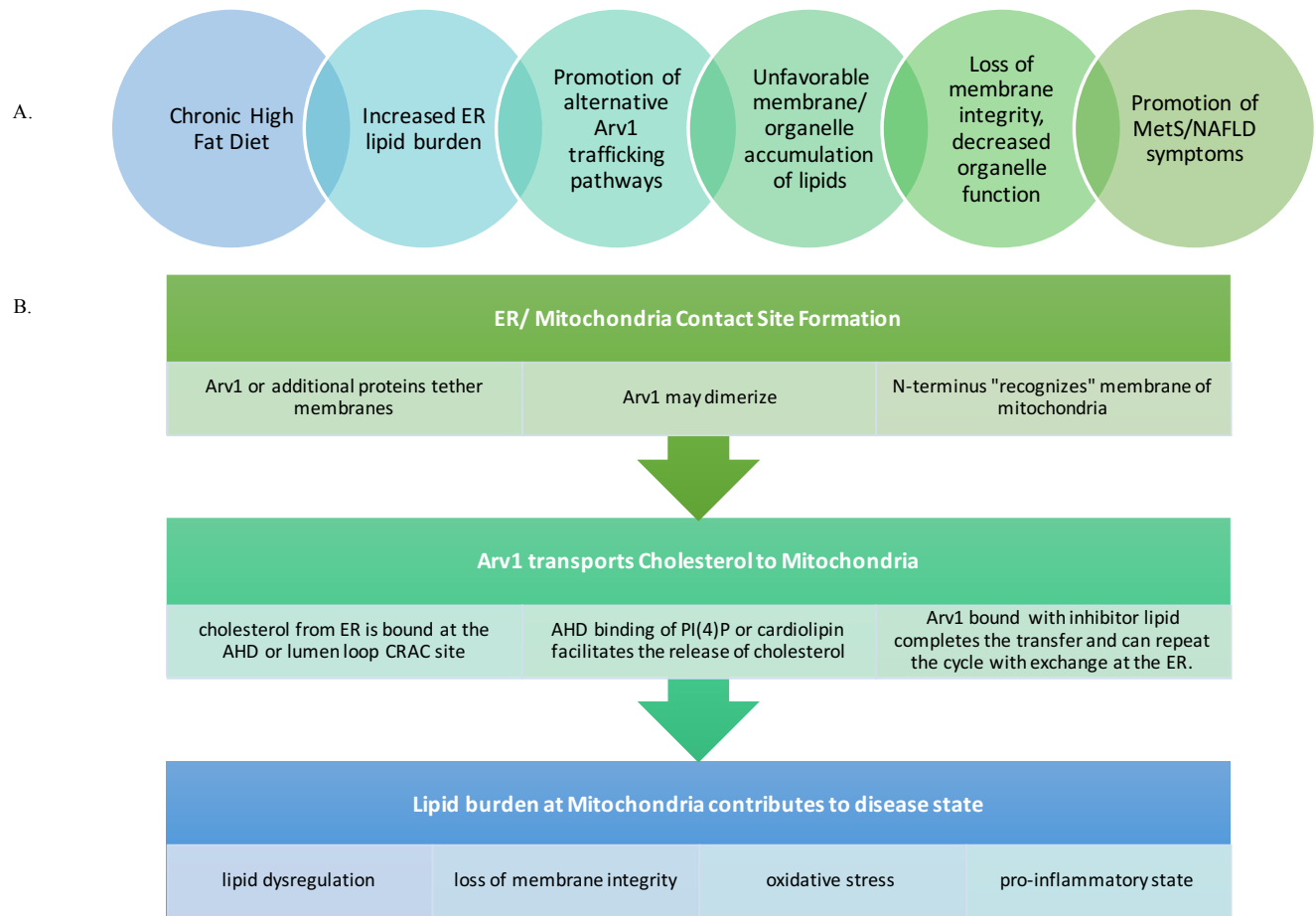
Figure 21. Predicted Mechanisms of Action of hArv1. [A.] Order of events for the role of Arv1 in the diet induced promotion of MetS/NAFLD. [B.] Order of events in the theoretical binding mechanism of Arv1 in the induced transport of cholesterol to the mitochondria.

6. Future Directions

The overall intention of this study was to aid in characterizing the protein-lipid binding interactions of human ARV1, a putative regulator of lipid transport. Even with the results herein described in conjunction with the current publications focused on Arv1 in relation to lipid dysregulation, a large expanse of information remains unresolved. What is the purpose of this membrane bound protein, what is its true structure and how does this structure confer the abilities of its predicted function of binding to and regulating cellular lipids? With the recent connections made between Arv1 and the initiation or progression of metabolic diseases, specifically NAFL/NASH, where treatment options are limited, there is a demand for more research to address these unanswered questions.

To further complement the work of this study, it would necessary to repeat HTRF assays with additional lipids as well as with additional mutations made within the AHD. Arv1 has been shown to bind to PS, a lipid that is involved in the initiation of pro-apoptotic pathways. Overlay result indicated the WT binds to PI(4)P and alteration at position expands its ability to bind to other phosphorylated species. Obtaining a quantifiable measurement of how well Arv1 can bind to all of the phosphoinositides could assist in identifying the regions where the ER bound protein interacts with other membranes of organelles, as PIPs localization represent an organelle "zip code" [34]. This study failed to show binding to cholesterol with lipid overlays. We were not able to look at cholesterol binding in our HTRF assay as biotinylated cholesterol is not available. With time, it may be possible to optimize a

modified form of the HTRF with liposomes. Liposomes could be created with phospholipids that lack the ability to be bound by Arv1, such as PC or PE, and with increasing concentrations of cholesterol. Preliminary work in our laboratory has used this system to show that N98 can bind to cholesterol at concentrations as low as 10% (*J. Francisco, unpublished* data). Liposomal binding assays provide a more physiology relevant model to study protein-lipid interactions, as having several phospholipids assembled allows their structures to be stabilized as they might be in the membrane. There is also the ability to make liposomes that mimic the lipid make up of various organelles. Moreover, there are acceptor/donor liposomal assays that can tell us whether Arv1 has the ability to not only transport lipid, be whether it has the ability to transfer it from one organelle bilayer to another.

Based on the data we obtained with our SDM studies, we could then look at the influence of critical residues involved in lipid transport/transfer in a cellular context through expression of full length constructs encoding the desired mutations. Immunohistochemistry studies would make it possible to detect the changes in localization of Arv1 within the cell involved in contact site formation as well as detect changes in metabolic burden in regards to lipid synthesis, storage, and trafficking. After assessing the cellular impact of these mutations, it would be beneficial to see if the changes induced can be "rescued" with supplemented Arv1protein and/or truncations.

7. Summary and Conclusion

Lipid Binding Characterization of hArv1 AHD Summary

Taken collectively, the AHD region of hArv1 has the ability to bind selectively to phospholipids in the absence of its transmembrane regions and lumen facing loop in vitro. Evidence suggests that the biding specificity is not completely dependent on the influence of charge as the N98 could bind anionic lipids, but not all of them. Further support of this was the removal of residues known to contribute to electrostatic interactions having not influenced binding or increasing the propensity to bind. We believe that the binding of lipids by Arv1 is lipid specific in that the protein is able to "recognize" specific lipids. The protein-lipid interaction occurs at differing apparent affinities in the order of PG > PA >> CL ~ PS > PE ~PC.

This study identified that position 94 is required to maintain the specificity of hArv1 AHD lipid binding denoted by an inverse change in PE and PG biding compared to the N98. Positions 67, 70, and 72 are required to maintain Arv1's affinity for PA. Position 84 may be involved in preventing increased PIP dependent signaling or localized binding events, as its removal increased the proteins apparent binding to PI(4)P, PI(4,5)P2, and PI(3,5)P2 compared to the N98 protein's binding of PI(4)P. We also believe that the AHD region is responsible for sulfatide binding as the majority of the mutations, which includes several regions of the AHD sequence, resulted in a substantial reduction of binding response. The results of this study have been mapped along the modified regions of the hArv1 AHD sequence (Figure 22).

Additional work is required to further support these findings in addition to identifying the lipid binding mechanisms through which hArv1 functions. Doing so will contribute to elucidating the true cellular behaviors of this punitive lipid transport protein in regards to lipid related diseases.
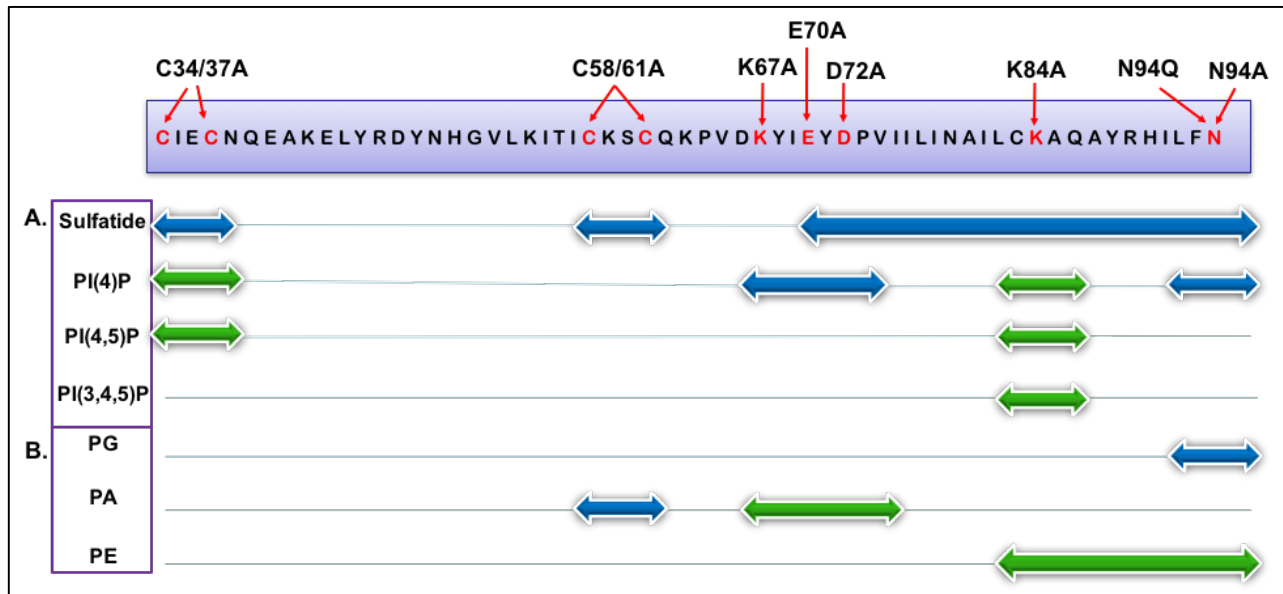
Figure 22. hArv1 homology domain regions associated with altered phospholipid binding. Collective schematic representing the effects of mutated amino acids within the hArv1 homology domain (top boxed sequence). Mutations listed above the AHD sequence with the affected amino acids are in red. Horizontal arrows indicate the portions of the amino acid sequence that when mutated, altered the described binding response for the phospholipid designated on the left. Green arrows indicate an apparent increase in binding and blue arrows indicate a loss of binding. [A.] Results obtained through protein-lipid overlays. [B.] Results obtained through HTRF assays.

8. References

1. Lagor, W., Tong, F., Jarrett, K., Lin, W., Conlon, D., & Smith, M. et al. (2015). Deletion of murine Arv1 results in a lean phenotype with increased energy expenditure. *Nutrition & Diabetes*, *5*(10), e181. http://dx.doi.org/10.1038/nutd.2015.32

2. Sherling, D., Perumareddi, P., & Hennekens, C. (2017). Metabolic Syndrome. *Journal of Cardiovascular Pharmacology and Therapeutics*, *22*(4), 365-367. http://dx.doi.org/10.1177/1074248416686187

3. O'Neill, S., & O'Driscoll, L. (2014). Metabolic syndrome: a closer look at the growing epidemic and its associated pathologies. *Obesity Reviews*, *16*(1), 1-12. http://dx.doi.org/10.1111/obr.12229

4. Aust, L. (1977). H. Haller, M. Hanefeld u. W. Jaross: Lipidstoffwechselstörungen - Diagnostik, Klinik und Therapie. 339 Seiten, 72 Abb., 60 Tab. VEB Gustav Fischer-Verlag, Jena 1975. Preis 38,50 M. *Food / Nahrung*, *21*(3), 276-277. http://dx.doi.org/10.1002/food.19770210332

5. Grundy, S. (2006). Drug therapy of the metabolic syndrome: minimizing the emerging crisis in polypharmacy. *Nature Reviews Drug Discovery*, *5*(4), 295-309. http://dx.doi.org/10.1038/nrd2005

6. Tsujimoto, T., & Yamamoto-Honda, R. (2014). Effectiveness of Combination Therapy with Statin and Another Lipid-Modifying Agent Compared with Intensified Statin Monotherapy. *Annals of Internal Medicine*, *161*(9), 678. http://dx.doi.org/10.7326/l14-5021-2

7. Pocha, C., Kolly, P., & Dufour, J. (2015). Nonalcoholic Fatty Liver Disease-Related Hepatocellular Carcinoma: A Problem of Growing Magnitude. *Seminars in Liver Disease*, *35*(03), 304-317. http://dx.doi.org/10.1055/s-0035-1562949

8. Thompson, T. (2017). *lipid | biochemistry*. *Encyclopedia Britannica*. Retrieved 17 April 2017, from https://www.britannica.com/science/lipid

9. Mathews, C. (2013). *Biochemistry*. Toronto: Pearson.

10. Berg, J., Tymoczko, J., & Stryer, L. (2007). *Biochemistry*. New York: W.H.Freeman & Co Ltd.

11. Bittman, R. (2013). Glycerolipids: Chemistry. *Encyclopedia of Biophysics*, 907-914. http://dx.doi.org/10.1007/978-3-642-16712-6_527

12. Yang, M., & Nickels, J. (2015). MOGAT2: A New Therapeutic Target for Metabolic Syndrome. *Diseases*, *3*(3), 176-192. http://dx.doi.org/10.3390/diseases3030176

13. Dufourc, E. (2008). Sterols and membrane dynamics. *Journal of Chemical Biology*, *1*(1-4), 63-77. http://dx.doi.org/10.1007/s12154-008-0010-6

14. Tong, F., Billheimer, J., Shechtman, C., Liu, Y., Crooke, R., & Graham, M. et al. (2010). Decreased Expression of ARV1 Results in Cholesterol Retention in the Endoplasmic Reticulum and Abnormal Bile Acid Metabolism. *Journal of Biological Chemistry*, *285*(44), 33632-33641. http://dx.doi.org/10.1074/jbc.m110.165761

15. Hishikawa, D., Hashidate, T., Shimizu, T., & Shindou, H. (2014). Diversity and function of membrane glycerophospholipids generated by the remodeling pathway in mammalian cells. *The Journal of Lipid Research*, *55*(5), 799-807. http://dx.doi.org/10.1194/jlr.r046094

16. Christie, W. (2017). *What is a Lipid? - AOCS Lipid Library*. *Lipidlibrary.aocs.org*. Retrieved 30 May 2017, from http://lipidlibrary.aocs.org/Primer/content.cfm?ItemNumber=39371#simple

17. Hiramine, Y., Emoto, H., Takasuga, S., & Hiramatsu, R. (2009). Novel acyl-coenzyme A:monoacylglycerol acyltransferase plays an important role in hepatic triacylglycerol secretion. *The Journal of Lipid Research*, *51*(6), 1424-1431. http://dx.doi.org/10.1194/jlr.m002584

18. Goldberg, MD, A. (2017). *Overview of Lipid Metabolism - Endocrine and Metabolic Disorders - MSD Manual Professional Edition*. *MSD Manual Professional Edition*. Retrieved 30 May 2017, from http://www.merckmanuals.com/professional/endocrine-and-metabolic-disorders/lipid-disorders/overview-of-lipid-metabolism

19. *Chapter 5: Atherosclerosis*. (2017). *Medicine and Health Articles*. Retrieved 12 April 2017, from https://healtheappointments.com/chapter-5-atherosclerosis-essays/2/

20. Fagone, P., & Jackowski, S. (2008). Membrane phospholipid synthesis and endoplasmic reticulum function. *The Journal of Lipid Research*, *50*(Supplement), S311-S316. http://dx.doi.org/10.1194/jlr.r800049-jlr200

21. Horton, J., Goldstein, J., & Brown, M. (2002). SREBPs: activators of the complete program of cholesterol and fatty acid synthesis in the liver. *Journal of Clinical Investigation*, *109*(9), 1125-1131. http://dx.doi.org/10.1172/jci15593

22. Ishii, S., IIzuka, K., Miller, B., & Uyeda, K. (2004). Carbohydrate response element binding protein directly promotes lipogenic enzyme gene transcription. *Proceedings of The National Academy of Sciences*, *101*(44), 15597-15602. http://dx.doi.org/10.1073/pnas.0405238101

23. Gavrilova, O., Haluzik, M., Matsusue, K., Cutson, J., Johnson, L., & Dietz, K. et al. (2003). Liver Peroxisome Proliferator-activated Receptor   Contributes to Hepatic Steatosis, Triglyceride Clearance, and Regulation of Body Fat Mass. *Journal of Biological Chemistry*, *278*(36), 34268-34276. http://dx.doi.org/10.1074/jbc.m300043200

24. Moon, Y. (2017). The SCAP/SREBP Pathway: A Mediator of Hepatic Steatosis. *Endocrinology and Metabolism*, *32*(1), 6. http://dx.doi.org/10.3803/enm.2017.32.1.6

25. Radhakrishnan, A., Sun, L., Espenshade, P., Goldstein, J., & Brown, M. (2010). The SREBP Pathway. *Handbook of Cell Signaling*, 2505-2510. http://dx.doi.org/10.1016/b978-0-12-374145-5.00298-9

26. van Meer, G., Voelker, D., & Feigenson, G. (2008). Membrane lipids: where they are and how they behave. *Nature Reviews Molecular Cell Biology*, *9*(2), 112-124. http://dx.doi.org/10.1038/nrm2330

27. Mitra, K., Ubarretxena-Belandia, I., Taguchi, T., Warren, G., & Engelman, D. (2004). Modulation of the bilayer thickness of exocytic pathway membranes by membrane proteins rather than cholesterol. *Proceedings of The National Academy of Sciences*, *101*(12), 4083-4088. http://dx.doi.org/10.1073/pnas.0307332101

28. Gibellini, F., & Smith, T. (2010). The Kennedy pathway-De novo synthesis of phosphatidylethanolamine and phosphatidylcholine. *IUBMB Life*, n/a-n/a. http://dx.doi.org/10.1002/iub.337

29. Holthuis, J., & Menon, A. (2014). Lipid landscapes and pipelines in membrane homeostasis. Nature, 510(7503), 48-57. http://dx.doi.org/10.1038/nature13474

30. Tanford, C. (1978). The hydrophobic effect and the organization of living matter. *Science*, *200*(4345), 1012-1018. http://dx.doi.org/10.1126/science.653353

31. Jackson, C., Walch, L., & Verbavatz, J. (2016). Lipids and Their Trafficking: An Integral Part of Cellular Organization. *Developmental Cell*, *39*(2), 139-153. http://dx.doi.org/10.1016/j.devcel.2016.09.030

32. Pomorski, T., Hrafnsdóttir, S., Devaux, P., & Meer, G. (2001). Lipid distribution and transport across cellular membranes. *Seminars in Cell & Developmental Biology*, *12*(2), 139-148. http://dx.doi.org/10.1006/scdb.2000.0231

33. Kaetzel, M., & Dedman, J. (2004). Annexin VI regulation of cardiac function. *Biochemical and Biophysical Research Communications*, *322*(4), 1171-1177. http://dx.doi.org/10.1016/j.bbrc.2004.07.127

34. McDermott, M., & Mousley, C. (2016). Lipid transfer proteins and the tuning of compartmental identity in the Golgi apparatus. *Chemistry and Physics of Lipids*, *200*, 42-61. http://dx.doi.org/10.1016/j.chemphyslip.2016.06.005

35. Mejia, E., & Hatch, G. (2015). Mitochondrial phospholipids: role in mitochondrial function. *Journal of Bioenergetics and Biomembranes*, *48*(2), 99-112. http://dx.doi.org/10.1007/s10863-015-9601-4

36. Fadeel, B., & Xue, D. (2009). The ins and outs of phospholipid asymmetry in the plasma membrane: roles in health and disease. *Critical Reviews in Biochemistry and Molecular Biology*, *44*(5), 264-277. http://dx.doi.org/10.1080/10409230903193307

37. Sprong, H., van der Sluijs, P., & van Meer, G. (2001). How proteins move lipids and lipids move proteins. *Nature Reviews Molecular Cell Biology*, *2*(7), 504-513. http://dx.doi.org/10.1038/35080071

38. Vance, J. (1990). Phospholipid synthesis in a membrane fraction associated with mitochondria. *Journal of Biological Chemistry*, *13*(265), 7248-7256.

39. Lebiedzinska, M., Szabadkai, G., Jones, A., Duszynski, J., & Wieckowski, M. (2009). Interactions between the endoplasmic reticulum, mitochondria, plasma membrane and other subcellular organelles. *The International Journal of Biochemistry & Cell Biology*, *41*(10), 1805-1816. http://dx.doi.org/10.1016/j.biocel.2009.02.017

40. SHIAO, Y., BALCERZAK, B., & VANCE, J. (1998). A mitochondrial membrane protein is required for translocation of phosphatidylserine from mitochondria-associated membranes to mitochondria. *Biochemical Journal*, *331*(1), 217-223. http://dx.doi.org/10.1042/bj3310217

41. Drin, G., von Filseck, J., & Čopič, A. (2016). New molecular mechanisms of inter-organelle lipid transport. *Biochemical Society Transactions*, *44*(2), 486-492. http://dx.doi.org/10.1042/bst20150265

42. Mesmin, B., Antonny, B., & Drin, G. (2013). Insights into the mechanisms of sterol transport between organelles. *Cellular and Molecular Life Sciences*, *70*(18), 3405-3421. http://dx.doi.org/10.1007/s00018-012-1247-3

43. Rogaski, B., & Klauda, J. (2011). Phospholipid Binding and Membrane Attachment of the Osh4 Protein. *Biophysical Journal*, *100*(3), 395a. http://dx.doi.org/10.1016/j.bpj.2010.12.2347

44. Sturley, S. (1997). Molecular aspects of intracellular sterol esterification: the acyl coenzyme A: cholesterol acyltransferase reaction. *Current Opinion in Lipidology*, *8*(3), 167-173. http://dx.doi.org/10.1097/00041433-199706000-00007

45. Lewis, T., Rodriguez, R., & Parks, L. (1987). Relationship between intracellular sterol content and sterol esterification and hydrolysis in Saccharomyces cerevisiae. *Biochimica Et Biophysica Acta (BBA) - Lipids and Lipid Metabolism*, *921*(2), 205-212. http://dx.doi.org/10.1016/0005-2760(87)90020-8

46. Tinkelenberg, A., Liu, Y., Alcantara, F., Khan, S., Guo, Z., Bard, M., & Sturley, S. (2000). Mutations in Yeast ARV1 Alter Intracellular Sterol Distribution and Are Complemented by Human ARV1. *Journal of Biological Chemistry*, *275*(52), 40667-40670. http://dx.doi.org/10.1074/jbc.c000710200

47. Kutateladze, T., Ogburn, K., Watson, W., de Beer, T., Emr, S., Burd, C., & Overduin, M. (1999). Phosphatidylinositol 3-Phosphate Recognition by the FYVE Domain. *Molecular Cell*, *3*(6), 805-811. http://dx.doi.org/10.1016/s1097-2765(01)80013-7

48. Hostager, B., Catlett, I., & Bishop, G. (2000). Recruitment of CD40 and Tumor Necrosis Factor Receptor-associated Factors 2 and 3 to Membrane Microdomains during CD40 Signaling. *Journal of Biological Chemistry*, *275*(20), 15392-15398. http://dx.doi.org/10.1074/jbc.m909520199

49. Gruenberg, J., Kobayashi, T., Beuchat, M., Lindsay, M., Frias, S., & Palmiter, R. et al. (1999). *Nature Cell Biology*, *1*(2), 113-118. http://dx.doi.org/10.1038/10084

50. Wu, W., McDonough, V., Nickels, J., Ko, J., Fischl, A., & Vales, T. et al. (1995). Regulation of Lipid Biosynthesis inSaccharomyces cerevisiaeby Fumonisin B1. *Journal Of Biological Chemistry*, *270*(22), 13171-13178. http://dx.doi.org/10.1074/jbc.270.22.13171

51. Swain, E., Stukey, J., McDonough, V., Germann, M., Liu, Y., Sturley, S., & Nickels, J. (2002). Yeast Cells Lacking the ARV1 Gene Harbor Defects in Sphingolipid Metabolism: COMPLEMENTATION BY HUMAN ARV1. *Journal of Biological Chemistry*, *277*(39), 36152-36160. http://dx.doi.org/10.1074/jbc.m206624200

52. Kajiwara, K., Watanabe, R., Pichler, H., Ihara, K., Murakami, S., Riezman, H., & Funato, K. (2008). Yeast ARV1 Is Required for Efficient Delivery of an Early GPI Intermediate to the First Mannosyltransferase during GPI Assembly and Controls Lipid Flow from the Endoplasmic Reticulum. *Molecular Biology of The Cell*, *19*(5), 2069-2082. http://dx.doi.org/10.1091/mbc.e07-08-0740

53. Radhakrishnan, A., Goldstein, J., McDonald, J., & Brown, M. (2008). Switch-like Control of SREBP-2 Transport Triggered by Small Changes in ER Cholesterol: A Delicate Balance. *Cell Metabolism*, *8*(6), 512-521. http://dx.doi.org/10.1016/j.cmet.2008.10.008

54. Sidrauski, C., & Walter, P. (1997). The Transmembrane Kinase Ire1p Is a Site-Specific Endonuclease That Initiates mRNA Splicing in the Unfolded Protein Response. *Cell*, *90*(6), 1031-1039. http://dx.doi.org/10.1016/s0092-8674(00)80369-4

55. Ruggles, K., Garbarino, J., Liu, Y., Moon, J., Schneider, K., & Henneberry, A. et al. (2013). A Functional, Genome-wide Evaluation of Liposensitive Yeast Identifies the "ARE2Required for Viability" (ARV1) Gene Product as a

Major Component of Eukaryotic Fatty Acid Resistance. *Journal of Biological Chemistry*, *289*(7), 4417-4431. http://dx.doi.org/10.1074/jbc.m113.515197

56. Villasmil, M., & Nickels Jr, J. (2011). Determination of the membrane topology of Arv1 and the requirement of the ER luminal region for Arv1 function in Saccharomyces cerevisiae. *FEMS Yeast Research*, *11*(6), 524-527. http://dx.doi.org/10.1111/j.1567-1364.2011.00737.x

57. Georgiev, A., Johansen, J., Ramanathan, V., Sere, Y., Beh, C., & Menon, A. (2013). Arv1 Regulates PM and ER Membrane Structure and Homeostasis But is Dispensable for Intracellular Sterol Transport. *Traffic*, *14*(8), 912-921. http://dx.doi.org/10.1111/tra.12082

58. Yki-Järvinen, H. (2014). Non-alcoholic fatty liver disease as a cause and a consequence of metabolic syndrome. *The Lancet Diabetes & Endocrinology*, *2*(11), 901-910. http://dx.doi.org/10.1016/s2213-8587(14)70032-4

59. Gaggini, M., Morelli, M., Buzzigoli, E., DeFronzo, R., Bugianesi, E., & Gastaldelli, A. (2013). Non-Alcoholic Fatty Liver Disease (NAFLD) and Its Connection with Insulin Resistance, Dyslipidemia, Atherosclerosis and Coronary Heart Disease. *Nutrients*, *5*(5), 1544-1560. http://dx.doi.org/10.3390/nu5051544

60. Fotbolcu, H., & Zorlu, E. (2016). Nonalcoholic fatty liver disease as a multi-systemic disease. *World Journal of Gastroenterology*, *22*(16), 4079. http://dx.doi.org/10.3748/wjg.v22.i16.4079

61. Sanyal, A., Campbell–Sargent, C., Mirshahi, F., Rizzo, W., Contos, M., & Sterling, R. et al. (2001). Nonalcoholic steatohepatitis: Association of insulin resistance and mitochondrial abnormalities. *Gastroenterology*, *120*(5), 1183-1192. http://dx.doi.org/10.1053/gast.2001.23256

62. Younossi, Z., Blissett, D., Blissett, R., Henry, L., Stepanova, M., & Younossi, Y. et al. (2016). The economic and clinical burden of nonalcoholic fatty liver disease in the United States and Europe. *Hepatology*, *64*(5), 1577-1586. http://dx.doi.org/10.1002/hep.28785

63. *Protter - interactive protein feature visualization*. (2017). *Wlab.ethz.ch*. Retrieved 13 June 2017, from http://wlab.ethz.ch/protter/start/

64. Munnik, T., & Wierzchowiecka, M. (2013). Lipid-Binding Analysis Using a Fat Blot Assay. *Methods in Molecular Biology*, 253-259. http://dx.doi.org/10.1007/978-1-62703-401-2_23

65. Fleury, L., Faux, C., Santos, C., Ballereau, S., Génisson, Y., & Ausseil, F. (2015). Development of a CERT START Domain–Ceramide HTRF Binding Assay and Application to Pharmacological Studies and Screening. *Journal of Biomolecular Screening*, *20*(6), 779-787. http://dx.doi.org/10.1177/1087057115573402

66. Degorce, F. (2009). HTRF: A Technology Tailored for Drug Discovery - A Review of Theoretical Aspects and Recent Applications. *Current Chemical Genomics*, *3*(1), 22-32. http://dx.doi.org/10.2174/1875397300903010022

67. *GraphPad Curve Fitting Guide*. (2017). *Graphpad.com*. Retrieved 4 December 2016, from http://www.graphpad.com/guides/prism/7/curve-fitting/index.htm?reg_the_ec50.htm

68. Acker, M., & Auld, D. (2014). Considerations for the design and reporting of enzyme assays in high-throughput screening applications. *Perspectives in Science*, *1*(1-6), 56-73. http://dx.doi.org/10.1016/j.pisc.2013.12.001

69. Carpenter, E., Beis, K., Cameron, A., & Iwata, S. (2008). Overcoming the challenges of membrane protein crystallography. *Current Opinion in Structural Biology*, *18*(5), 581-586. http://dx.doi.org/10.1016/j.sbi.2008.07.001

70. Olkkonen, V., & Li, S. (2013). Oxysterol-binding proteins: Sterol and phosphoinositide sensors coordinating transport, signaling and metabolism. *Progress in Lipid Research*, *52*(4), 529-538. http://dx.doi.org/10.1016/j.plipres.2013.06.004

71. Krahmer, N., Farese, R., & Walther, T. (2013). Balancing the fat: lipid droplets and human disease. *EMBO Molecular Medicine*, *5*(7), 973-983. http://dx.doi.org/10.1002/emmm.201100671

72. Vanier, M. (2013). Niemann–Pick diseases. *Handbook of Clinical Neurology*, 1717-1721. http://dx.doi.org/10.1016/b978-0-444-59565-2.00041-1

73. Maxfield, F., & Tabas, I. (2005). Role of cholesterol and lipid organization in disease. *Nature*, *438*(7068), 612-621. http://dx.doi.org/10.1038/nature04399

74. Jackson, C., Walch, L., & Verbavatz, J. (2016). Lipids and Their Trafficking: An Integral Part of Cellular Organization. *Developmental Cell*, *39*(2), 139-153. http://dx.doi.org/10.1016/j.devcel.2016.09.030

75. Sundvold, H., Sundvold-Gjerstad, V., Malerød-Fjeld, H., Haglund, K., Stenmark, H., & Malerød, L. (2016). Arv1 promotes cell division by recruiting IQGAP1 and myosin to the cleavage furrow. *Cell Cycle*, *15*(5), 628-643. http://dx.doi.org/10.1080/15384101.2016.1146834

76. Buschard, K., Bracey, A., McElroy, D., Magis, A., Osterbye, T., & Atkinson, M. et al. (2016). Sulfatide Preserves Insulin Crystals Not by Being Integrated in the Lattice but by Stabilizing Their Surface. *Journal of Diabetes Research*, *2016*, 1-4. http://dx.doi.org/10.1155/2016/6179635

77. Takahashi, T., & Suzuki, T. (2012). Role of sulfatide in normal and pathological cells and tissues. *The Journal of Lipid Research*, *53*(8), 1437-1450. http://dx.doi.org/10.1194/jlr.r026682

78. Fantini, J., & Barrantes, F. (2013). How cholesterol interacts with membrane proteins: an exploration of cholesterol-binding sites including CRAC, CARC, and tilted domains. *Frontiers in Physiology*, *4*. http://dx.doi.org/10.3389/fphys.2013.00031

79. Shechtman, C., Henneberry, A., Seimon, T., Tinkelenberg, A., Wilcox, L., & Lee, E. et al. (2011). Loss of Subcellular Lipid Transport Due to ARV1 Deficiency Disrupts Organelle Homeostasis and Activates the Unfolded Protein Response. *Journal of Biological Chemistry*, *286*(14), 11951-11959. http://dx.doi.org/10.1074/jbc.m110.215038

80. Suetsugu, S., Kurisu, S., & Takenawa, T. (2014). Dynamic Shaping of Cellular Membranes by Phospholipids and Membrane-Deforming Proteins. *Physiological Reviews*, *94*(4), 1219-1248. http://dx.doi.org/10.1152/physrev.00040.2013

81. Tatsuta, T., Scharwey, M., & Langer, T. (2014). Mitochondrial lipid trafficking. *Trends in Cell Biology*, *24*(1), 44-52. http://dx.doi.org/10.1016/j.tcb.2013.07.011

82. Fon Tacer, K., & Rozman, D. (2011). Nonalcoholic Fatty Liver Disease: Focus on Lipoprotein and Lipid Deregulation. *Journal of Lipids*, *2011*, 1-14. http://dx.doi.org/10.1155/2011/783976

83. Gallo-Ebert, C., Francisco, J., Liu, H., Hayward, M., Li-Wang, B., & Jones, B. et al. Mice lacking mARV1 are resistant to high fat diet-induced obesity and show reduced signs of non-alcoholic steatohepatitis and metabolic syndrome. *Manuscript submitted*.

9. Abbreviations

A	Alanine
ABC	ATP-Binding Cassette Transporters
ACAT	A:Cholesterol O-Acyltransferase
AGPAT	Acylglycerol-3-Phosphate Acyltransferase
AHD	Harv1 Homology Domain
Apo_	Apolipoproteins
ARE1/2	ACAT Related Enzymes ½
Arv1	Acyl-Coenzyme-A: Cholesterol O-Acyl Transferase Related Enzyme Required For Viability-1
ASCVD	Atherosclerotic Cardiovascular Disease
ASO	Antisense Oligonucleotide
ATF6	Activating Transcription Factor-6
Biopl	Biotinylated Phospholipid
BSA	Bovine Serum Albumin
C	Cysteine
CDP-DAG	Cytidine Diphosphate Diacylglycerol
CERT	Ceramide Transfer Protein
CHOL	Cholesterol
CHOP	C/EBP Homologous Protein
ChREBP	Carbohydrate Response Element Binding Protein
CL	Cardiolipin
Co-IP	Co-Immunoprecipitation

CRAC	Cholesterol Recognition/Interaction Amino Acid Consensus
CRP	C-Reactive Protein
CVD	Cardiovascular Disease
D	Aspartate
DAG	Diacylglycerol
DGAT	Diacylglycerolacyltransferase
DHE	22,33-Dihydroergosterol
E	Glutamate
EC50	Half Maximal Effective Concentration
EDTA	Ethylenediaminetetraacetic Acid
ER	Endoplasmic Reticulum
ERG	Ergosterol
FA	Fatty Acids
FRET	Fluorescence Resonance Energy Transfer Technology
FXR	Farnesoid X Receptor
G3P	Glycerol-3-Phosphate
Galcer	Galactosylceramide
GPAT	Glycerol-3-Phosphate Acyltransferase
Gsls	Glycosphingolipids
HCC	Hepatocellular Carcinoma
HDL	High Density Lipoprotein
HEPES	4-(2-Hydroxyethyl)-1-Piperazineethanesulfonic Acid
Hepg2	Hepatocellular Carcinoma Cell Lines

HFD	High Fat Diet
HMG-CoA	3-Hydroxy-3-Methylglutaryl-Coenzyme A
HRP	Horseradish Peroxidase
HTRF	Homogeneous Time Resolved Fluorescence
IC50	Half Inhibitory Efective Concentration
IDL	Intermediate Density Lipoprotein
IFG	Impaired Fasting Glucose
IGT	Impaired Glucose Tolerance
IL	Interleukin
IMAC	Immobilized Metal Ion Affinity Chromatography
IMM	Inner Mitochondrial Membrane
INSIG-1	Insulin Induced Gene 1
IPTG	Isopropyl B-D-1-Thiogalactopyranoside
IR	Insulin Resistance
IRE1	Inositol-Requiring Enzyme-1
ISL	Inositol Sphingolipid
K	Lysine
KAN	Kanamycin
KD	Knock Down
KO	Knock Out
LB	Luria Broth
LDL	Low Density Lipoprotein
LDLR	Low Density Lipoprotein Receptor

LPA	Lysophosphatidic Acid
LPL	Lipoprotein Lipase
LTP	Lipid Transporter Protein
Mab	Monoclonal Antibody
MAG	Monoacylglycerol
MAM	Mitochondrial Associated Membranes
Mets	Metabolic Syndrome
MGAT	Monoacylglycerol Acyltransferase
N	Asparagine
N98	Amino Terminus 98 Amino Acids
NAFLD	Nonalcoholic Fatty Liver Disease
NASH	Nonalcoholic Steatohepatitis
NFM	Nonfat Milk
OD	Optical Density
OMM	Outer Mitochondrial Membrane
OSBP	Oxysterol Binding Protein
Osh	Oxysterol Binding Protein Homolog
PA	Phosphatidic Acid
PAI1	Plasminogen- Activator Inhibitor 1
PAM	Plasma Membrane Associated Membranes
PC	Phosphatidylcholine
PDME	Phosphatidyl-N,N-Dimethylethanolamine
PE	Phosphatidylethanolamine

PERK	Protein Kinase RNA (PKR)-Like ER Kinase
PG	Phosphatidylglycerol
PI	Phosphatidylinositol
PI	Protease Inhibitor
PIPs	Phosphoinositides
PL	Phospholipid
PLO	Protein Lipid Overlays
PM	Plasma Membrane
PMME	Phosphatidyl-N-Monomethylethanolamine
PPAR Γ	Peroxisome Proliferator-Activated Receptor-Γ
PS	Phosphatidylserine
PSS	Phosphatidylserine Synthase
Q	Glutamine
S1P	Sphingosine-1-Phosphate
S1P, S2P	SCAP Activated Site 1 And 2 Proteases
SAA	Serum Amyloid A Protein
Sapb	Saposin B
Sc	Saccharomyces Cervisiae
SCAP	SREBP Cleavage-Activating Protein
SDM	Site Directed Mutagenesis
SDS-PAGE	Sodium Dodecyl Sulphate-Polyacrylamide Gel Sequences
SNARE	Soluble NSF Attachment Protein Receptor

SREBP	Sterol Regulatory Element Binding Protein
T2D	Type II Diabetes
TAG	Triglyceride
TBST	Tris-Buffered Saline (TBS) And Polysorbate 20
Tnfα	Tumor-Necrosis Factor-A
TR	Time-Resolved
UPR	Unfolded Protein Response
VLDL	Very Low Density Lipoprotein
WAT	White Adipose Tissue
WT	Wild Type
Y2H	Yeast 2 Hybrid

11. Attributes

Figure 1; Illustration modified from Grundy, et al. 2006

Figure 2; Illustration from "*Chapter 5: Atherosclerosis", 2017*

Figure 3; Illustration from *Radhakrishnan, Sun, Espenshade, Goldstein & Brown, 2010*

Figure 4; Illustration *Christie et al, 2017*

Figure 5; Illustration by *van Meer, Voelker & Feigenson, 2008*

Figure 6; Illustration modified from *van Meer, Voelker & Feigenson, 2008*

Figure 7; *Model from Villasmil et al 2011, adapted and illustrated by Hsing-yin Liu, 2015*

Figure 8; Preliminary data obtained from manuscript submitted by *Gallo-Ebert et al*

Figure 9; Illustration by Jessie Lee Cunningham, modified from Hsing-Yin Liu's adaptation from *Villasmil*, et al. 2011

Figure 10; Illustration by Jessie Lee Cunningham (Protter program)

Figure 11; Illustration by Jessie Lee Cunningham *modified from model by Fleury et al, 2015*

Table 1; Illustration by Jessie Lee Cunningham

Table 2; Illustration by Jessie Lee Cunningham

Figure 12; All work done by Jessie Lee Cunningham

Table 3; Illustration by Jessie Lee Cunningham

Figure 13; All work done by Jessie Lee Cunningham

Figure 14; All work done by Jessie Lee Cunningham

Figure 15; All work done by Jessie Lee Cunningham

Figure 16; All work done by Jessie Lee Cunningham

Figure 17; All work done by Jessie Lee Cunningham

Figure 18; All work done by Jessie Lee Cunningham

Figure 19; All work done by Jessie Lee Cunningham

Figure 20; All work done by Jessie Lee Cunningham

Figure 21; Illustration by Jessie Lee Cunningham

Figure 22; Illustration by Jessie Lee Cunningham